Role of Wnt/GSK3β/β-catenin signaling pathway in cardiac and pulmonary vascular remodeling

Inaugural Dissertation
submitted to the
Faculty of Medicine
in partial fulfillment of the requirements
for the PhD-Degree
of the Faculties of Veterinary Medicine and Medicine
of the Justus Liebig University Giessen

by
Sklepkiewicz, Piotr Lukasz
of
Torun, Poland

Giessen 2010

From the Department of Medicine
Director / Chairman: Prof. Dr. Werner Seeger
of Medicine of the Justus Liebig University Giessen

First Supervisor and Committee Member: Prof. Ralph Theo Schermuly, PhD
Second Supervisor and Committee Member: Prof. Jeanine D'Armiento, MD, PhD
Committee Members:
Date of Doctoral Defense:

Table of Content

Table of Content ..... **I**

List of Figures: ..... **IV**

List of Tables: ..... **VI**

List of Abreviations: ..... **VII**

1. Introduction **1**

1.1. **Pulmonary Hypertension** **1**

1.1.1. Definition and research history of Pulmonary Hypertension 1

1.1.2. Classification of Pulmonary Hypertension 1

1.1.3. Pathogenesis of Pulmonary Arterial Hypertension 4

1.1.4. Cellular crosstalk in vascular remodeling of PAH 8

1.1.5. Molecular mediators of vascular remodeling in PAH 9

1.1.6. Pharmacological treatment of PAH 12

1.2. **Cardiac remodeling** **15**

1.2.1. Right heart failure in PAH 15

1.2.2. Left ventricular remodeling 16

1.3. **Wnt signaling pathway** **17**

1.3.1. Wnt ligands 18

1.3.2. Wnt receptors 19

1.3.3. Canonical Wnt signaling 20

1.3.4. GSK3β as Wnt-independent multi tasking kinase 21

1.3.5. Non-canonical Wnt signaling pathway 23

1.3.6. Extracellular modulation of Wnt signaling by secreted Frizzled related proteins (sFRPs) 24

1.4. **Wnt signaling pathway in vascular homeostasis** **25**

1.5. **Animal model of Monocrotaline (MCT)-induced PAH in rats** **26**

2. Aims of the study **27**

3. Materials and methods **29**

3.1. **Materials** **29**

3.1.1. Equipment 29

3.1.2. Reagents 31

3.2. **Methods** **34**

3.2.1. RNA isolation 34

3.2.2. Reverse transcription 34

3.2.3. Polymerase chain reaction (PCR) 35

3.2.4. Real-Time Polymerase chain reaction 37

3.2.5. Agarose gel electrophoresis 38

3.2.6. Protein isolation 38

3.2.7. Cytoplasmic and nuclear fractionation 39

3.2.8. Protein quantity estimation 39

3.2.9. SDS polyacrylamide gel electrophoresis 39

3.2.10. Protein blotting 40

3.2.11. Protein detection 41

3.2.12. Densitometry 41

3.2.13. Immunohistochemistry 41

3.2.14. Molecular cloning 42

3.2.15. Cell culture condition 51

3.2.16. Transfection of primary PASMCS 53

3.2.17. ^{3}H- Thymidine incorporation assay 53

3.2.18. Experimental model of Pulmonary Hypertension 54
3.2.19. Statistical analysis 54
3.2.20. sFRP-1 KO mice generetion. 54
3.2.21. Pathway-Focused gene expression profiling using Real-Time PCR 55
3.2.22. Immunohistofluorescence 55
3.2.23. Echocardiographic analysis 56
3.2.24. Histological analysis 56

4. Results 57
4.1. **Wnt signaling expression in an experimental Pulmonary Hypertension 57**
4.1.1. mRNA expression profile of Wnt signaling in experimental Pulmonary Hypertension 57
4.1.2. Protein expression profiling of the Wnt signaling intracellular effectors in an experimental Pulmonary Hypertension 58
4.1.3. Wnt signaling expression in PASMC's 59
4.1.4. GSK3β/β-Catenin signaling axis protein expression in PASMC's of MCT-induced Pulmonary Hypertension 60
4.2. **The role of GSK3β/β-Catenin signaling axis in PDGF-BB mitogenic signaling in MCT-PASMC 61**
4.2.1. Phosphorylation of GSK3β by PDGF-BB mitogen in MCT-PASMC's 61
4.2.2. GSK3β/β-Catenin system is differentially regulated by PDGF-BB and Wnt3A signaling pathways in MCT-PH PASMC's 62
4.2.3. Phosphorylation status of GSK3β by PDGF-BB mitogen in MCT-PH PASMC's is restored by Imatinib treatment. 63
4.2.4. The generation of human GSK3β constructs with point mutations at the main functional phosphorylation residues. 64
4.2.5. Overexpression of human wild type GSK3β and point mutated variants influences PASMC's proliferation 66
4.3. **Upregulation of GSK3β in human lungs of IPAH 69**
4.4. **Canonical Wnt signaling in PASMC's of MCT-induced Pulmonary Hypertension 70**
4.5. **Wnt signaling in cardiac remodeling. Cardiac phenotype of sFRP-1 KO mice 71**
4.5.1. Pattern of sFRP-1 expression in normal mice hearts 71
4.5.2. sFRP-1 KO mice increase heart size 72
4.5.3. sFRP-1 KO mice increase forming fibrotic lesions in heart myocardium 74
4.5.4. Dysregulation of Wnt signaling pathway in sFRP-1 KO hearts 75
4.5.5. Increased protein expression profile of the main canonical Wnt signaling molecules in the sFRP-1 KO hypertrophy model 77
4.5.6. An increase in β-catenin accumulation in the intercalated disks of sFRP-1 cardiomyopathic hearts 79
4.5.7. Suppression of canonical Wnt transcriptional activity in sFRP-1 KO hearts 80
4.5.8. Decreased expression of Connexin43 in sFRP-1 KO remodeled hearts 81

5. Discussion 83
5.1. **Dysregulation of Wnt signaling pathway in experimental Pulmonary Hypertension 83**
5.2. **Contribution of the GSK3β/β-catenin pathway to growth factors induced signaling in MCT-PASMC 86**
5.3. **Individual role of GSK3β in regulation of MCT-PASMC proliferation 89**
5.4. **Canonical Wnt signaling and its potential role in regulating PASMC proliferation 91**
5.5. **Role of Wnt signaling in heart failure. Loss of sFRP-1 leads to cardiac remodeling and loss of heart function 92**

5. Outlook 97

7. Summary 99

8. Zusammenfassung 101

9. Appendix 103
10. References 106
11. Curriculum Vitae 120
12. Declaration 123
13. Acknowledgements 124

List of Figures:

Figure 1.1. Scheme of series of events governing pathology of PAH
Figure 1.2. Characteristic histopathology of pulmonary arteries in PAH
Figure 1.3. Scheme representing three signaling pathways which are main targets for existing therapeutical strategies in Pulmonary Hypertension focusing on vasodilation
Figure 1.4. Schematic molecular mechanism of reversing vascular remodeling in PAH by Imatinib mesylate a potent PDGFR inhibitor
Figure 1.5. Scheme representing distinct Wnt signaling pathways.
Figure 1.6. Motifs present in Frizzled proteins.
Figure 1.7. Scheme representing mechanisms of canonical Wnt signaling action within the cell.
Figure 1.8. Scheme representing two isoforms of GSK3 of the mammalian genome.
Figure 1.9. Putative substrates of GSK3ß protein**.**
Figure 1.10. Wnt signaling modulation by sFRPs
Figure 1.11. Scheme representing potential implication of Wnt signaling in homeostasis and pathogenesis of blood vessels.
Figure 3.1. pGEM-T Easy Vector
Figure 3.2. pcDNA3.1 TOPO directional expression vector
Figure 4.1. Expression of Wnt signaling ligands and receptors in lung tissues of control and MCT-induced PAH rats
Figure 4.2. Expression of Wnt signaling intracellular effectors in lung tissues of control and MCT-induced AH rats
Figure 4.3. Expression of GSK3ß/ß-Catenin signaling molecules axis in lung tissues of control and MCT-induced PAH rats
Figure 4.4. Expression of Wnt signaling in primary pulmonary arterial smooth muscle cells isolated from control and MCT-induced PAH rats
Figure 4.5. Regulation of GSK3ß/ß-Catenin signaling molecules axis in primary PASMC's isolated from control and MCT-induced PAH rats
Figure 4.6. Increased phosphorylation of GSK3ß in primary PASMCs after stimulation with PDGF-BB.
Figure 4.7. GSK3ß/β-Catenin axis is differentially regulated by PDGF-BB and Wnt3A stimulation in primary PASMCs.
Figure 4.8. Detection of two GSK3ß splice variants in human lungs.
Figure 4.9. Sequence alignment of human GSK3β constructs designed for overexpression in primary PASMC's.
Figure 4.10. Transient transfection of wild type and mutants of GSK3ß influences MCT-PAH PASMCs proliferation
Figure 4.11. Transient transfection of wild type and constitutively active GSK3ß influences ERK phosphorylation
Figure 4.12. Expression of GSK3ß/ß-Catenin signaling molecules axis in human lungs of healthy and IPAH patients
Figure 4.13. Canonical Wnt3A decreases MCT-PAH PASMCs proliferation
Figure 4.14. Lithium Chloride decreases serum-induced MCT-PAH PASMCs proliferation
Figure 4.15. Abundant expression of sFRP-1 in normal heart during mice adult life
Figure 4.16. sFRP-1 KO mice develop heart hypertrophy at 1 year of age.
Figure 4.17. Developmnet of dilated cardiomyopathy with worsened LV functional parameters

Figure 4.18. Fibrotic lesions formation in myocardium of sFRP-1 KO hearts.
Figure 4.19. Wnt Signaling Real-Time based mRNA expression profile
Figure 4.20. Main canonical Wnt signaling molecules are upregulated in sFRP-1 KO heart homogenates.
Figure 4.21. β-Catenin accumulates in intercalated disks of sFRP-1 KO cardiomyopathic hearts.
Figure 4.22. Loss of sFRP-1 in hearts leads to age dependent loss of canonical Wnt signaling transcriptional activity
Figure 4.23. Loss of sFRP-1 leads to downregulation of Connexin43 in heart myocardium.
Figure 5.1. Possible role for GSK3β in Imatinib-induced reversal of vascular remodeling in MCT-PAH.
Figure 5.2. Speculative role for GSK3β overexpression on proliferation of MCT-PASMC
Figure 5.3. Potential mechanism of sFRP-1 KO-induced cardiac remodeling in mice.

List of Tables:

Table 1.1. Newest Clinical Classification of Pulmonary Hypertension (Dana Point, 2008)
Table 1.2. WHO functional classification of pulmonary hypertension
Table 1.App List of primers used for PCR amplification
Table 2.App List of primers used for PCR fragments sequencing
Table 3.App List of primers used for PCR GSK3β splice variant detection
Table 4.App List of primary antibodies used
Table 5.App List of secondary antibodies use

List of Abreviations:

A	Alanine
ABC	Avidin-Biotin Complex
AEC	3-Amino-9-Ethylcarbazole
AF	Adventitial Fibroblasts
Akt	Aktivin, Protein Kinase B
ALK1	Activin receptor-like Kinase 1
APC	Adenomatosis Polyposis Coli
AR**VC**	Arrhythmogenic Right Ventricular Cardiomyopathy
BAX	Bcl2 assosiated X protein
Bcl	B-cell CLL/lymphoma 2
BCR-ABL	Philadelphia Chromosome, chromosomal abnormality associated with CML
BMP-2	Bone Morphogenetic Protein 2
BMPR2	Bone morphogenic Protein Receptor 2
BSA	Bovine Serum Albumin
Ca^{2+}	Calcium
cDNA	single stranded DNA
cGMP	cyclic guanosine monophoshate
c-Jun	protein which, in combination with c-Fos, forms the AP-1
c-kit	Tyrosine Kinese Receptor (target of Imatinib)
CML	Chronic Myelogenous Leukemia
CRD	Cystein rich domain
CREB	cAMP Response Element Binding
CTEPH	Chronic Thromboembolic Pulmonary Hypertension
Cx43	Connexin 43
D	Aspartic Acid
DEP	protein module of ~90 amino acids that was first discovered in three proteins, Discheveled, EGL-10 and Pleckstrin hence the term
DHEA	Dehydroepiandrosterone
DMEM	Dulbecco's Modified Eagle Medium
DNA	Deoxyrybonucleic acid
DOTMA	N-[1-(2,3-dioleyloxy)propyl]-N,N,N-trimethylammonium chloride
DTT	Dithiothreitol
Dvl	Dishevelled
EC	Endothelial Cells
ECM	Extracellular Matrix
EDTA	Ethylenediaminetetraacetic acid
EGF	Epidermal Growth Factor
EGTA	Ethylene glycol tetraacetic acid
eIF2	Eucaryotic Initiation Factor 2
EMT	Epithelial to Mesenchymal Transition
eNOS	endothelial Nitric Oxide Synthase

ERK	Extracellular signal-regulated Kinase
ET-1	Endothelin 1
ETRA	Endothelin Receptor A
ETRB	Endothelin Receptor B
EV	Empty Vector
FCS	Fetal Calf Serum
FGF2	Fibroblast Growht Factor 2
FPAH	Familial Pulmonary Arterial Hypertension
FrzA	Frizzled A =sFRP-1
FS	Fractional shortening
Fzd	Frizzled
GAPDH	Glyceraldehyde 3-phosphate dehydrogenase
Gleevec	STI571=Imatinib, PDGFR inhibitor
GTP	Guanosine triphosphate
H1	Histone 1
HCM	Hypertrophic Cardiomyopathy
HPV	Hypoxic Pulmonary Vasoconstriction
HRP	Horseradish Peroxidase
IAP	Inhibitor of Apoptosis Protein
ICM	Idiopathic Cardiomyopathy
IGF	Insulin Growth Factor
IgG	Immunoglobulin
IPAH	idiopathic Pulmonary Arterial Hypertension
IPTG	Isopropyl β-D-1-thiogalactopyranoside
KO	Knock Out
Kv channel	Pottassium Channel
LB	Lysogeny Broth
LEF	Lymphoid Enhancer Factor
LF	Lipofectamine
LiCl	Lithium Chloride
LRP	LDL related protein
LVEDD	Left Ventricle End Diastolic Dimension
MAPK	Mitogen activated Protein Kinase
MCTP	Monocrotaline pyrrole
MCT-PAH	Monocrotaline-induced Pulmonary Arterial Hypertension
MCT-PASMC	Pulmonary Arterial Smooth Muscle Cells isolated from MCT-PAH rats
$MgCl_2$	Magnesium Chloride
MHC	Myosin Heavy Chain
MI	Myocardial Infarction
MMP	Matrix Metalloproteinase
mRNA	messenger Rybonucleic Acid
Myc	Family of oncogenic transcription factors
NFAT	Nuclear factor of activated T-cells, transcription factor
NFkB	nuclear factor kappa-light-chain-enhancer of activated B cells
NO	Nitric Oxide

NOS	Nitric Oxide Synthase
NYHA	New York Heart Association
PA	Pulmonary Artery
PAEC	Pulmonary Arterial Endothelial Cells
PAH	Pulmonarry Arterial Hypertension
PAP	Pulmonary Arterial Pressure
PASMC	Pulmonary Arterial Smooth Muscle Cells
PBGD	porphobilinogen deaminase
PBS	Phosphate Buffered Saline
PCH	Pulmonary capillary hemangiomatosis
PCP	Planar Cell Polarity
PCR	Polymerase Chain Reaction
PDE5	Phosphodiesterase 5
PDZ	an acronym combining the first letters of three proteins: post synaptic density protein (PSD95), Drosophila disc large tumor suppressor (DlgA), and zonula occludens-1 protein (zo-1)
PGI_2	Prostacyclin
PH	Pulmonary Hypertension
PI3K	Phosphoinositide 3-kinase
PMSF	phenylmethylsulphonyl fluoride
PDGF	Platelet Derived Growth Factor
PPH	Primary Pulmonary Hypertension
PVH	Pulmonary Venous Hypertension
PVOD	Pulmonary veno-occlusive disease
PVR	Pulmonary Vascular Ressistance
PW	Posterior Wall Thickness
Rac	a subfamily of the Rho family of GTPases
Real-Time PCR	quantitative Polymerase Chain Reaction
RNA	Rybonucleic Acid
ROCK	intracellular-signaling serine threonine kinases that bind to Rho GTP-binding proteins.
Ror2	Receptor like tyrosine kinase
ROS	Reactive Oxygen Species
ROX	Real-Time PCR Passive Reference Dye
RT	Reverse transcriptase
RTK	Receptor Tyrosine Kinase
RV	Right Ventricle
RVSP	Right Ventricular Systolic Pressure
Ryk	Receptor like tyrosine kinase
S	Serine
SDS	Sodium Dodecyl Sulfate
SDS-PAGE	Sodium Dodecyl Sulfate PolyAcrylamide Gel Elepctrophoresis
sFRP-1	secreted Frizzled Related Protein 1
SM	Smooth Muscle
SMC	Smooth Muscle Cells
SPH	Secondary Pulmonary Hypertension

SYBR Green	asymmetrical cyanine dye used as a nucleic acid stain in molecular biology
TAE	Tris base, acetic acid and EDTA buffer
TBS	Tris Buffered Saline
TBST	Tris Buffered Saline + Tween 20
TCA	Trichloroacetic acid
TCF	T-Cell Factor
TEMED	Tetramethylethylenediamine
TN-C	Tenascin - C
UTR	Untranslated Region
VEGF	Vascular Endothelial Growht Factor
VSMC	Vascular Smooth Muscle Cells
Wnt	combined as a combination of Wg (wingless) and Int
WT	Wild Type
Xgal	bromo-chloro-indolyl-galactopyranoside
Y	Tyrosine

1. Introduction

1.1. Pulmonary Hypertension

1.1.1. Definition and research history of Pulmonary Hypertension

Pulmonary Hypertension (PH) is a progressive disorder of the pulmonary circulation, which is naturally a low-pressure system with high-flow. This rare disease (1) is characterized by progressive and sustained elevation of the pulmonary arterial pressure (PAP) with increased pulmonary vascular resistance (PVR). As a consequence it leads to increased right ventricle afterload followed by heart failure and death (2). PH is a rare and fatal disease with a yearly incidence around 2-3 cases per million (3) with a median survival of approximately 2.8 years after diagnosis (3,4).

Research on Pulmonary Hypertension spans over 100 years and since the observation of the first case described as "pulmonary vascular sclerosis" by Ernst Romberg in 1891 (5) our understanding of this disease has progressed and changed dramatically. The modern understanding of PH started with the development of pulmonary catheterization in the 1940s (6), which began a new era of research in this field and helped with determination of many important factors for future disease classification. Since that time multiple pathophysiological mechanisms of Pulmonary Hypertension had been identified and multiple therapies based on animal models and human studies had been developed. Although there is no final cure for PH many therapeutical strategies shows improvement in survival and quality of life of PAH patients.

1.1.2. Classification of Pulmonary Hypertension

Clinically pulmonary hypertension is defined by mean pulmonary arterial pressure (PAP) more than 25mm Hg at rest or more than 30mm Hg with exercise (7). As a disease associated with a diverse etiology, classification of pulmonary hypertension is essential in order to facilitate the diagnosis. The initial classification system was demonstrated during the first Pulmonary Hypertension international meeting held at The World Health Organization Symposium in 1973 (7). At that time PH was classified into 2 categories: Primary Pulmonary Hypertension (PPH) or Secondary Pulmonary Hypertension (SPH) depending on the absence or the presence of identifiable causes or risk factors respectively (7,8). In 1998 in Evian, France, a new classification system for pulmonary hypertension was developed (9). The aim of the ''Evian classification'' was defined to individualise categories sharing similarities in

pathophysiological mechanisms, clinical presentation and therapeutic options (10). This was a much broader, more precise classification, with 5 major categories; pulmonary arterial hypertension (PAH), pulmonary venous hypertension (PVH), PH associated with disorders of the respiratory system or hypoxemia, PH caused by thrombotic or embolic diseases, and PH caused by diseases affecting the pulmonary vasculature. The new classification allowed investigators to conduct clinical trials in a well-defined group of patients with a shared underlying pathogenesis. The 3rd World Symposium revised the "Evian classification" where modest changes were made. The most prominent alteration was to change the well accepted term in the literature Primary Pulmonary Hypertension used initially by Dresdale in 1951 (11) and replace it with Idiopathic Pulmonary Hypertension (IPAH). The current classification of Pulmonary Hypertension (12) was prepared during the 4th World Symposium on PH in Dana Point, California in 2008 to reflect recent publications as well as to address areas of research that remain unclear. The new classification still retains the general idea and structure of the "Evian classification" (Table 1.1). In addition, the New York Heart Association (NYHA) functional classification was prepared for heart diseases (13) to allow comparisons of patients with respect to the clinical severity of the disease process (Table 1.2).

Table 1.1. Clinical Classification of Pulmonary Hypertension (Dana Point, 2008)

1. Pulmonary arterial hypertension (PAH)

1.1. Idiopathic PAH
1.2. Heritable
  1.2.1. BMPR2
  1.2.2. ALK1, endoglin (with or without hereditary hemorrhagic telangiectasia)
  1.2.3. Unknown
1.3. Drug- and toxin-induced
1.4. Associated with
  1.4.1. Connective tissue diseases
  1.4.2. HIV infection
  1.4.3. Portal hypertension
  1.4.4. Congenital heart diseases
  1.4.5. Schistosomiasis
  1.4.6. Chronic hemolytic anemia
1.5 Persistent pulmonary hypertension of the newborn
1.6 Pulmonary veno-occlusive disease (PVOD) and/or pulmonary capillary hemangiomatosis (PCH)

2. Pulmonary hypertension owing to left heart disease

2.1. Systolic dysfunction
2.2. Diastolic dysfunction
2.3. Valvular disease

3. Pulmonary hypertension owing to lung diseases and/or hypoxia

3.1. Chronic obstructive pulmonary disease
3.2. Interstitial lung disease
3.3. Other pulmonary diseases with mixed restrictive and obstructive pattern
3.4. Sleep-disordered breathing
3.5. Alveolar hypoventilation disorders
3.6. Chronic exposure to high altitude
3.7. Developmental abnormalities

4. Chronic thromboembolic pulmonary hypertension (CTEPH)

5. Pulmonary hypertension with unclear multifactorial mechanisms

5.1. Hematologic disorders: myeloproliferative disorders, splenectomy
5.2. Systemic disorders: sarcoidosis, pulmonary Langerhans cell histiocytosis: lymphangioleiomyomatosis, neurofibromatosis, vasculitis
5.3. Metabolic disorders: glycogen storage disease, Gaucher disease, thyroid disorders
5.4. Others: tumoral obstruction, fibrosing mediastinitis, chronic renal failure on dialysis

Table 1.2. WHO functional classification of pulmonary hypertension

Class	Description
I	Patients with pulmonary hypertension but without resulting limitation of physical activity. Ordinary physical activity does not cause undue dyspnea or fatigue, chest pain or near syncope.
II	Patients with pulmonary hypertension resulting in slight limitation of physical activity. They are comfortable at rest. Ordinary physical activity causes undue dyspnea or fatigue, chest pain or near syncope.
III	Patients with pulmonary hypertension resulting in marked limitation of physical activity. They are comfortable at rest. Less than ordinary physical activity causes undue dyspnea or fatigue, chest pain or near syncope.
IV	Patients with pulmonary hypertension with inability to carry out any physical activity without symptoms. These patients manifest signs of right heart failure. Dyspnea and/or fatigue may even be present at rest. Discomfort is increased by any physical activity.

1.1.3. **Pathogenesis of Pulmonary Arterial Hypertension**

Pathogenesis of Pulmonary Arterial Hypertension is complex and it is unlikely to explain that one single factor causes all types of PAH. Increased PAP caused by increased Pulmonary Vascular Resistance (PVR) is the main PAH recognition marker. An increase in vascular resistance in PAH is caused by a series of physiological events many of which are likely due to a combination of pulmonary vasoconstriction, remodeling of the pulmonary artery wall and *in situ* thrombosis (Figure 1.1.). However now it is believed that pulmonary arterial obstruction by abnormal vascular proliferation is the hallmark of PAH pathogenesis (14).

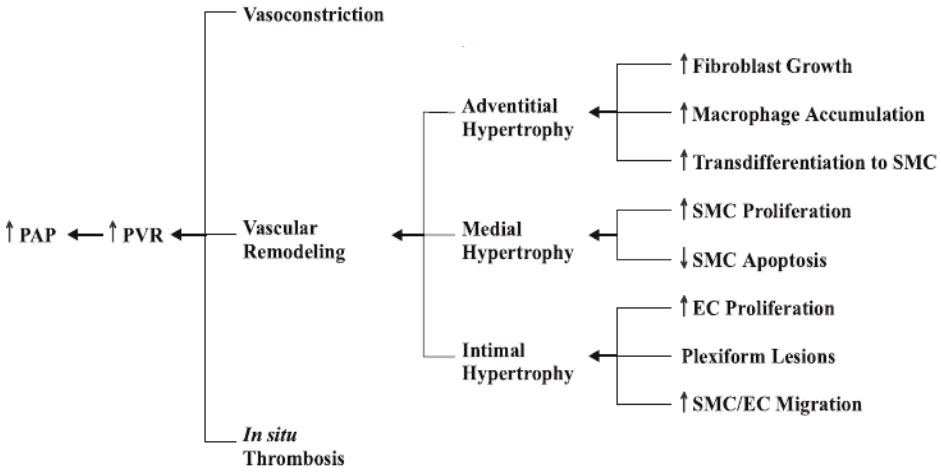

Figure 1.1. Scheme of series of events governing pathology of PAH (Modified from Mandegar et al. 2004) (15)

1.1.3.1 Pulmonary vasoconstriction

Pulmonary vasoconstriction defined as narrowing of the lumen of the vessel is one of the main contributing factors in the pathology of PAH. Sustained pulmonary vasoconstriction in PAH is mediated by various clinical vasoactive therapies like nitric oxide (NO) and prostacyclin (PGI) administration or inhibition of Endothelin-1 (ET-1) signaling pathway. Causes of pulmonary vasoconstriction in PAH are yet to be fully understood although endothelial dysfunction or hypoxia are two of the major factors that are involved in PAH pathogenesis could contribute to the functional changes. Impairment of the endothelial cell layer can results in an imbalance of vasoactive agents like NO, PGI, ET-1 and growth factors which regulate the physical and biochemical poperties of the vessels (1,16). Elevated PAP and ensuing vasoconstriction can influence pulmonary arterial smooth muscle cells (PASMC) hypertrophy and hyperplasia (17). Another major mechanism inducing narrowing of the vessels is hypoxia. Hypoxic Pulmonary Vasoconstriction (HPV) is an adaptive mechanism, unique to the lungs, believed to be major culprit in high- attitude PH (15). Hypoxia has been shown to induce vasoconstriction in isolated pulmonary arteries (18) and to cause contraction in isolated cultured PASMC (19). These observations indicate that sustained pulmonary vasoconstriction is an important contributor to the elevated PVR and PAP in some cases of PAH.

1.1.3.2 Pulmonary artery wall remodeling

The normal pulmonary artery is a compliant structure with few muscle fibres, which allows the pulmonary vascular bed to function as a high-flow, low-pressure circuit. The vascular histopathological features of pulmonary arteries in PAH are: intimal thickening and hyperplasia, medial hypertrophy, adventitial thickening (Figure 1.2. A) and in-situ thrombosis (18). In most cases of PAH a unique structure reffered to as a plexiform lesion is formed (Figure 1.2. B) (18). The pathological diagnosis of pulmonary vascular remodeling depends on the histological assessment of the cellular composition of pulmonary vascular walls, which if abnormal, are described as pulmonary vascular ‘lesions’. The functional status of the pulmonary circulation and the level of pulmonary vascular resistance and pulmonary artery pressure ultimately determine the outcome and treatment of patients with PH (19).

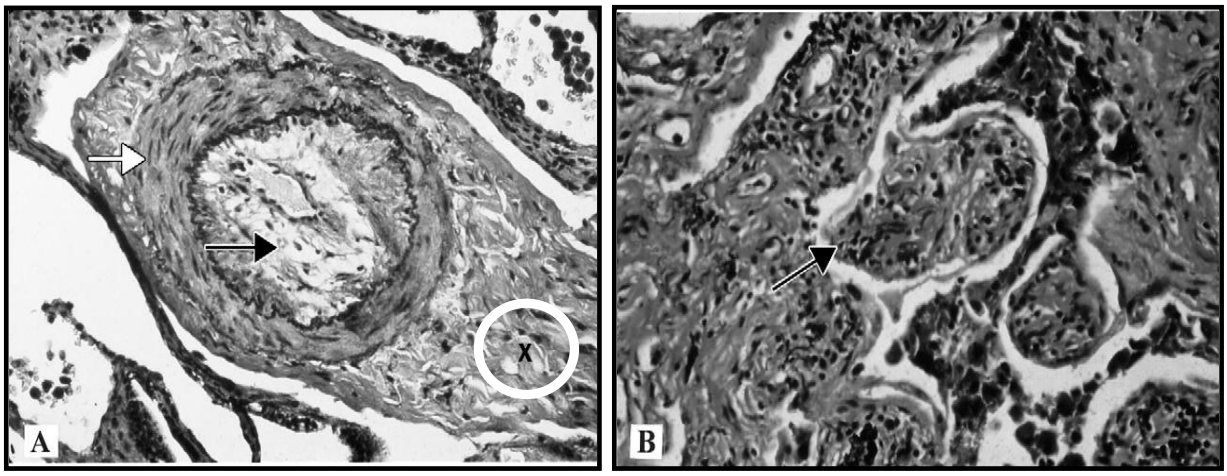

Figure 1.2. Characteristic histopathology of pulmonary arteries in PAH A. Muscular pulmonary artery from a PPH patient with medial hypertrophy (white arrow), luminal narrowing by intimal proliferation (black arrow), and proliferation of adventitia (X in white circle). **B.** Characteristic plexiform lesion from an obstructed muscular pulmonary artery (black arrow). (Adapted from Gaine et al. 1998)

1.1.3.2.1 Intima lesions

Intimal lesions account for most of the reduction of luminal area of small pulmonary arteries and potentially influence the overall pulmonary vascular resistance. Intimal lesions consist of eccentric intima thickening, and fibrotic, concentric plexiform lesions (19).

Intima thickening: Due to migration and proliferation of smooth muscle (SM) like cells (SMC, fibroblasts and myofibroblasts) into the intima layer (Figure 1.2. A) (20). These changes may be concentric laminar, eccentric or concentric non-laminar. More advanced lesions acquire a 'fibrotic' pattern, with interspersed myofibroblasts and marked accumulation of mucopolyssacharides (19) becoming acellular with abundant extracellular matrix deposition.

Plexiform lesions: (Figure 1.2. B) Are typically located at branching point of muscular arteries (22), consists of a network of vascular channels lined up by focal proliferation of endothelial cells (23) and a core of myofibroblastic or less well-differentiated cells (24) with an increase in connective tissue matrix.

1.1.3.2.2 Medial vascular remodeling

Medial hypertrophy (Figure 1.2. A) is a characteristic pathologic feature of PAH that involves muscularized arteries (ranging between 70 and 500 μm in diameter), and precapillary vessels (below 70 μm in diameter) (19). The increase in the cross sectional area of the media of pulmonary arteries is due to both hypertrophy and hyperplasia of smooth muscle fibers

with a simultaneous decrease in the state of apoptosis rate as well as an increase in connective tissue matrix and elastic fibers in the media of muscular arteries (21). The medial layer represents approximately 10-15% of the outside diameter of the normal muscularized pulmonary arteries, and 30–60% of the outside diameter in vessels of IPAH lungs (25,26). It is well established that medial layer hypertrophy is most prominent in IPAH cases. Smooth muscle cells proliferation and medial hypertrophy is one of a major focus of this dissertation.

1.1.3.2.3 Adventitial remodeling

The adventitial layer surrounding the blood vessels has long been exclusively considered as a supporting tissue with main function to provide structural support to the medial layer. Thickening of the adventitia (Figure 1.2. A) is primarily due to adventitial fibroblast proliferation and extracellular matrix deposition (19). Already existing hypothesis in the field is that in response to various inducing factors such as hypoxia or vascular distension, a heterogenous cell population is activated. This compartment can be considered as the main "injury sensing tissue" of pulmonary arteries in PAH. The response is more than just a fibroblast proliferation (27). Now in the PH field, it is thought that the adventitial layer is a reservoir of multiple subpopulations of fibroblasts with a range of proliferation capacity consisting of recruited circulating monocytes, fibrocytes and resident progenitor cells that provide cells and molecules with the capacity to influence vascular remodeling in all of the layers of pulmonary arteries (27,28). Animal studies show that adventitial cells can differentiate into myofibroblasts (30), which can accumulate in the adventitia or migrate to the medial and further to the intimal layer influencing neointima formation (28,29).

1.1.3.3 *In situ* Thrombosis

Pulmonary arterial thrombosis is mainly caused by the dysregulation of the clotting cascade as well as a dysfunction of endothelial cells and platelets. Thrombotic lesions and platelet dysfunction are important processes in the development of PAH (31). Prothrombotic abnormalities have been demonstrated in PAH patients (32) and thrombi are present in both microcirculation and elastic pulmonary arteries (33). Moreover fibrinopeptide A levels that reflect thrombin activity (34) and Thromboxane A2 levels (inducer of platelet aggregation) (35) are both elevated in patients with IPAH. In addition to Thromboxane A2 other procoagulant, vasoactive and mitogenic agents factors are released from platelets like serotonin, PDGF and TGFβ, which may contribute to thrombin and clot generation. Although,

thrombotic lesions in pulmonary arteries have never been correlated with the severity of PH, the studies have shown that in all forms of severe PH, thrombotic lesions could be found in pulmonary arteries (36). However, it remains unclear if thrombosis and platelet dysfunction are a cause or result of PH (1, 31).

1.1.4. **Cellular crosstalk in vascular remodeling of PAH**

Under normal conditions the thickness and tissue mass of pulmonary arteries are maintained by keeping the balance between proliferation and apoptosis of fibroblasts, pulmonary artery smooth muscle cells and pulmonary arterial endothelial cells. An imbalance favoring proliferation of cells leads to thickening of PA wall, narrowing and eventual obliteration of the vessel lumen and finally to an increase in PVR and PAP (15).

Vascular cells constantly interact keeping homeostasis within the wall of the pulmonary artery. Each cell type (endothelial, smooth muscle, and fibroblast) in the pulmonary vascular wall plays a specific role in the response to injury in PAH (1,14). The mechanism of medial SMC hyperplasia is potentially one of the most important in human iPAH and it remains unclear whether hyperplasia results from inherent dysfunction of PASMCs or from an imbalance between proliferation and apoptosis that governs the PASMC growth coming from signals originating from the injured endothelial cells (37,38).

Endothelial cells (ECs) are recognized as major regulators of vascular function, and in response to hypoxia, shear stress, inflammation, drugs or toxins that affect endothelial homeostasis. This affects vascular tone, but also promotes vascular remodeling. Paracrine crosstalk between PAEC and PASMCs tested *in vitro* demonstrated clearly that exposure of PASMCs to culture medium from PAECs induces PASMC proliferation (39). This effect was exaggerated when PAECs were isolated from patients with PAH.

Medial SMC are thought to interact also with adventitial fibroblasts (AF) (37). Several interesting findings from animal models also support this concept. For instance, adventitial fibroblasts are activated rapidly in response to pathological stimuli. An early marker of AF activation in response to stress is increase in reactive oxygen species (ROS) particularly superoxide (27). Increased superoxide can have direct effects on neighboring SMC to increase their contraction (40). Moreover AF in response to ROS and other microenvironmental stimuli are capable of releasing a number of mediators such as ET-1, PDGF, EGF (27) that potentially affect SMCs as well as general vascular tone. In response to injury, fibroblasts dramatically change the production of extracellular matrix molecules (ECM) and a marked increase in collagen production and elastin are observed in the adventitia during the

development of pulmonary hypertension (41). Marked increase in the accumulation of fibronectin, tenascin-C (TN-C), and elastin in the adventitial compartment of models of hypoxia-induced pulmonary hypertension have been observed (42). Fibronectin appears to play a critical role in facilitating the proliferation of fibroblasts as well as in their differentiation into myofibroblasts (43). Tenascin-C (TN-C) expression has been shown to be upregulated in pulmonary hypertensive vessels (44-45). TN-C, like fibronectin, is associated with fibroblast and SMC proliferation.

1.1.5. **Molecular mediators of vascular remodeling in PAH**

1.1.5.1 Vascular tone mediators and regulators

Prostacyclin and NO. Impaired endothelium-derived vasodilation is one of the most studied mechanism in pulmonary hypertension. Prostacyclin is a strong vasodilator produced by cyclooxygenase metabolism of arachidonic acid. Prostacyclin also exhibits anti-proliferative effects on vascular smooth muscle cells and anti-aggregative effect on platelets. Prostacyclin synthesis is decreased in endothelial cells from PAH patients. Analysis of urinary metabolites of prostacyclin demonstrated a decrease in the amount of excreted 6-ketoprostaglandin F1α, a stable metabolite of prostacyclin, in patients with idiopathic PAH (46). Moreover, pulmonary endothelial cells of PAH patients are characterized by reduced expression of prostacyclin synthase (47). In addition, PGI_2-receptor knockout mice develop more severe hypoxia-induced pulmonary hypertension (PH) (48). While PGI_2-overexpressing mice are protected against hypoxia-induced PH (49) supporting a significant role for a PGI_2 in PH.

Nitric oxide (NO) signaling is mediated mainly by the guanylate cyclase/cyclic guanosine monophosphate (cGMP) pathway. NO is synthesized mainly by endothelial NO synthase (eNOS) which is significantly decreased in the ECs of the pulmonary circulation from PAH patients (50), and is a vasodilator and suppressor of SMC proliferation. In PAH a reduction in NO is thought to be related to high arginase levels (51) because l-arginine, the substrate of NO synthase, is required to produce NO (52). Degradation of the second messenger of NO, cGMP, by phosphodiesterases is mainly accomplished by phosphodiesterase-5 (PDE5) which is also upregulated in PAH patients.

Endothelin-1 (ET-1) is a potent vasoconstrictor studied for many years as one of the main targets for PAH therapy mainly due to increase in levels of lung and circulating ET-1 in patients with pulmonary hypertension of various etiologies (53). Besides its vasoconstrictive function ET-1 can also be a potent mitogenic factor. The proliferative action of ET-1 is

mainly transduced by two subtypes of Endothelin Receptors A and B (ETRA, ETRB) possibly through early activation of p42/p44 isoforms of mitogen-activated protein kinase (MAPK) (1,14). Both ET-1 receptors are found in SMCs of blood vessels, and can mediate vasoconstriction, but ETRB on ECs may mediate vasodilatation and endothelin clearance particularly in microvessels (52). Studies in rats with hypoxia-induced PH (54), coupled with clinical studies both document an increase in expression of endothelin in the lungs of patients with PAH (52,53).

Potassium channels. Potassium channels are tetrameric, membrane-spanning proteins that selectively conduct potassium at near diffusion-limited rates. The classical function of K^+ channels is the regulation of membrane potential and vascular tone. PASMCs express voltage-gated (Kv) channels, which had recently been considered to participate in vascular remodeling by regulating cell proliferation and apoptosis (58). The selective loss of these Kv channels leads to pulmonary artery smooth muscle cell depolarization, an increase in the intracellular calcium, and both vasoconstriction and cell proliferation. Microarray studies have shown that Kv channel genes are downregulated in PAH lungs (55). Kv1.5 is downregulated in pulmonary artery smooth muscle cells in humans with PAH (56), and both Kv1.5 and Kv2.1 subunits are downregulated in rats with chronic hypoxia-induced pulmonary hypertension (57).

1.1.5.2 Pro-proliferative mediators

Recently vascular remodeling has been considered as pseudo-malignant disorder and mediators from cancer research has been described as targets for therapeutic interventions for PAH. Therapies against mitogenic factors (PDGF-BB, EGF FGF2, survivin) are extremely effective on not only normalize physiological parameters of PAH such as PAP and the RVSP but also reverse vascular remodeling in the animal models of PH.

Survivin. A member of the family of inhibitor of apoptosis proteins (IAP) is a key regulator of mitosis and programmed cell death. In PAH, survivin was found to be exclusively expressed in remodeled PA from PAH patients (59) suggesting its importance in vascular remodeling. In addition, gene therapy using adenoviral vectors carrying phosphorylation deficient survivin reversed monocrotaline-induced PAH in rats by lowering PVR, RV hypertrophy, induction of PASMC apoptosis and inhibition of PASMC proliferation. The opposite effects were observed for gene therapy using WT survivin (59).

Nuclear factor of activated T cells (NFAT). The current and recent findings suggest that the NFAT–Kv channel–mitochondria axis regulates ionic and metabolic remodeling and apoptosis under diverse conditions ranging from vascular disease and myocardial hypertrophy to cancer. NFAT a calcium/calcineurin sensitive transcription factor has recently been implicated in PAH pathogenesis. Increased activation of NFATc was observed in human remodeled pulmonary arteries as well as in human IPAH PASMCs. Inhibition of NFATc by cyclosporine A reversed the downregulation of potassium chanels, inhibited apoptosis and decreased proliferation of vascular cells in MCT-induced PAH by an as yet not fully understood mechanism (153) which makes NFAT a very promising therapeutical target for PAH treatment.

PDGF-BB. Platelet-derived growth factor (PDGF) signaling has been implicated in many proliferatory diseases. PDGFs are a family of ligands inducing a mitogenic response through tyrosine kinase receptors, PDGFRα and β, known to be involved in cancer (61). PDGF induces the proliferation and migration of SMCs and fibroblasts and is proposed as a key mediator in the progression of vascular diseases such as atherosclerosis and PH (62-63). PDGF plays an important part of the progression of experimental pulmonary hypertension, but its role and effective downstream signaling pathway in human pulmonary arterial hypertension is only partly elucidated (61). Schermuly et al. in 2005 (64) presented the importance of PDGF signaling in the development of pulmonary vascular remodeling of PH. In addition to reporting PDGF signaling being highly disregulated in two animal models as well as in PAH patients this particular study was a milestone in developing anti-malignant therapy against PAH through blockade of PDGF signaling. Subsequently an increase in PDGF-BB and PDGF receptors has been reported in the pulmonary arteries of patients with pulmonary arterial hypertension where PDGF induces proliferation and migration of human pulmonary artery smooth muscle cells (65). These results taken together strengthen the concept that PDGF signaling is overactive in PAH and has a crucial role in the vascular remodeling processes of PAH.

Other growth factors such as epidermal growth factor (EGF) (66), fibroblast growth factor -2 (FGF2) (67) and transforming growth factor β (TGFβ) (60,67) were also implicated recently in the development of the pulmonary vascular remodeling.

EGF signaling is disregulated in monocrotaline-induced PAH in rats. In PAH patients, EGF colocalizes with TN-C in vascular lesions suggesting its crucial role in disease progression (68). Most interestingly, inhibition *in vitro* and in organ culture of EGF signaling results in an increase in SMCs apoptosis and a decrease of SMCs proliferation which suggests that EGF

signaling alone or in connection to serine elastase activity or extracellular matrix remodeling releasing active growth factor and inducing matrix metalloproteinases (MMPs) plays a role in PAH pathogenesis (69-72).

Recent studies demonstrate that **FGF2 signaling** contributes to the the human as well as the rodent disease progression (67). FGF2 is mainly described as endothelial derived factor based on *in situ* hybridization study which identified FGF2 overproduction in remodeled vascular endothelium of lungs from patients with PAH. The level of FGF2 was significantly increased in the medium of PAH isolated endothelial cells. Finally inhibition of FGF2 signaling reversed established PH in a rat model suggesting this factor as very promising target for future treatments against pulmonary hypertension.

Transforming growth factor β (TGFβ) signaling also contributes to the progression of vascular remodeling in PAH patients. Alterations in two TGFβ signaling pathways, bone morphogenetic protein receptor II (BMPR2) and TGFβ receptor I are linked to the pathogenesis of PAH. Genetic studies of familial PAH (FPAH) revealed that 80% of FPAH patients posses a germline mutation in one copy of BMPR2 (73-74). Although results may vary, an increase in TGFβ signaling in PH seems to be the case since inhibition of this TGF β receptor I signaling results in blockade of MCT-induced PAH progression in rats (74).

1.1.6. **Pharmacological treatment of PAH**

Pulmonary Hypertension is a disease associated with a very poor prognosis and up to now there is no therapy available to completely reverse this disease. Although there is no final cure for PH, many therapeutical strategies shows improvement in survival and quality of life of PAH patients. In the early phase of treatment conventional therapies are used such as oral anticoagulant application (warfarin) which proved to be effective in improving survival from 21 to 49% (79-80), duretics and low-flow supplemental oxygen therapy (75-77). In the last two decades considerable increase of clinical interest in this disease was observed and simultaneously large amount of experimental work has been performed in labs and clinics to understand the basic pathogenesis of PAH which has evolved to several therapies. Current treatments of PH target mainly aspects of vasoconstriction and vascular remodeling (78-79). Nevertheless, therapies targeting vasodilation are considered the most effective for now. The main purpose of vasodilatory treatment is to decrease PAP and reduce right ventricle afterload. There are now three classes of medications with vasodilatory effect and those are prostanoids, endothelin receptor antagonists and PDE5 inhibitors (79) that have shown

efficacy in the treatment of PH focusing on three major pathways involved in abnormal proliferation and contraction of PASMCs in PAH (Figure 1.3.).

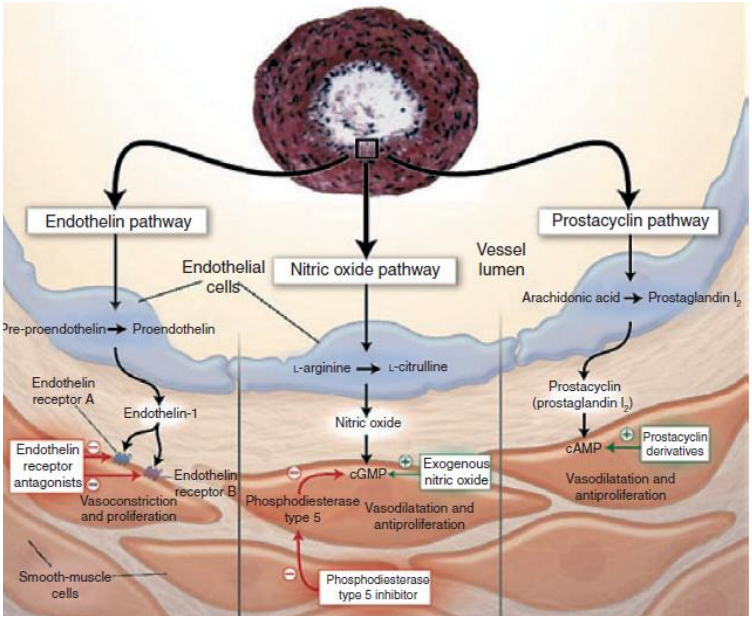

Figure 1.3. Scheme representing three signaling pathways which are main targets for existing therapeutical strategies in Pulmonary Hypertension focusing on vasodilation (adapted from Lee SH and Rubin LJ 2005)

Prostacyclin pathway. To target this signaling pathway prostacyclin analogues are used in the treatment of PAH patients. The main disadvantage of prostacyclins is the extremely short half-life of these compounds. The first successful study using continuous intravenous prostacyclin (epoprostenol) (81) led to the development of prostacyclins with improved stability. Due to this study new compounds (prostacyclin analogues) and new method of its administration were developed such as iloprost – intravenous and inhaled (82), beraprost – oral (83) and the most stable (up to 4,5hrs) treprostinil- oral, inhaled (84).

NO pathway. Inhaled NO proved to be effective in decreasing PAP but due to its extreme side effects it is not considered as main therapy and requires improvement. Alternative methods to target this pathway (Figure 1.3.) are phosphodiesterase 5 inhibitors (sildenafil citrate), which thus far demonstrated significant improvements in PAH patients (85).

The Endothelin pathway is important pathway in PAH and endothelin receptor antagonists are used for treatment of PAH. Two therapies are now available targeting these receptors using dual endothelial receptor A and B antagonist Bosentan (86) and single endothelial receptor A antagonists Sitaxentan (87-88) and Ambrisentan. Since endothelin binding to

receptor A has been described in vascular remodeling process (78) a selective inhibitior of endothelin receptor A may have advantages over non-selective inhibition of both receptors.

All of the compounds mentioned above have proven to be effective by improving hemodynamics, exercise capacity and provide small increements in survival in PAH patients (78). The main problem of therapies targeting vasodilation is that asides from providing relief to the patients, they fail to reverse the disease process and therefore the focus of treatment in recent years has changed from vasodilators to anti-proliferative agents and new treatments are needed.

Tyrosine Kinase Inhibitors. Reversal of lung vascular remodeling rather than prolonged vasodilation is the concept underlying the use of RTKs inhibitors in pulmonary hypertension. Most promising drug to reverse vascular remodeling in PAH is Imatinib Mesylate (Gleevec=STI571) a drug already approved to treat Chronic Myelogenous Leukemia (CML) and gastrointestinal stromal tumors. Imatinib is a selective inhibitor of RTK c-kit, BCR-ABL and PDGFRβ. RTKs like PDGFR have already been implicated to play an important role in PAH in humans as well as in PH animal models. The role of PDGF signaling inhibition by Imatinib in hypoxia and monocrotaline induced PH on vascular remodeling has been shown recently (61) (Figure 1.4.). The molecular mechanisms of Imatinib besides preventing PDGFRβ phosphorylation and ERK dephosphorylation (64) however remain undefined and needs to be clarified.

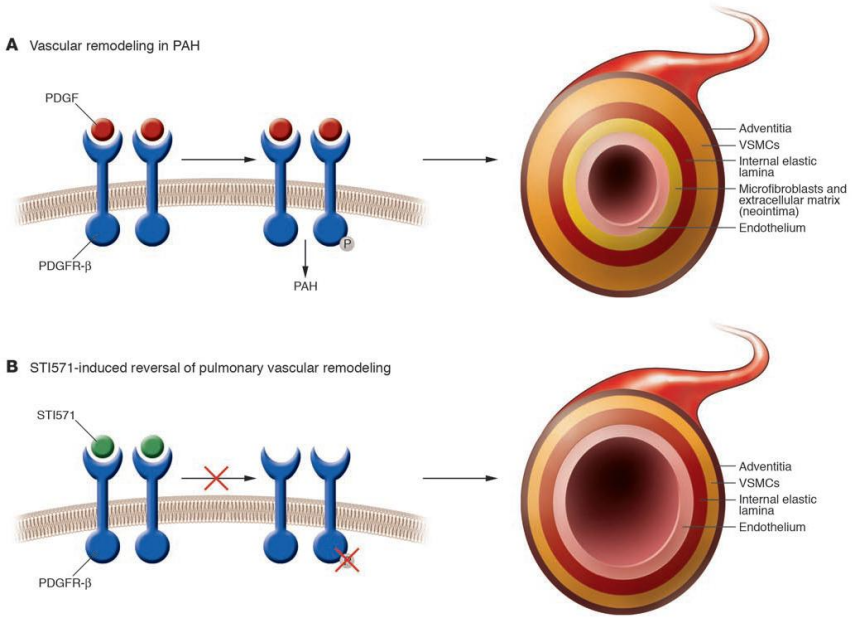

Figure 1.4. Schematic molecular mechanism of reversing vascular remodeling in PH by Imatinib mesylate a potent PDGFR inhibitor (Adapted from Barst R 2005)

In 2005, Imatinib was first used by Dr. Ghofrani (89) for compassionate cases. This effort provided evidence for Imatinib with regard to PAH regression. Phase III randomized controlled trials with tyrosine kinase inhibitors in PAH are expected to begin soon (90).

Other tyrosine kinase inhibitors like EGFR (Iressa) or multiple kinase inhibitor Sorafenib are also promising for future treatment of PAH. Sorafenib and Iressa already proved to be effective in the regression of PAH in animal models (66,91). These and other findings presenting PAH as a pseudomalignant disease open the new possibility for researchers to target signaling pathways previously implicated in cancer research governing uncontrolled proliferation (92-93). Another possible interesting pathway for further investigation in PAH is the Wnt signaling pathway that plays a crucial role in development and cancerous diseases and should be further investigated in the disease of PAH (92).

1.2. **Cardiac remodeling**

Cardiac enlargement refers to an increase in the size of the heart, which can occur eighter through hypertrophy, or dilation of the heart but occasionally occurring in concert. Cardiac hypertrophy is a thickening of the heart muscle (myocardium), which results in a decrease in the size of the chamber of the heart, including the left and right ventricles. Dilation involves an increase in the size of the inside cavity of a chamber of the heart. Hypertrophy, or thickening of the heart muscle occurs in response to increased stress on the heart leads to an increase in the workload of the heart or under conditions stimulating myocyte growth. Hypertrophy typically involves one of the ventricles. The increase in heart size reduces the elevated ventricular wall stress and/or compensates for the increased hemodynamic demand. Therefore, normal physiological conditions, e.g. physical exercise, induce hypertrophy of the heart. Unlike physiological hypertrophy, pathological stimuli like arterial hypertension lead to interstitial fibrosis and expression of genes associated with hypertrophy. These changes ultimately lead to myocardial stiffness and a decrease in cardiac output followed by possible heart failure (157). High blood pressure, or hypertension, is the most frequent cause of left ventricular hypertrophy. The most common causes of right ventricular hypertrophy are diseases that damage the lung like primary pulmonary hypertension or emphysema.

1.2.1. **Right heart failure in PAH**

Right heart failure is a direct cause of death in most of PAH patients. In PAH, development of right ventricular (RV) hypertrophy and an increase in right ventricle systolic pressure is associated directly with pulmonary vasculopathy and increased pulmonary vascular resistance (158). The RV is thinner than the LV with a slightly different shape. This is a major explanation for the low pressure in the pulmonary circulation and enables a quick adaptation to changes in preload. Increased wall stress caused by high PAP in PAH leads to RV adaptation, an increase in wall thickness by accumulation of muscle mass (158). RV hypertrophy is the result of an increase in protein synthesis due to stretch and its enhancement through autocrine and paracrine influences in cardiac cells (myocytes, fibroblasts and endothelial cells) (159). Pressure induced growth of cardiomyocytes is also associated with an increase in ECM synthesis and growth of supporting vessels (158). Interconnecting individual myocytes, myofibrils, muscle fibers of abnormal ECM production is likely to influence diastolic and systolic function as well as the size and shape of the ventricle (160-161). Adaptation of the RV to pressure overload does not last long and ultimately the cardiac contractile force decreases and the RV dilates. During the development of cardiac hypertrophy, a mismatch between the number of capillaries and the size of cardiomyocytes can lead to myocardial hypoxia, contractile dysfunction and apoptosis (162). Sano et al. (163) showed that the development of systolic dysfunction is associated with decreased number of microvessels. In monocrotaline induced-PAH chronic RV overload associates with decreased capillary density and decreased VEGF expression while opposite phenomenon was observed in chronic hypoxic-induced PH (164).

1.2.2. **Left ventricular remodeling**

The concept that enlargement of left ventricle can affect function of the right ventricle was advanced in 1910 (254). It is now recognized that the most common cause of pulmonary hypertension is that associated with left ventricular failure. Reeves and Groves (255) reported that 44% of patients with coronary artery disease at the time of coronary arteriography and right heart catheterization have pulmonary hypertension. Current classification of Pulmonary Hypertension formed at Dana Point, California in 2008 shows that PH owing to left heart disease consist of a very prominent group of patients comparing to other forms of PH (12).

Right ventricular dysfunction can develop in association with left ventricular dysfunction via multiple mechanisms: (1.) left ventricular failure increases afterload by increasing pulmonary venous and ultimately pulmonary arterial pressure, partly as a

protective mechanism against pulmonary edema; (2.) the same cardiomyopathic process can simultaneously affect the right ventricle; (3.) myocardial ischemia can involve both ventricles; (4.) left ventricular dysfunction can lead to decreased systolic driving pressure of right ventricular coronary perfusion, which may be a significant determinant of right ventricular function; (5.) ventricular interdependence due to septal dysfunction may occur; and (6.) left ventricular dilation in a limited pericardial compartment may restrict right ventricular diastolic function (256). 90% of patients with heart failure develop this disease on the basis of ischemic and/or hypertensive heart disease. Ischemic heart failure is the result of one or several infarcts resulting in regional loss of contractile force and compensatory growth of the remaining myocardium. Cardiac contraction depends on left ventricular (LV) geometry and contractile mass. Diastolic function is affected by the extent of LV wall hypertrophy and ventricular "stiffness", which are both affected by the degree of fibrosis. The term "left ventricular remodeling" summarizes the sequential changes following extensive cardiac damage finally leading to progressive loss of systolic function and heart dilation despite cardiomyocyte hypertrophy. Because of the multiple influences affecting right ventricular function due to left ventricular failure, right ventricular status may constitute a "common final pathway" in the progression of congestive heart failure and therefore may be a sensitive indicator of impending decompensation or poor prognosis (256).

1.3. **Wnt signaling pathway**

Wnt signaling pathway regulates numerous developmental processes and has been implicated in tissue homeostasis in adult organisms and disease. Based on studies in mice in addition to regulating development, the Wnt signaling pathway is also commonly altered in human cancers (94). The function of this signaling pathway has been the subject of investigation for more than 20 years and one conclusion from this work is that Wnts seem to activate more than one type of signaling pathway and govern cell proliferation, survival, differentiation, polarization, and migration by modulating both cellular and transcriptional events (94). Wnt molecules bind to main Wnt receptors Frizzled (Fzd) receptor/low density lipoprotein (LDL) receptor-related protein (LRP) co-receptor complex at the cell surface. To date the major signaling branches downstream of the Fzd receptor have been identified including a traditional and most studied canonical or Wnt/β-catenin pathway and the non-canonical or β-catenin-independent pathway (97) which can be divided into the Planar Cell Polarity (PCP) pathway and the Wnt/Ca^{2+} pathway (Figure 1.5.).

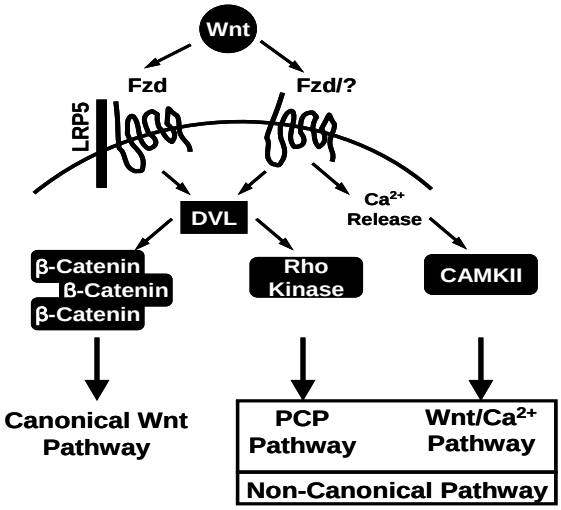

Figure 1.5. Scheme representing distinct Wnt signaling pathways. (author's scheme)

After binding of Wnt to the receptor complex, the signal is transduced to the cytoplasmic phosphoprotein Dishevelled (Dvl). At the level of Dvl, the Wnt signal branches into three major cascades, canonical, Planar Cell Polarity and Wnt/Ca^{2+}. Dishevelled (Dvl) is an important downstream component of Wnt transduction pathway and is the first cytoplasmic protein that is pivotally involved in all three major branches of Wnt signaling (Figure 1.5.) (99). However, it still remains unclear how Dvl protein regulates and channels signaling into each of these pathways (97).

1.3.1. **Wnt ligands**

Wnts ligands are highly conserved among species. In mammals, the complexity and specificity of Wnt signaling is initiated by 19 Wnt ligands, which are cysteine-rich glycoproteins of approximately 350–400 amino acids that contain an N-terminal signal peptide for secretion (95). Wnt ligands have only recently been characterized due to difficulties with purification because of complicated posttranslational modifications (glycosylation, lipidation and palmitoylation) (96). The First and most biochemically characterized of the Wnts is Wnt3A because of its efficient secretion contrary to other Wnt ligands (98). Wnt molecules are defined by the sequence and not by the function so that some Wnts tend to activate β-catenin signaling, others preferentially activate β-catenin independent pathways. For example, Wnt1, Wnt2, Wnt3, Wnt3a, Wnt6, Wnt7b and Wnt8 are often referred to as canonical β-catenin Wnts, whereas Wnt4, Wnt5a, Wntb and Wnt11 are considered non-canonical Wnts (100-102). New development are made every year to

determine Wnt molecules function and controversy are raising in the field as some Wnts can induce both canonical and non-canonical signals like Wnt3A, Wnt7a, Wnt7b and Wnt11 (103-106).

1.3.2. **Wnt receptors**

Each Wnt protein can activate distinct intracellular responses in a variety of experimental assays. The diversity of responses seen to different Wnt ligands is likely due, at least in part, to the repertoire of receptors present at the cell surface.

Frizzled receptors. Frizzled proteins range in length from about 500 to 700 amino acids. These proteins consist of three main regions: the amino terminus is predicted to be extracellular and contains cystein reach domain (CRD), which is the Wnt ligand binding domain. Further 7 hydrophobic domains classify these receptors to 7 pass-transmembrane receptors. Carboxy-terminal domain is an intracellular domain that has a different length and is not well conserved among different family members. The presence of the KTXXXW sequence is most probably involved in the determination of the downstream signaling pathway (Figure 1.6.) (129).

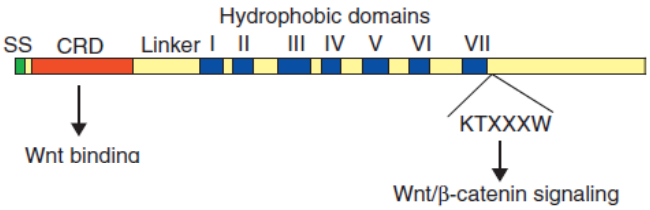

Figure 1.6. Motifs present in Frizzled proteins. (Adapted from Huang and Klein 2004)

The mammalian genome has 10 Fz genes, most of which have variable capacities to activate β-catenin signaling. The Fzd Receptors known to induce the canonical pathway are Fzd1 and 2. Fzd4 is known to induce non-canonical signaling (124). Although compelling evidence exists that Fzds act as a Wnt receptors, it is becoming clear that other cell surface and extracellular molecules also play crucial roles in the reception of Wnt signals and are important Fzd co-receptors. **Fzd co-receptors.** Most known Fzd co-receptors are the low density lipoprotein (LDL) receptor-related protein (LRP) in particular LRP5/6. The Fzd-LRP5/6 coreceptor complex demonstrates that a Wnt/Fzd complex is capable of recruiting LRP5/6 and activating the β-catenin pathway, consistent with the specific requirement of

LRP5/6 in canonical signaling (130). To date a better understanding of the non-canonical signaling will require the identification of newly discovered Ryk and Ror2 co-receptors (131).

1.3.3. **Canonical Wnt signaling**

The best understood Wnt signaling pathway is canonical signaling also called the Wnt/β-catenin pathway. It has been characterized by a combination of genetics and biochemistry. A hallmark of canonical Wnt pathway activation is the elevation of cytoplasmic β-catenin protein levels of the subsequent nuclear translocation and further affecting activation of β-catenin specific gene transcription (Figure 1.7.).

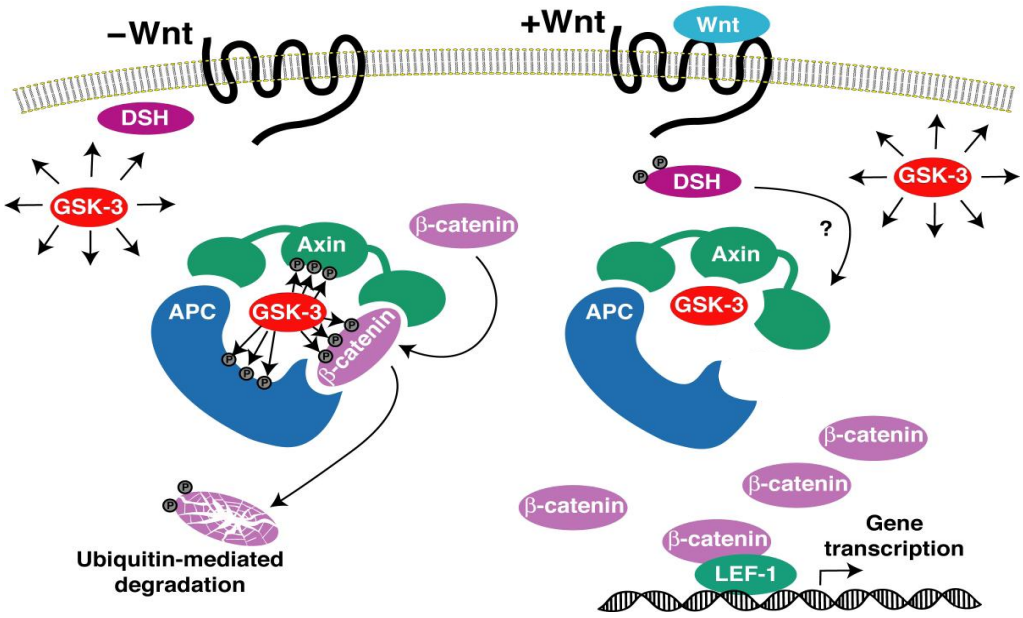

Figure 1.7. Scheme representing mechanisms of canonical Wnt signaling action within the cell. (Adapted from James R. Woodgett 2001)

In the absence of Wnt ligands, β-catenin is recruited into a 'destruction complex' that contains adenomatous polyposis coli (APC) and Axin, which facilitate the phosphorylation of β-catenin by glycogen synthase kinase 3 β (GSK3β). GSK3β phosphorylates the N-terminal domain of β-catenin, thereby targeting it for ubiquitylation and proteasomal degradation (94). So, in the so called 'canonical off state', cells maintain low cytoplasmic and nuclear levels of β-catenin, although β-catenin is associated with cadherins at the plasma membrane, an association that spares it from the degradative pathway (137). The binding of Wnt to Fzd leads to activation of the phosphoprotein Dvl. The Dvl recruits Axin and the destruction complex to the plasma membrane, where Axin directly binds to the cytoplasmic tail of LRP5/6. Axin is degraded, which decreases β-catenin degradation (138). The activation of Dvl also leads to the inhibition of GSK3β by phosphorylation at serine 9 residue, which

further reduces the phosphorylation and degradation of β-catenin. So-called 'canonical on state' involves increasing the post-translational stability of β-catenin, through Wnt dependent degradation of Axin and inhibition of GSK3β. As β-catenin levels rise and it accumulates in the nucleus, where it can interact with DNA bound TCF and LEF family members to activate the transcription of target genes (94).

Importantly GSK3β is a very important protein for canonical Wnt signaling but its disregulation can lead to alteration of multiple signaling pathways, which are also crucial for many hypertrophic, proproliferative and neurodegenerative diseases (138).

1.3.4. **GSK3β as Wnt-independent multi tasking kinase**

Glycogen synthase kinase 3 is a multifunctional serine/threonine kinase found in all eukaryotes. The enzyme is a key regulator of numerous signaling pathways, including cellular responses to Wnt, receptor tyrosine kinases and G-protein-coupled receptors and is involved in a wide range of cellular processes, ranging from glycogen metabolism to cell cycle regulation and proliferation (139). There are two mammalian GSK-3 isoforms encoded by distinct genes: GSK3α and GSK3β (Figure 1.8.) (140).

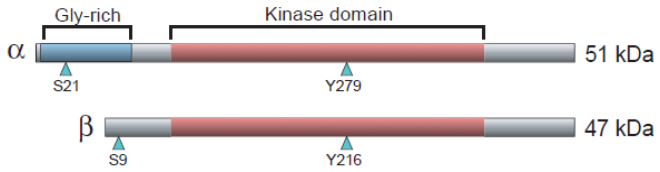

Figure 1.8. Scheme representing two isoforms of GSK3 of the mammalian genome. N-terminal Glycine rich domain α isoform is unique for the α isoform and the Kinase domain is present in both isoform. The main sites of phosphorylation are indicated by blue arrows. (adapted from Bradley W. et al 2003)

GSK3α and GSK3β are structurally similar but functionally extremely different. This became clear upon knocking-out of the GSK3β isoform in mice, which results in an embryonic lethal phenotype (141) suggesting great significance of the β isoform which unfortunately could not be rescued by the α isoform. GSK3β itself has two splice variants. Recently it was discovered that a minor (~15% of total) splice variant of GSK3β, GSK3β2 contains a 13-residue insert within the kinase domain (142). *In Vitro* analysis of these isoforms revealed that GSK3β2 has reduced activity towards the microtubule-associated protein tau, compared with shorter unspliced GSK3β. The difference also lays in the localization of these two splice variants to neuronal cell bodies in case of GSK3β2, unlike unspliced GSK3β, which has much wider spectrum of localization.

Apart from the crucial role of GSK3β in regulating β-Catenin translocation to the nucleus in the canonical Wnt signaling pathway this enzyme is regulated on multiple levels. GSK3β was first identified in 1978 as a consequence of its phosphorylation activity toward glycogen synthase to be the main regulator of glycogen metabolism. Although its original name did not change, this enzyme's sphere of influence extends well beyond intermediary metabolism (143). It is presently known that GSK3β is regulated by multiple hypertrophic, proliferative signaling pathways such as growth factors (IGF, EGF, PDGF) and Wnt molecules (144), which are central core that facilitates GSK3β inhibition through the main regulatory serine 9 phosphorylation. GSK3β is catalysed by protein kinase B (Akt) in the case of growth factors or Dvl in the case of Wnt signaling.

The inactivation of GSK3β in was shown to cause a reduction in the phosphorylation status of its substrates, ß-Catenin, CREB Binding Proteins, cyclin D, c-Myc, c-Jun, and the translation initiation factors eIF2 and eIF2B, BAX, BCL2, NF-kB, NFAT etc. (145-148). Most importantly, phosphorylation of these substrates by GSK3ß usually has an inhibitory effect or negatively regulates downstream signaling pathways. Thus, GSK3β acts like a double-edged sword by regulating several of its substrates (Figure 1.9.), participates in a wide spectrum of cellular processes, including glycogen metabolism, transcription, translation, cytoskeleton regulation, intracellular vesicular transport, cell cycle progression, and apoptosis.

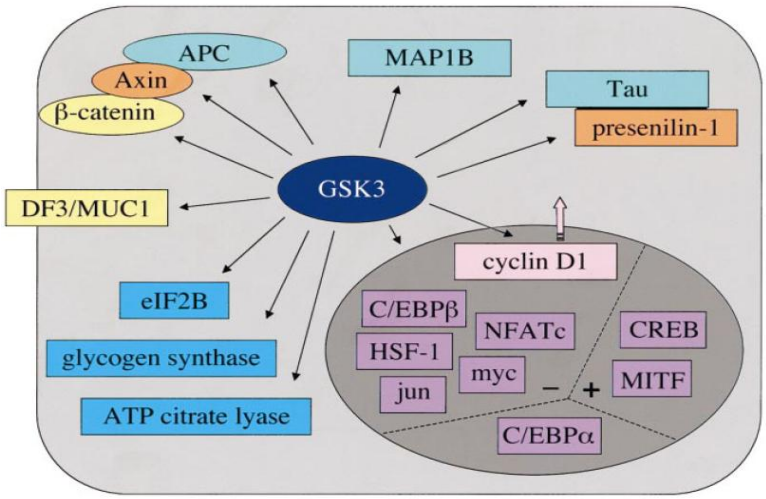

Figure 1.9. Putative substrates of GSK3ß protein. Alterations in GSK3ß activity can cause many disorders associated with transcription factors (mauve), enzymes that regulate metabolism (blue), proteins bound to microtubules (turquoise), scaffold proteins (orange), or components of the cell division cycle machinery (pink) or involved in cell adhesion (yellow). Adapted from Sheelagh Frame and Philip Cohen 2001.

Besides the well known GSK3β inhibitory mechanism involving phosphorylation of the serine 9 residue, GSK3β posses an additional probable regulatory phosphorylation site at

tyrosine 216 residue (Y216). Protein kinases related to GSK3β, such as ERK2, require phosphorylation of residues in their activation loops (T-loops) as a prerequisite for activity (149). Y216 phosphorylation could play a role in forcing open the substrate-binding site, but is not strictly required for kinase activity (150). The literature suggests potential circumstantial role for tyrosine phosphorylation in cell apoptosis (151) as well as in response to transient increases in intracellular calcium (152), however, the exact role of Y216 remains to be elucidated.

1.3.5. **Non-canonical Wnt signaling pathway**

PCP pathway. The PCP pathway emerged from genetic studies in Drosophila in which mutations in Wnt signaling components including Fzd and Dvl were found to randomize the orientation of epithelial structures including cuticle hairs and sensory bristles (107). In the non-canonical pathway, the Wnt signal is thought to be mediated through Fzd independent from the LRP co-receptor (108). Fzd co-receptors are not yet clearly defined but there are several possible candidates like Ryk (111), PTK7 (112) and ROR2 (113). The induction of these kinases further activates both PDZ and DEP domains of Dvl, which are both, utilized to activate two parallel pathways that activate the small GTPases Rho and Rac. Final activation of Rho GTPase leads to the activation of the Rho-associated kinase (ROCK) (109) and myosin (110), which leads to modification of the actin cytoskeleton and cytoskeletal rearrangement. However, the involvement of Dvl in this process seems to be crucial. Overexpression or downregulation of Dvl was observed to disrupt membrane localization and mediolateral cell polarity. Thus, asymmetric and membrane accumulation of the Dvl protein and activation of the PCP pathway seem to be required for convergent extension (114).

Wnt/Ca^{2+} pathway. Discovery of this pathway began with the finding that some Wnts and Fzd receptors can stimulate intracellular Ca^{2+} release from the endoplasmatic reticulum in a G-protein dependent manner (115-116). In response to this finding new evidences raise for the role of the non-canonical Wnt signaling pathway in intracellular calcium release and the main Wnt pathway components known so far are: Wnt5a (119-121), Wnt5b (125), Wnt11 (122-123), Fzd4 (124). Dvl protein plays an important role in this pathway as well by activation of phospholipase C (PLC), which in turn can lead to intracellular calcium release (97). The calcium release and intracellular accumulation activates several Ca^{2+} sensitive proteins like protein kinase C (PKC) (117) or Calcium-dependent protein kinase II (118)

which in turn can stimulate nuclear factor of activated T-cells (NFAT) transcription factor, important factor for ventral cell fate (117).

Further studies discovered another very interesting aspect of non-canonical Wnt signaling; that it can also inhibit Wnt/β-catenin signaling (126-127). Initial studies showing that overexpression of Wnt-5a in Xenopus could inhibit the effects of canonical Wnt-1 isoform provided the first hints that these two pathways could have antagonistic effects (128).

1.3.6. **Extracellular modulation of Wnt signaling by secreted Frizzled related proteins (sFRPs)**

Wnt signaling is extracellularly regulated on several levels. Besides Wnt ligands, there is also a family of secreted protein which are thought to antagonize or modulate canonical and non-canonical Wnt signaling, secreted Frizzled-related proteins (sFRPs) (Figure 1.10.).

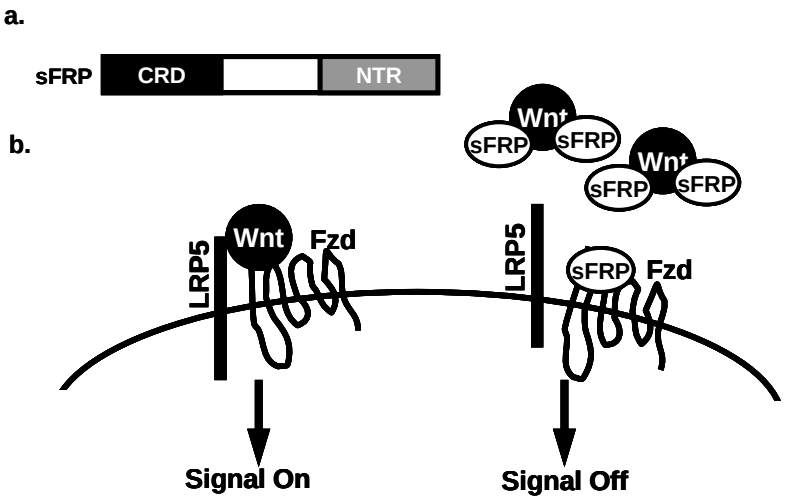

Figure 1.10. Wnt signaling modulation by secreted frizzled related proteins A. Motiffs present in sFRP proteins (CRD-cystein rich domain, NTR- netrin rich domain) B. Inhibitory mechanism of sFRP (author's scheme)

sFRPs were first identified around 1996 and postulated to be potential modulators of Wnt signaling (133). Although the sFRPs contain an N-terminal CRD domain same as the Wnt-binding domain of the Frizzled receptor (Figure 1.6. a), mechanism of binding to Wnt ligand is still unclear (135). Interestingly, this cysteine-rich domain in sFRPs can dimerize with other sFRPs and also bind Frizzled itself, suggesting that dual inhibition of Wnt signaling by sFRPs could potentially occur either through the binding of soluble Wnt ligand or the formation of non-functional receptor complexes with cell-surface Frizzled receptors

(136). Loss-of-function studies in mice have revealed significant redundancy for the sFRP genes (132). Currently, there are five members of the sFRP family in humans (sFRP1-5) (103). Of the five sFRPs, sFRP-1 is the predominant form and is highly expressed in human heart during development and adult (134).

1.4. **Wnt signaling pathway in vascular homeostasis**

Wnt signaling has recently been linked to the pathogenesis of important diseases, in particular cancer by controlling abnormal proliferation (167-168) and tumorigenesis (169-170). The Wnt genes and components of intracellular Wnt signaling pathways provide one of the most striking examples of this connection. In particular, the discovery that activating mutations in β-catenin are associated with a variety of human cancers has fueled an extraordinary explosion of interest into the relationship between Wnt signaling and oncogenesis. Activation of the Wnt signaling pathway may lead to angiogenesis or vessel remodeling, whereas inhibition of Wnt signaling may lead to vessel stability or even regression (Figure 1.11.). In order to better understand this system, identification of the Wnt signaling components present in vascular cells must be completed (166).

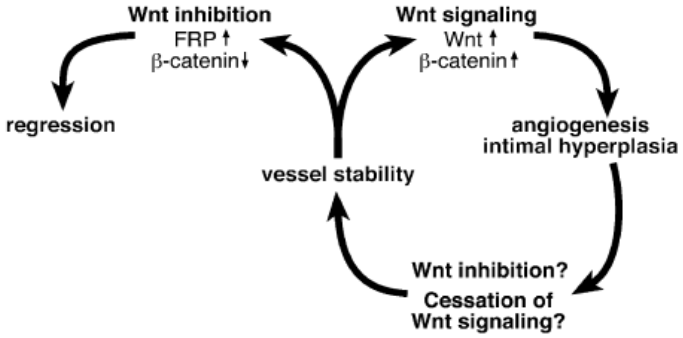

Figure 1.11. Scheme representing potential implication of Wnt signaling in homeostasis and pathogenesis of blood vessels. (Adapted from Goodwin A.M and D'Amore P.A. 2002)

Fascinatingly, very recently it was elucidated that, Wnt/β-catenin signaling plays a very profound role in atherosclerosis but the downstream pathways, which are involved, still remains a mystery. Besides Wnt/β-catenin (171), interestingly GSK3β acts as a β-catenin independent signal plays a crucial role in the regulation of cell proliferation (172-174) and is a possibly a key player in vascular homeostasis (175).

PAH is characterized by cellular and structural changes in pulmonary arteries. Gene expression analysis of pulmonary arterial resistance vessels revealed differentially regulated canonical and noncanonical Wnt genes in PAH (165). It was also shown that recruitment of

both canonical and noncanonical Wnt pathways are required in BMP-2-mediated angiogenesis (176) leaving the door open to investigate the possible role of this signaling in vascular remodeling.

Wnt signaling pathways are also known to be involved in heart development and the dysregulation of some of the Wnt components is associated with heart disorders. Profound changes in pulmonary vasculature in PAH are followed by heart hypertrophy and heart failure at the last stages of disease. GSK3 is an essential negative regulator of cardiac development (176) and hypertrophy and its inhibition by Wnts and growth factors hypertrophic stimuli (177) is an important mechanism contributing to the development of cardiac hypertrophy. sFRP-1 the main Wnt modulator was also shown to be important in heart disorders during ischemic rupture.

Crosstalk between the Wnt signaling and growth factors signaling pathways both shown to inhibit GSK3β could be crucial for vascular remodeling as well as induction of heart hypertrophy in PAH.

1.5. **Animal model of Monocrotaline (MCT)-induced PAH in rats**

One of most established animal models of PAH is monocrotaline induced PAH in rats. Monocrotaline is a pyrrolizidine alkaloid extracted from the crushed seeds of *Crotalaria spectabilis*. This phytotoxin is known to induce severe pulmonary hypertension in rats (154-155). Following single subcutaneous or intraperitoneal injection (156) monocrotaline is activated in the liver to the electrophile monocrotaline pyrrole (MCTP) (155) and then transported to the lung where it causes damage. Between 3rd and 5th week after injection monocrotaline induces severe pulmonary hypertension similar to many human forms characterized by increase in PAP and significant right ventricular hypertrophy (156). Pathologically PAH is characterized by vascular remodeling with significant increase in vessel muscularization and decreased lumen (155). Rodent species differs in sensitivity to monocrotaline and mice are completely resistant to lung changes.

2. **Aims of the study**

Pulmonary arterial hypertension (PAH) is a rare progressive pulmonary vascular disorder associated with vascular remodeling followed by right heart failure. Vascular remodeling involves numerous signaling cascades governing pulmonary arterial smooth muscle cell (PASMC) proliferation, migration and differentiation. Concerning the fact that new targets for future therapies are needed we focused on the Wnt signalling pathway.

Wnt signaling is known to play a crucial role in controlling proliferation in development as well as in cancer and recently has been implicated as a crucial pathway for cardiovascular system maintenance. One of the main function of GSK3ß/β-catenin axis is that it can act as a downstream regulatory switch for numerous signaling pathways. Hence we hypothesized that Wnt/GSK3ß/β-catenin axis plays a crucial role in pulmonary vascular remodeling and heart failure. In this context our research focus was to obtain:

- mRNA and protein expression profile of the canonical Wnt/GSK3ß/β-catenin system associated molecules in lungs of experimental model of MCT-induced PAH in rats 3 and 5 weeks after monocrotaline injection
- mRNA and protein expression profile of the canonical Wnt/GSK3ß/β-catenin system in PASMCs isolated from healthy and MCT-induced PAH lungs 5 weeks after monocrotaline injection
- Role of the GSK3ß/β-catenin axis in PDGF-induced signalling and proliferation of MCT-PASMC
- Individual role of the GSK3ß/β-catenin axis in the pathogenesis of MCT-PASMC by overexpression of GSK3ß
- Crosstalk of Wnt and PDGF signaling in pathogenesis of MCT-PASMC

The Wnt signaling pathways are also known to be involved in heart development and dysregulation is associated with heart disorders. Profound changes in pulmonary vasculature in PAH are followed by heart hypertrophy and heart failure occurs at the last stages of disease. GSK3β as a multi tasking kinase and sFRP-1, the main Wnt signaling modulators were shown to be very important in cardiac remodeling and heart disorders during ischemic rupture. Therefore we hypothesized that Wnt signaling might be of interest to study. To address this issue our research was focused on estimation of protein expression levels of

GSK3ß/β-catenin axis in hearts of MCT-induced PAH. To address the role of Wnt signaling *in vivo* in cardiac remodeling, mice lacking the Wnt modulator, sFRP-1 were used. In this context our research focus was to obtain:

- Expression of sFRP-1 in the normal heart during adult life
- Heart to body weight ratio of sFRP-1 KO mice at 6 month and one year of age
- Efect of the loss of sFRP-1 on fibrosis in the myocardium
- mRNA expression profile of Wnt signaling using PCR-Array
- Protein expression levels of canonical Wnt/GSK3ß/β-catenin
- Assessment of β-catenin translocation *in vivo* by immunohistochemichal staining and protein expression profile of β-catenin transcriptional targets like cyclin D, cMyc
- Effect of loss of sFRP-1 on Connexins

3. **Materials and methods**

3.1. **Materials**

3.1.1. **Equipment**

Name	**Company**
Autoclave	Tuttnauer Systec, Germany
Beta Counter	Canberra Packard, Germany
Cell Culture Incubator, Hera Cell	Heraeus, Germany
Chromatography Columns	Bio-Rad, USA
Electrophoresis Chambers	Biometra, Germany
Falcon Tubes	Greiner Bio-One, Germany
Film Casette	Kodak, USA
Filter Tips: 10; 100; 1000µl	Eppendorf, Germany
Fluorescence Microscope, LEICA	Leica, Germany
Frezer -80˚C	Bosh, Germany
Freezer -20˚C	Bosch, Germany
Freezer +4˚C	Bosch, Germany
Gel Blotting Paper	Bio-Rad, USA
Glass Bottles: 0,1; 0,2; 1l	Schott Duran, Germany
Glass Pipetek	Greiner Bio-One, Germany
Light Microscope	Hund, Germany
Lysis&Homogenization automated equipment	PeQLab, Germany
Microplate Reader Infinite 200	TECAN, Germany
Multifuge Centrifuge	Heraeus, Germany
NanoDrop	PeqLab, Germany
PCR-thermocycler	Biometria, Germany
PCR- Real Time Mx3000P	Stratagene, Germany
PCR-Real Time 7300	Applied Biosystems, USA
Petri Dish	Greiner Bio-One, Germany
Pipetboy	Eppendorf, Germany
Pipets	Eppendorf, Germany

Power Supply	Biometria, Germany
Radiographic Film Hypersensitive	Amersham Bioscences, UK
Radiographic Film Kodak	Kodak, USA
Serological pipette: 5, 10, 25, 50 ml	BD Falcon, USA
Tissue Culture Chamber Slides	BD Falcon, USA
Tissue Culture Dish 100mm	Greiner Bio-One, Germany
Tissue Culture Flask 250mm	Greiner Bio-One, Germany
Tissue Culture 6well Plate	Greiner Bio-One, Germany
Transilluminator BioDocAnalyzer	Biometria, Germany
Water Bath for Cell Culture	Medingen, Germany
Western Blot Chambers	Biometra, Germany
Vortex Machine	VWR, Germany

3.1.2. **Reagents**

Product Name	**Company**
Ammonium persulfate	Sigma-Aldrich, Germany
AEC Chromogen staining kit	Zymed Labs, Germany
Ampicilin	Invitrogen
2-Mercapto-ethanol	Sigma-Aldrich, Germany
2-Propanol	Fluka, Germany
Acetic Acid, Glacial 99+%	Sigma-Aldrich, Germany
Acrylamide solution, Rotiphorese gel 30	Roth, Germany
Agarose	Fluka, Germany
Albumine, Bovine serum	Sigma-Aldrich, Germany
Ammonium Acetate	Sigma-Aldrich, Germany
Ammonium formate	Sigma-Aldrich, Germany
Brillant Blue G	Sigma-Aldrich, Germany
Calcium Chloride	Sigma-Aldrich, Germany
EDTA-free protease inhibitor coctail	Roche, Germany
DMEM-F12 medium	Gibco BRL, Germany
Dimethyl Sulfoxide	Sigma-Aldrich, Germany
DTT	Sigma, Germany
DNA Ladder (100bp, 1kb)	Promega, USA
Dulbecco’s phosphate buffered saline 1x	PAN, Germany
Ethanol absolut	Riedel-de Haen, Germany
Ethidium Bromide	Sigma-Aldrich, Germany
Ethylene glycol-bis(ß-amino-ethylether)-N,N,N',N'tetraacetic acid (EGTA)	Sigma-Aldrich, Germany
Ethylenediamine-Tetraacetic acid (EDTA)	Sigma-Aldrich, Germany
ECL Plus Western Blotting Detection System	Amersham Biosciences
Endofree plasmid maxi kit	Qiagen, Germany
Fetal Calf Serum (FCS)	Biowest, USA
Formaldehyde	Sigma-Aldrich, Germany
Gel Extraction Kit	Qiagen, Germany
Glycerol	Sigma-Aldrich, Germany

Glycine, minimum 99% TLC	Sigma-Aldrich, Germany
GoTaq ® Flexi DNA polymerase	Promega, USA
2-(-4-2-hydroxyethyl)-piperazinyl-1-ethansulfonate (HEPES)	Sigma-Aldrich, Germany
Hydrochloric Acid	Sigma-Aldrich, Germany
IPTG	Promesa, Germany
ImProm-II™ Reverse Transcriptase	Promega, USA
Isopropanol	Roth, Germany
JM109 competent cells	Promesa, Germany
LB agar	Invitrogen, Germany
LB base	Invitrogen, Germany
Lipofectamine 2000	Invitrogen, Germany
Magnesium chloride (anhydrous)	Sigma-Aldrich, Germany
Methanol	Fluka, Germany
Methyl-[*3H*]-Thymidine, 250µCi	Amersham, Germany
Mini Prep Kit	Qiagen, Germany
Milk Powder	Roth, Germany
Nonidet-P40 (NP-40) Substitute	Fluka, Germany
N,N,N',N'-Tetramethyl-1-,2-diaminomethane (TEMED)	Sigma-Aldrich, Germany
Oligo(dT) Primer	Promega, USA
Opti MEM-I +glutaMax-I	Gibco, Germany
Penicillin-Streptomycin	PAA Laboratories, Austria
Hydrochloric Acid	Promega, USA
pcDNA3.1 directional TOPO cloning kit	Invitrogen, Germany
pGEM-T easy vector system II	Promesa, Germany
Platinum High Fidelity Taq Polymerase	Invitrogen, Germany
Platinum SYBR Green qPCR SuperMix-UDG	Invitrogen, Germany
Ponceau S Solution	Sigma-Aldrich, Germany
Potassium Chloride	Roth, Germany
Potassium dihydrogen phosphate (KH_2PO_4)	Roth, Germany
Potassium hydroxide, Sigma Ultra	Sigma-Aldrich, Germany
Potassium Phosphate monobasic	Sigma-Aldrich, Germany
Phenymethanesulfonyl fluoride (PMSF) (0.1M)	Fluka, Germany

Rainbow Protein Marker	Amersham Biosciences
RNase Awal	Molecular Bioproducts
RNeasy mini kit	Qiagen, Germany
RNAsin inhibitor	Promega, USA
RT^2Profiler WNT signaling PCR array (Mouse)	SABiosciences, USA
RT^2 PCR Real-Time SYBR Green Master Mix	SABiosciences, USA
RIPA buffer	Santa Cruz, Germany
SDS Solution, 10% w/v	Promega, USA
SOC Medium	Sigma, Germany
Sodium Chloride	Riedel-de Haen, Germany
Sodium citrate tribasic dihydrate	Sigma-Aldrich, Germany
Sodium hydroxide	Sigma-Aldrich, Germany
Sodium Fluoride	Sigma, Germany
Sodium orthovanadate	Sigma, Germany
Sodium Phosphate (monobasic, anhydrous)	Sigma-Aldrich, Germany
Scintillation liquid (Rotiszint eco plus)	Roth, Germany
Tris-HCl 1M	Sigma-Aldrich, Germany
Trizma base, minimum 99.9% titration	Sigma-Aldrich, Germany
Trizol Reagent	Invitrogen
Trichloroacetic acid (TCA), minimum 99%	Sigma, Germany
Trypsin/EDTA	Sigma Aldrich, Germany
Tween 20	Promesa, Germany
Vectastain Universal Elite ABC kit, VIP substrate	Vector Labs, Germany
Xgal	Promesa, Germany
Xylol	Merck, Germany

3.2. Methods

3.2.1. RNA isolation

Total RNA was isolated from both tissue rat lung homogenates and rat primary isolated PASMC's using TRIzol™ reagent. For tissue extraction, 100mg of rat lung in 1ml of TRIzol™ was placed in tissue homogenizer for 30s in three repeats and in between samples were cooled down on ice 20s. For PASMC's 1ml of TRIzol™ reagent was applied directly on culture dish and after 5 min of incubation on ice samples were collected to 1,5ml tubes with rubber policeman. After homogenization samples were incubated for 5 min in room temperature. After adding 0.2 ml of chloroform, mixing well 2 min at room temperature samples were centrifuged for 30min at 4°C (12000xg). The aqueous phase was transferred to a fresh tube, mixed with 0.5ml of isopropanol, incubated for 15min at room temperature and again centrifuged for 20min at 4°C (12000xg). After removing the supernatant, the RNA precipitated pellet was washed with 75% ethanol and centrifuged for 5min at room temperature (7.500xg). RNA pellet was dried and dissolved in RNase free water for 10min at 55°C.

RNA concentration and purity was determined by applying 1µl of a sample to a NanoDrop analyzer and spectroscopical absorbance analysis was set as the ratio of 260/280 nm wavelengths. Only the most pure RNA was further used in next experiments which 260/280 nm ratio was around 1,8.

3.2.2. Reverse transcription

Reverse transcription is enzymatic reactions, which enables the conversion of total RNA and amplify robust complementary, full length single stranded cDNA using powerful enzyme called reverse transcriptase.

cDNA was produced from cells or tissue isolated total RNA (section 3.2.1) using ImpromII Reverse Transcriptase Kit. The Reverse transcription (RT) reaction was held in two steps according to the manufacturer's protocol in the final volume of 20µl. First step was the combination of 1µg of total experimental RNA with 1µl oligo $(dT)_{15}$ primers (100µg/ml) in a 5µl volume. The primer/template mix was thermally denatured at 70°C for 5min and chilled on ice. In the second step a reverse transcription reaction mix was assembled on ice as follows: Primer/Template combination then was added to reverse transcription reaction mix. Following an initial annealing at 25°C for 5 min, the reaction is incubated at 42°C for 1h.

Product of reverse transcription was directly added for further polymerase chain reaction analysis.

Reaction components	Final concentration	Volume
Nuclease free water	-	4µl
ImProm-II. 5X Reaction Buffer	1x	4µl
25 mM $MgCl_2$	5mM	4µl
10 mM dNTP Mix	0,5mM	1µl
RNasin® Ribonuclease Inhibitor (1U/µl)	1U	1µl
ImProm-II. Reverse Transcriptase (1U/µl)	1U	1µl
Final Volume		**15µl**

The primer/template combination was then added to the reverse transcription reaction mix. Following an initial annealing at 25°C for 5 min, the reaction is incubated at 42°C for 1h. The product of reverse transcription was directly added for further polymerase chain reaction analysis.

3.2.3. **Polymerase chain reaction (PCR)**

PCR is an enzymatic reaction used to generate copies of a particular template DNA sequence using an enzyme heat-stable DNA polymerase, such as *Taq* Polymerase. This method relies on thermal cycling consisting of cycles of repeated heating and cooling of the reaction for DNA denaturation (separation of DNA template and primers by disrupting hydrogen bonds between complementary bases of DNA strands into single stranded DNA), annealing (primers binding to complementary sequence in single stranded DNA) and elongation (synthesis of new DNA strand complementary to template DNA by DNA polymerase by adding dNTP that are complementary to DNA template in 5' to 3' direction).

PCR was used to amplify different templates of DNA (cDNA section 3.2.2, plasmid DNA section 3.2.14.2). The PCR reaction on the cDNA template obtained as described above utilized two polymareses based systems: Platinum High Fidelity Taq Polymerase (Invitrogen) to amplify full length gene sequence for subsequent cloning and protein overexpression in PASMC's or to conduct point mutagenenesis on a full length gene inserted into plasmid DNA and GoTaq® Flex DNA Polymerase (Promega) for normal PCR analysis. The PCR reaction was conducted under conditions as follows:

PCR component	Final concentration	Volume per reaction
Platinum High Fidelity Taq Polymerase		
10x High fidelity PCR Buffer	1x	5µl
10mM dNTP mix	0,2mM	1µl
50mM $MgSO_4$	5mM	5µl
10µM full length forward primer	0,2µM	1µl
10µM full length reverse primer	0,2µM	1µl
High Fidelity Taq Polymerase	1U	0,2µl
Template cDNA		2µl
Distilled water		34,8µl
GoTaq® Flex DNA Polymerase		
5x PCR Buffer	1x	10µl
10mM dNTP mix	0,2nM	1µl
25mM $MgCl_2$	2,5mM	5µl
10 µM forward primer	0,2µM	1µl
10 µM reverse primer	0,2µM	1µl
GoTaq® Flex DNA Polymerase	1,25U	0,25µl
Template		2µl
Distilled water		29,75µl
Final Volume		**50µl**

The PCR components were mixed carefully on ice and after spinning down were placed in the PCR Thermal Cycler. Annealing temperatures for the primers (* Appendix Table 1.) were different according to the primers melting temperatures. Additionally the final elongation step timecourse was depending on the amplified sequences (5min- for fragments <500bp, 10min- for fragments up to 1,5kb). PCR was conducted under following conditions:

Step	Temperature	Time
Activation	95°C	2-5min
Denaturation	95°C	30s
Annealing	*	20-30s
Elongation	68-72°C	1min
Final Elongation	68-72°C	5-10min

The PCR reaction used to perform point mutations on the template DNA of the full length gene built in the plasmid was conducted using Platinum High Fidelity Taq Polymerase (Invitrogen) system with the same PCR reaction components as described above for this system. For the pcDNA3.1-full length gene insert TOPO amplification which length was >5kb following conditions were used:

Step	Temperature	Time
Activation	95°C	90s
Denaturation	95°C	30s
Annealing	62°C	30s
Elongation	68°C	900s
Final Elongation	68°C	1200s

3.2.4. **Real-Time Polymerase chain reaction**

Real-Time PCR also called quantitative PCR is a technique based on polymarease chain reaction which is used to amplify and simultaneously determine quantification of a targeted DNA. Quantification is expressed as an absolute number of copies or relative amount when normalized to control DNA input or housekeeping genes.

Real-Time PCR was performed on cDNA templates obtained from cells or tissue as described above in 25µl reaction using Platinum SYBR Green qPCR SuperMix-UDG (Invitrogen) with ROX reference dye. The Reaction was prepared as follows:

PCR component	Final concentration	Volume per reaction
SYBR Green qPCR SuperMix-UDG 2x	1x	12,5µl
50mM $MgCl_2$	5mM	2µl
ROX		0,5µl
10 µM full length forward primer	0,2µM	1µl
10 µM full length reverse primer	0,2µM	1µl
Template cDNA		1µl
Distilled water		7µl

The Real-Time PCR reaction components were well mixed on 96-well PCR plates, vortexed and spun down for 1min. The thermal cycle conditions used for all of the reactions were as follows:

Step	Temperature	Time
Activation	50°C	2min
Denaturation	95°C	2min
Annealing	59°C*	30s
Elongation	72°C	30s

All reactions was carried out with the same number of cycles which was 40 and the same annealing temperature for specific primers designed to melt at the same temperature (* Appendix Table 1.).

3.2.5. **Agarose gel electrophoresis**

To analyze the PCR products, plasmid DNA or restriction mapping of cloned DNA agarose gel electrophoresis (a method to separate DNA based on its size) was conducted. Pending on DNA size different percentage of gels were used in a range 0,7-1,5%. To perform electrophoresis agarose was mixed with 1x TAE buffer with the addition of ethidium bromide (1μg/ml) which enables the visualization of DNA under UV light condition. The gels were run in 1x TAE buffer in the 80-100V ranges.
DNA bands were visualized under UV light in a transilluminator (Biometra).

1xTAE Buffer (40mM Tris-acetate, pH=8.0, 1mM EDTA, pH=8.0)

3.2.6. **Protein isolation**

Tissues and cell samples were homogenized in the same manner as described above (Section 3.2.1) with exeption of tissue lysis in RIPA buffer (Santa Cruz) containing DMSO, a protease inhibitor cocktail and PMSF. After lysis proteins were incubated 15-20min on ice and subsequently centrifuged for 30min at 4°C (13000xg). Then supernatants were transferred to fresh 1,5ml tube and directly stored at -80°C.

3.2.7. **Cytoplasmic and nuclear fractionation**

To prepare nuclear extracts cells were washed with PBS and trypsinized. After 2min the medium supplemented with FCS was added to inactivate trypsin and cells were centrifuged for 5min (800xg). The pellet was resuspended in 200-300µl of Buffer-A and immediately 0.125% NP-40 V/V (3.75µl to 300µl) added to maintain the nuclear membrane structure. After 5min of incubation on ice the cells were spin down for 10min at 4°C (1000xg). The supernatant (cytosolic fraction) was then transferred to a fresh 1,5ml tube. The pellet was washed with 300µl of Buffer-A and spun down for 10min at 4°C (1000xg). The supernatant was decantedand the pellet was resuspended in 30µl of Buffer-C and spun down for 10min at 4°C (12000xg). The supernatant (nuclear fraction) was transferred to a new 1,5ml tube. The protein of both fractions were directly stored at -80°C.

Buffer-A Composition

10mM Tris pH-7.9, 10mM KCl, 1.5mM $MgCl_2$, 10% Glycerol, 10mM K_2HPO_4. Directly before lysis following was added: 1mM Sodium vanadate, 10mM NaF, 0.5mM DTT, 1mM PMSF, 1X-protease inhibitors)

Buffer –C Composition (20mM Tris (pH-7.9), 0.42M NaCl, 1.5mM $MgCl_2$, 2mM EDTA, 10% Glycerol, 10mM K_2HPO_4. Directly before lysis following was added: 1mM Sodium Vanadate, 10mM NaF, 0.5mM DTT, 1mM ABSF, 1X protease inhibitors)

3.2.8. **Protein quantity estimation**

The quantity of protein was estimated using the Quick Start™ Bradford Dye Reagent (Biorad). The Bradford assay method involves the incorporation of Coomassie Brilliant Blue G-250 dye to proteins. After binding of the dye to protein it is converted to a stable blue form. Protein/dye complexes were detected at 595nm using TECAN microplate reader. BSA was used as a standard solution in a range from 0,2-2µg to determine an exact protein concentration in the sample.

3.2.9. **SDS polyacrylamide gel electrophoresis**

SDS polyacrylamide gel electrophoresis was conducted to separate proteins according to its size for further immunoblotting analysis. Tissue and cell lysates before substracting on

the gel were prepared with SDS loading dye containg DTT to negatively charge protein in the sample and subsequently boiled at 100°C. Electrophoretical separatation of the proteins was performed in 1x Running buffer at 120V with the usage of polyacrylamide gels with a different separation ability in the range of 7-15% pending on the proteins sizes.

SDS-running buffer (25mM Tris, 250mM Glycine, 0,1% (w/v) SDS)

5xSDS-loading buffer (250mM Tris pH 6.8, 50% glycerol , 5% SDS, 0.05% bromophenol blue, 200mM DTT)

Stacking gel (5%)

Gel component	Volume
Distilled water	3ml
0,5M Tris; pH=6,8	1,25ml
10% SDS	0,1ml
Acrylamide/Bis-acrylamide	0,67ml
10% Amonium Persulfate	0,05ml
TEMED	0,005ml

Resolving gel (7-15%)

Gel component	Percentage of gel		
	5%	10%	15%
Distilled water	5,1ml	4,1ml	2,4ml
1,5M Tris; pH=8,8	2,5ml	2,5ml	2,5ml
10% SDS	0,2ml	0,2ml	0,2ml
Acrylamide/Bis-acrylamide	2,3ml	3,4ml	5ml
10% Amonium Persulfate	0,05ml	0,05ml	0,05ml
TEMED	0,007ml	0,007ml	0,007ml

3.2.10. **Protein blotting**

Electrophoretically separated proteins on the polyacrylamide gels were transferred to 0,45µM nitrocellulose membranes (BioRad). Wet transfer technique was conducted in transfer buffer for 1h at 120V.

Transfer buffer (25mM Tris, 192mM Glycine, 20% (v/v) Methanol)

3.2.11. **Protein detection**

The protein transfer membranes were subsequently blocked in 5% dry non-fat milk for 1h at room temperature. After blocking the membranes were probed with primary antibodies (Appendix Table 4.) diluted in 5% dry non-fat milk overnight at 4°C in different dilutions. After overnight incubation the membranes were washed 3 times 10min with 1x TBST buffer and subsequently incubated 1h with secondary HRP-conjugated antibodies (Appendix Table 5.) diluted in 5% dry non-fat milk. The secondary antibodies left over was washed 3 times 10min with 1x TBST buffer and the signal was detected with ECL Western Blotting Reagent (Amersham Bioscencies) and visualized on the hyper or low sensitive films according to signal intensity. According to the experiment need membranes were stripped in a stripping buffer and reprobed with control genes antibodies like total protein or housekeeping controls in order to quantify more precisely.

1xTBST (1xTBS, 0,1% (v/v) Tween 20)
Blocking milk solution (5% non-fat dry milk, 1xTBST)
Stripping buffer (62,5 mM Tris-HCl, pH=6,8, 2% (w/v) SDS, 100mM β-mercaptoethanol)

3.2.12. **Densitometry**

Western blots were quantified using densitometry, which was performed on the Biometra Illuminator with BioDoc software. Expression was quantified using bands intensity values which were normalized to GAPDH when performing cytoplasmic and total fraction analysis and to histone H1 for nuclear fraction.

3.2.13. **Immunohistochemistry**

Microtome cut 6 μm paraffin-embedded lung sections from healthy and MCT-injected after 5 weeks were incubated 45min at 65°C and subsequently deparaffinized in xylene three times for 3 minutes. Then slides were hydrated with decreasing concentration of alcohol at the range from100% to 80% ethanol concentration. After slides were washed with running tap water antigen was retrieved by incubation in trypsin for 20 minutes at 37°C. Subsequently sections were incubated in 3% hydrogen peroxide for 20 minutes at room temperature, washed and blocked for 30 minutes in 2% bovine serum albumine. Then sections were probed

overnight in 4°C with primary antibodies (Appendix Table 4.) usually in 1:100 dilution. Biotinylated anti-rabbit secondary antibody and HRP-streptavidin enzyme conjugate were added and sections were incubated for 1h at room temperature and subsequently washed with PBS (3xtimes). sFRP-1 or Connexin 43 signal was detected by incubation with AEC substrate (red color) for HRP 10 min (Histostain SP Rabbit Primary AEC Kit (ZYMED Laboratories). In the end sections were counterstained with hematoxylin (blue color), mounted in aqueous GVA mount media, cover slipped and further analysed by light microscope (Leica) when properly dried.

3.2.14. **Molecular cloning**

The cloning procedure is a molecular technique most frequently used to amplify DNA fragments containing whole genes for further gene overexpression in mammalian cells but also widely used for many purposes ranging from amplifying any DNA sequence for example promoters, non-coding sequences of randomly fragmented DNA, genetic fingerprinting or creating transgenic animals.

3.2.14.1. Vector systems

Molecular cloning vectors are DNA molecules used as a vehicle to carry inserted DNA (f.e gene of interest). Four major types of vectors are used in molecular biology: plasmids, bacteriophages and other viral types of vetors and cosmids. The main characteristic of a vector is to contain origin of replication, multicloning site to build in insert and selectable marker (often antibiotic resistance genes).

To conduct cloning experiments and finnaly overexpress protein in mammalian cells two types of plasmid vectors were used: pGEM-T Easy Vector which is normal TA cloning vector (Promega) (Figure 3.1.) and subsequently pcDNA3.1 TOPO directional expression vector (Invitrogen) (Figure 3.2.) used for overexpression of gene of interest in the mammalian cell system.

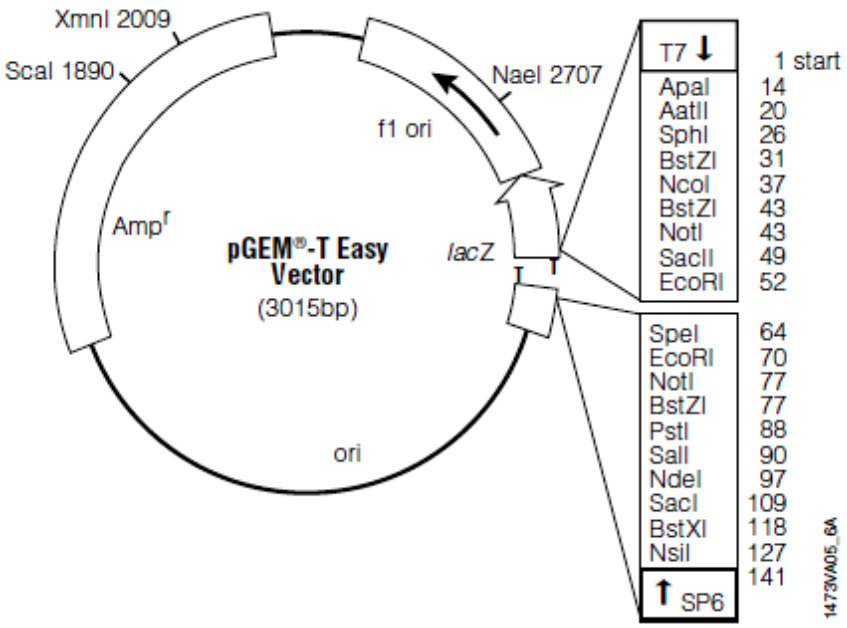

Figure 3.1. pGEM-T Easy Vector. pGEM-T Easy Vector schematic map and reference points.

A.

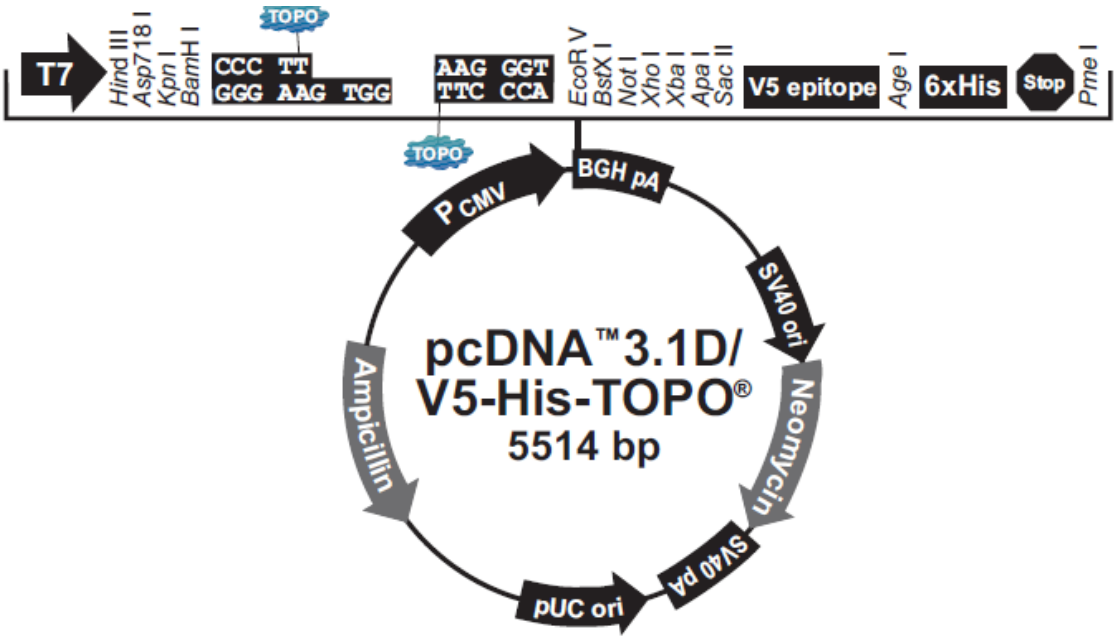

B.

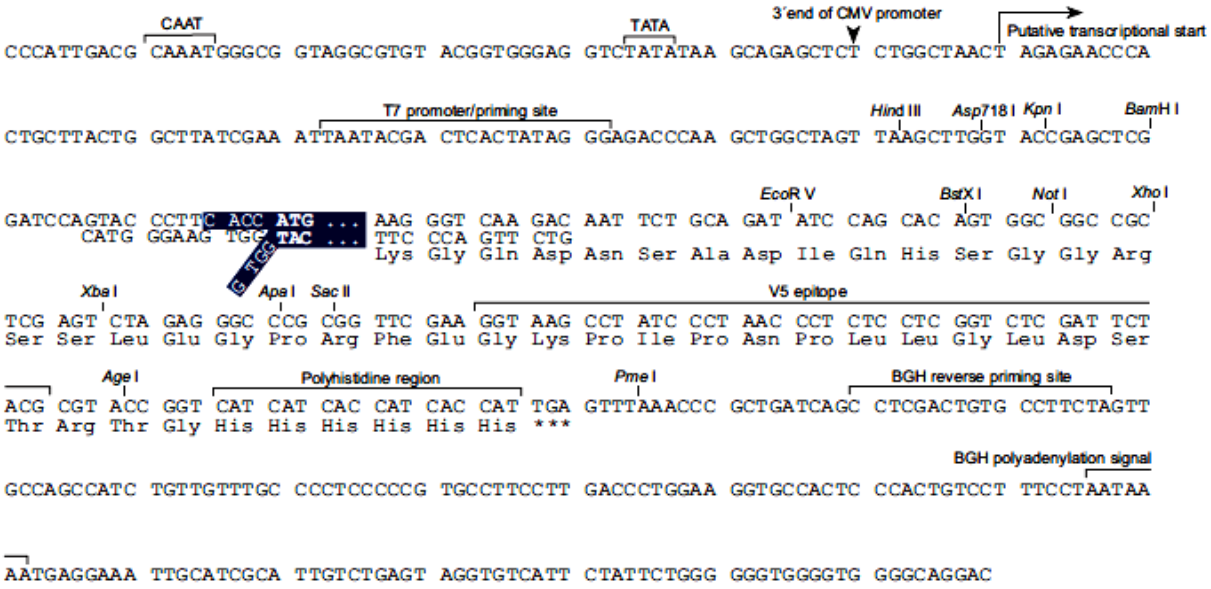

Figure 3.2. pcDNA3.1 TOPO directional expression vector A. pcDNA3.1 Vector schematic map and reference points. B. Multiple cloning site sequence

3.2.14.2. Generation of full length gene insert and PCR product purification

Considering the two vector systems described above which have different requirements for DNA fragment to be inserted due of its 5' and 3' ends desired full length gene of interest DNA was amplified using two sets of specific primers one for each vector system.

To create the full length gene insert in the expression vector the first step is to amplify the full length gene of interest on human specific cell type cDNA template with 5' and 3' UTR overhangs using specific pair of primers (Appendix Table 1.). Insertion in the pGEM-T Easy TA cloning vector which specifically required the insert to be A-tailed. An additional A-tailing step was unnecessary because of the usage of the Platinum High Fidelity Taq Polymerase (Section 3.2.3).

To procced the second step was to amplify a pure full length gene of interest on a pGEM-T Easy carrying insert with UTR overhangs template. To insert into pcDNA3.1 Directional Expression Vector the full length gene of interest was amplified using a specific pair of primers (Appendix Table 1.) to add CACC on 5' end right before start codon (ATG) and delete stop codon (TCA) on 3' end.

PCR reaction used to amplify the full length gene sequences for both pGEM-T Easy Vector and pcDNA3.1 TOPO directional expression vector was conducted in conditions described previously for DNA fragments up to 1,5kb using Platinum High Fidelity Taq Polymerase (Section 3.2.3).

The desired DNA fragments prepared according to the vector requirements were purified by qel extraction using the QIAquick gel extraction kit (Qiagen) technology. The PCR products were run on low-melting point agarose gel. The desired DNA band was excised from the gel using a scalpel. Gel slices were incubated at 50°C for 15min to melt the agarose. Pure DNA up to 10µg were recovered by absorption onto a special silica membrane in the presence of a high concentration of chaotropic salts while all contaminants passed through the membrane. Pure DNA inserts were eluted in low salt concentration conditions and subsequently inserted to the described plasmids.

3.2.14.3. Ligation

Ligation is an enzymatic reaction which uses an enzyme called T4 Ligase to insert the desired fragment of DNA into a carrier vehicle plasmid DNA mixing them in a range from

1:1 to 1:3 molar ratio. To calculate the proper vector:insert DNA ratio a standard equation was used:

$$\frac{100ng(pGEM-Tvector)x1,4kb(insert)}{3,014kb(pGEM-Tvector)} = 45ng(insert)$$

The standard ligation reaction procedure was used only for the pGEM-T Easy vector and the reaction components were prepared as follows:

Reaction components	Concentration	Volume
2X Rapid Ligation Buffer, T4 DNA Ligase	1x	5µl
pGEM®-T Easy Vector (50ng/µl)	100ng/10µl	2µl
Purified full-length gene with UTR overhangs (45ng/µl)	45ng/10µl	1µl
T4 DNA Ligase (3U/µl)	3U/10µl	1µl
Water		2µl
Final volume		**10µl**

Reaction components were mixed properly, spun down and incubated 1h at room temperature. After incubation T4 ligase was inactivated by heating the ligation mixture at 70°C for 15min.

Before transformation, the ligation mixture needed to be desalted in a special made desalination tube. To prepare desalination tubes a solution of: 1% agarose + 100mM Glucose in deionized H_2O boiled in microwave was prepared. Afterwards this warm solution was poured into 1,5ml tubes with small 200µl tubes on the top (self constructed). When the solution got solid 200µl tubes were taken out and holes left inside were filled with H_2O to avoid drying. This hand made desalt-tubes were stored at 4°C.

To desalt the sample 10µl of ligation reaction mixture was put into whole in desalt-tubes. Incubate 1h on ice. After desalination ligation mixture was ready to be transform to *E.coli* (section 3.2.14.5). Instead of desalination tubes DNA precipitation procedure could be used.

3.2.14.4. TOPO cloning reaction

Cloning of the DNA full lengtht insert into the pcDNA3.1 Directional expression TOPO vector did not require T4 ligase. In this system based on topoisomerase I activity, PCR products are directionally cloned by adding four bases to the forward primer (CACC). The overhang in the cloning vector (GTGG) (Figure 3.2. B) invades the 5′ end of the PCR product, anneals to the added bases, and stabilizes the PCR product in the correct orientation. Inserts can be cloned in the correct orientation with efficiencies equal to or greater than 90%. The TOPO cloning reaction mixture was prepared as follows:

TOPO cloning reagents	**Volume for chemically competent *E.coli***
Purified PCR product with 5' CACC overhang	4µl
Salt solution (1,2M NaCl; 0,06M $MgCl_2$)	1µl
pcDNA3.1 TOPO vector	1µl
Final volume	**5µl**

Reagents were mixed properly, spun down and incubated 5-30min at room temperature. Both for further transformation to chemically competent *E.coli* strain JM-109 (Promega) by heat shock procedure.

3.2.14.5. *E.Coli* heat shock transformation

Chemically competent JM109 strain of *E.coli* cells (Promega) was thawn on ice in 100µl aliquots. The ligation reaction mixture was diluted 1:10. To each 100µl transformation reaction 5-10µl of approximately 10-20ng of DNA was added. Component were mixed by flicking the tube extremely gently and incubated on ice 30min. Cells were transformed by heat shock 30-45sec at 42°C, placed on ice for 2min and 900µl SOC media was immediately added to increase transformation efficiency. Then tubes were incubated 1h at 37°C without shaking and 10-100µl of the transformation reaction was spread by a plastic sterile stick onto pre-warmed LB/IPTG/Xgal plates with appropriate ampicilin selection suitable for blue-white screening. LB agar plates were incubated up to 14h at 37°C to avoid satellite colonies formation.

LB/IPTG/Xgal agar plates (Dissolve 32mg of LB agar per 1l of ddH_2O and autoclave. After LB agar solution cooled down following was added: 50μg/ml Ampicilin, 100μM IPTG, 50μg/ml Xgal)

25ml of still warm mixed liquid was aliquoted on Petri dishes and kept at room temperature until get solid and further stored at 4°C.

3.2.14.6. Clones selection and analysis

Bacterial colonies containing an insert with the pGEM-T Easy vector were simply recognized by blue and white screening. This technique allows for the quick and easy detection of successful ligation without the need to individually test each colony based on βgalactosidase gene activity. pGEM-T Easy vector encodes the α subunit of LacZ protein with an internal multiple cloning site, while the chromosome of the *E.coli* strain encodes the remaining Ω subunit to form a functional βgalactosidase enzyme. The full lengtht gene inserted within the LacZα gene, disrupts the production of functional βgalactosidase. Xgal, a colorless modified galactose sugar is metabolized by βgalactosidase to form an insoluble product (5-bromo-4 chloroindole) which is bright blue and is an indicator for this reaction. Isopropyl β-D-1-thiogalactopyranoside (IPTG) induces Lac operon. The hydrolysis of colorless X-gal by the β-galactosidase causes the characteristic blue colour in the colonies which simply shows that the colonies contain pGEM-T Easy vector without insert. White colonies (loss of ability to hydrolyze the marker indicate pGEM-T Easy vector containing an insert as first step of analysis. The second step was to linearize the vector with *Bam*HI restriction enzyme followed by 0,7% agarose gel electrophoresis (Section 3.2.14.7). The third step was to perform PCR with full length gene primers followed by sequencing with appropriate primers for pGEM-T Easy vector (Section 3.2.14.11).

Single colonies contain pcDNA3.1 TOPO directional expression vector as it does not encode βgalactosidase gene for blue and white screening were analysed by restriction and further sequenced with proper for pcDNA3.1 vector primers (Sequencing). PCR reaction was additionally performed with full length gene insert primers.

3.2.14.7. Restriction digestion

Recombinant clones were analysed using restriction enzyme digestion. For this purpose the *Bam*HI (Invitrogen) enzyme was used to digest and linearize both pGEM-T Easy

and pcDNA3.1 TOPO vector carrying an insert. The reaction was conduction under the following conditions:

Reaction component	Volume
10x Ligation Buffer (ReACT3)	2µl
Template (plasmid DNA with insert)	5µl (max 1µg)
Sterile H_2O	12µl
*Bam*HI (4U/µl)	1µl
Final Volume	**20µl**

The reaction components were mixed properly, spin down and incubated for 60-90min At 37°C. Subsequently mixture together with not digested empty vector control was apllied on 0,7% agarose gel analysis. Vectors containing inserts were positively identified by the expected size (pGEM-T Easy carrying insert ±4,4kb; pcDNA3.1 TOPO vector carrying insert ±5,9kb).

3.2.14.8. Plasmid isolation

E.coli carrying plasmid DNA with full length gene inserts were amplified in liquid LB medium supplemented with 50µg/ml ampicilin selection marker in 5ml (mini culture) and 250ml (maxi culture) volume. Plasmids were isolated with QIAPrep technology (Qiagen). This technology basic principles are based on modified alkaline lysis procedure followed by adsorption of plasmid DNA to special designed silica membrane and further elution in specific salt concentration and pH.

For a small amount of plasmid isolation, a single pGEM-T Easy vector white colonies were picked with a sterile tip and inoculated in LB medium with ampicilin. Bacterial cultures were grown at 37°C and simultaneously shaked with 250rpm for 14h. Bacterial cells were harvested by centrifugation (10000rpm) for 5min at room temperature. Plasmids were isolated using QIAPrep miniprep spin isolation kit (Qiagen). This method utilizes silica membranes for selective adsorption of plasmid DNA in high salt concentration and elution in low salt concentrations and pH between 7-8,5. After isolation the plasmid was subjected to sequencing (sequencing) and further used as a starting template for TOPO cloning reaction.

For large amounts of plasmid isolation single pcDNA3.1 vector colonies were picked with a sterile tip and inoculated in 2ml of LB medium with ampicilin, shaked (250rpm) for 6-

8h at 37°C. A further 2ml of the starter bacterial culture was diluted 1:1000 in 250ml of LB medium supplemented with ampicilin, grown at 37°C and simultaneously shaked with 250rpm for 14h. Bacterial cells were harvested by centrifugation (6000xg) for 25min at 4°C. Plasmids were isolated using Endo-Free Plasmid Maxi Kit (Qiagen). This plasmid purification method is based on alkaline lysis followed by plasmid adsorption on an Anion-Exchange resin under low salt concentration and pH. Contrary to the miniprep procedure plasmids are eluted with high-salt concentration and desalted by isopropanol precipitation. This procedure provides much more pure yields of isolated plasmid DNA.

Plasmid DNA yield was measured on Nanodrop and stored in -20°C for further experiments.

3.2.14.9. Clones storage

Recmbinant clones were stored in 7% DMSO stocks. To 930µl of bacterial cultures in LB medium supplemented with ampicilin 70µl of DMSO was added, properly mixed by pipeting and stored for long term at -80°C.

3.2.14.10. Mutagenesis

To study the function of the gene in its on and off stage in mammalian cells several point aminoacid mutation was performed. Three mutants of GSK3ß were constructed each represents a regulatory phosphorylation residues of this protein: GSK3ß S9A - where serine 9 residue was substituted with alanine, GSK3ß Y216D – where tyrosine at 216 residue was substituted by aspartic acid and GSK3ß Y216E – where tyrosine at 216 residue was substituted with glutamic acid.

To conduct mutagenesis long product PCR reaction was performed where full length wild type gene (GSK3ß) was inserted in pcDNA3.1 directional expression vector methylated in *dam* positive *E.coli* strain JM109 was used as a template for performing point mutations with specific primers (Appendix Table 1.). The PCR reaction components were prepared as described (Section 3.2.3) for Platinum High Fidelity Taq Polymarase and whole reaction was held in conditions described for long PCR product (>5kb) (PCRsection). PCR raction mixture which contained both methylated pcDNA3.1 with wild type full length gene and unmethylated pcDNA3.1 with point mutated full length gene was then digested by restriction endonuclease enzyme *Dpn*I (New England Biolabs) which degrades methylated DNA. Digestion reaction was prepared as follows:

Reaction components	Volume
10x NEBuffer 4	5µl
Template DNA – long PCR reaction mixture of methylated and unmethylated plasmids	20µl (0,5µg)
*Dpn*I (10U/µl)	5µl
Sterile water	20µl
Final volume	**50µl**

The reaction components were mixed properly, spun down and incubated 4h at 37°C. After incubation *Dpn*I enzyme was inactivated by 20min incubation at 80°C and unmethylated pcDNA3.1 vector carrying mutated insert was further transformed by heat shock (heat shock transformation) into *E.coli* strain JM109 and isolated in large amounts using Endo-Free Plasmid Maxi Kit (Qiagen) (plasmid isolation section) and stored in glycerol stocks (clones storage). Mutations were validated by sequencing (Section 3.2.14.11). Primers sequences used for mutagenesis PCR reaction for S9A and Y216D mutant and melting temperature are described in (Appendix Table 1.).

3.2.14.11. Sequencing

Full length gene inserts were sent for sequencing to AGOWA GmbH Sequencing service (Berlin, Germany). Gene inserts built in pGEM-T Easy vector were sequenced with T7 and SP6 primers (Appendix Table 2.) whereas wild type and mutated gene inserts inserted into pcDNA3.1 directional expression vector were sequenced with T7 and BGH primers (Appendix Table 2.).

3.2.15. **Cell culture condition**

In vitro cell culture experiments were performed using primary pulmonary arterial smooth muscle cells isolated from healthy rat lungs and pulmonary hypertensive rats 5 weeks after monocrotaline injection. These cells were previously isolated by manual dissection of the rat pulmonary artery. Briefly, proximal and distal parts of the rat pulmonary artery were separated and endothelial cells were mechanically removed to expose the smooth muscle

layer. The PAMSC's from the distal part of the pulmonary artery were used further *in vitro* experiments.

Primary rat PASMCs cultures were maintained at 37°C in a humidified 5% CO_2/95 % O_2 atmosphere in DMEMF-12 medium supplemented with 10% Fetal Calf Serum (FCS), 5% streptomycin/penicillin and 5% glutamate. Growth of cells was checked everyday by contrast phase microscopy and the medium was changed ever third day. After reaching 80% confluence cells were passaged and plated to 10cm^2, 6-well and 48-well plates depending on the experimental need. To passage, cells were first washed twice with pre-warmed PBS to minimize serum amount and 1x trypsin solution was applied (0,025% Trypsin/EDTA, 1xPBS). Trypsin/EDTA solution was neutralized by DMEMF12 medium supplemented with FCS. Cells were further counted and seeded on a new culture dishes.

Before stimulation cells were starved for 24h in DMEMF12 medium supplemented with 0,1% FCS to obtain a pure response for proper stimulation that would not be affected by serum factors. Stimulants used for experiments were as follows:

Stimulants	**Final concentration**
Growth factors	
Platelet derived growth factor BB (PDGF-BB)	60ng/ml
Wnt3A	10-50ng/ml
Inhibitors	
Imatinib (Gleevec)	5μM
Lithium Chloride	1-10mM

10% FCS cell culture médium (F-12 DMEM Medium, 1% Penicillin/Streptamycin, 1% Glutamine, 10% FCS)
0,1% FCS cell culture médium (F-12 DMEM Medium, 1% Penicillin/Streptomycin, 1% Glutamine, 10% FCS)

For long term storage of the cells harvested the cell pellet after trypsinization was resuspended in DMEMF12 medium supplemented with 10% FCS and 5% DMSO and subsequently frozen first at -20°C for up to 4 hours and finally in liquid nitrogen in cryogenic vials. For furthr use of frozen cells cryogenic vials containing cells were fast thawn at 37°C

diluted 1:10 in fresh DMEMF12 supplemented with 10% FCS and spread equally onto culture dishes. The next day, the medium was changed to remove the last traces of DMSO.

3.2.16. **Transfection of primary PASMCS**

Transfection is a process of introducing nucleic acids into cells by non-viral procedures. In this study lipofection (liposome transfection) was used as a method of plasmid DNA introduction into mammalian cells. Lipofection is a transfection procedure which uses synthetic cationic lipid, N-[1-(2,3-dioleyloxy)propyl]-N,N,N-trimethylammonium chloride (DOTMA). Small liposomes containing DOTMA interact with plasmid DNA to form lipid-DNA complexes with very efficient entrapment of the DNA. DOTMA is responsible for facilitating fusion of the complex with the plasma membrane of cells, resulting in the uptake of DNA and further expression of the gene carried by the plasmid DNA.

Smooth muscle cells were maintained as described (Section 3.2.15) and by the time they reach 70% confluence the cells were transfected with pcDNA3.1 TOPO directional expression vector carrying GSK3ß WT, S9A, Y216D and empty vector (EV) on 6-well plates (for protein expression) and 48-well plates (for proliferation assessment) using Lipofectamine 2000 (Invitrogen) reagent. Before transfection the DNA was diluted (1μg/ml in 6-well plate and 0,2μg/ml in 48-well plates) in Opti-MEM Glutamax medium with no FCS. At the same time Lipofectamine 2000 reagent was mixed with Opti-MEM medium (5μl/ml) and incubated 5min at room temperature. After 5min the diluted plasmid DNA and Lipofectimine 2000 were gently mixed and incubated for 20 min at room temperature to allow complexes formation. The complex was further diluted in no FCS Opti-MEM Glutamax medium added to the cells. Due to complexes stability after 6h medium was aspirated and changed to DMEMF12 supplemented with 10% FCS to allow cells recovery. Depending on the application, the cells were incubated for 48h for protein analysis of the targeted GSK3ß and its mutated forms, cellular signaling analysis or proliferation assessment.

3.2.17. ^{3}**H- Thymidine incorporation assay**

The proliferation of primary rat PASMC's cells was assessed by ^{3}H- Thymidine incorporation assay. This technology is based on deoxythymidine DNA nucleoside T, which pairs with deoxyadenosine A in cellular double stranded DNA. During S phase when the DNA is being replicated thymidine binds to the newly synthesized DNA and is an indicator of cells proliferation based on DNA content.

Transiently transfected or growth factors stimulated prepared as described (Section 3.2.15 and 3.2.16) PASMC's isolated from pulmonary hypertensive rats 5 weeks after monocrotaline injection after 24h of incubation were subjected to ^{3}H- Thymidine incorporation assay. Cells were labeled 4h before readout with 0,1μCi per well (48-well plate) at 37°C. After 4h incubation with thymidine cells were washed twice with HBSS buffer and subsequently fixed with 250μl per well ice cold methanol and incubated 15min at 4°C. Then to precipitate the nucleic acids 250μl per well of 10% TCA solution was applied. Precipitation was carried out 15min by incubation at 4°C. After the two step washing with sterile water the cells were lysed with 250μl per well of 0,1M NaOH and incubated with shaking (200rpm) for 1h at room temperature. Proliferation of cells was determined by scintillation counting (Canberra-Packard β-counter) and quantified based on β radiation counts per minute (cpm).

3.2.18. **Experimental model of Pulmonary Hypertension**

Experiments were performed on male CD rats 300 – 350 g body weight, Charles River, Sulzfeld, Germany). Pulmonary hypertension was induced by a single subcutaneous injection of monocrotaline (MCT, 60 mg/kg, Sigma, Deishofen, Germany), dissolved in 0.1 M NaOH, adjusted to pH 7.4 with 0.1 M HCl, as described by Schermuly et al. (64). In these experiments 3 study groups were used: healthy rats, MCT-injected rats sacrificed after 3 weeks and after 5 weeks injection.

3.2.19. **Statistical analysis**

Data are expessed as means and standard error of mean (SEM). All statistical analysis was made by Student's *t*-test for paired and unpaired data between two groups, as appropriate or 1-way ANOVA with Newman-Keuls post hoc test for studies with more than two groups. Difference between groups was considered significant when $p<0,05$.

3.2.20. **sFRP-1 KO mice genereation.**

The sFRP-1 KO mice were obtained from Peter V. N. Bodine (Women's Health Research Institute, Wyeth Research) where they were produced by Lexicon Genetics, Inc. Briefly, the sFRP-1 KO (-/-) mouse line was constructed by deleting 1176 bp of exon 1 and subsequently replacing it with a LacZ/MC1-Neo selection cassette. Four targeted ES cell clones were identified and injected into C57BL/6 (albino) blastocyts. The chimeras were

mated to C57BL/6(albino) females to generate $sFRP^{+/-}$ animals which were subsequently intercrossed to produce WT (+/+), Heterozygous (+/-) and KO (-/-) animals.

3.2.21. **Pathway-Focused gene expression profiling using Real-Time PCR**

Total RNA was isolated from the tissue heart homogenates from sFPR-1 WT versus KO mice at one year of age with Qiagen RNeasy Mini Kit which combines the selective binding properties of a silica-based membrane with the speed of microspin technology. Up to 100μg of RNA longer than 200 bases binds to specific RNeasy silica membrane. 2mm cubicles of heart samples were homogenized and lysed using highly denaturing guanidine-thiocyanate–containing buffer, which immediately inactivates RNases to ensure purification of intact RNA. Efficient binding conditions of total RNA are created by specialized high-salt buffer system with addition of ethanol on RNeasy Mini spin column where conatminants are successfully washed out. Total RNA is eluted with 30μl of water.

With use of Nano Drop we determined the quantity and quality of extracted RNA. The recommended 1μg of total DNase treated RNA was added to the reverse transcription reaction (RT) to produce cDNA. Subsequently produced cDNA was used to perform Wnt signaling mouse PCR Array with the RT^2 Profiler PCR Array system (SABiosciences). Briefly, cDNA was added to ready made RT^2 PCR Master Mix containing SYBR Green and ROX reference dye. Prepared cDNA/PCR master mix solution was applied on Wnt signaling PCR Array 96-well plate. Each PCR Array Profiles the Expresion of 84 Pathway-Specific Genes plus control housekeeping genes. Real-Time PCR reaction was perform in Applied Biosystems Real-Time PCR 7300 machine and further analyzed on SABiosciences website according to provided instructions.

3.2.22. **Immunohistofluorescence**

6μm paraffin-embedded heart sections were cutted bu the microtome and incubated 45 minutes at 65°C and subsequently deparaffinized in xylene three times 3 minutes. Then slides were hydrated with 100% to 80% ethanol concentration. After the slides were washed with running tap water, the antigen was unmasked by microwaving 20 minutes in the retrieval buffer. Sections were incubated in 3% hydrogen peroxide in methanol for 20 minutes at room temperature, washed and blocked for 30 minutes in 2% bovine serum albumine. Then sections were probed overnight at 4°C with primary anti-rabbit antibody. Subsequently sections were

incubated with fluorescent secondary antibody (Appendix Table 5.). Primary antibody and DAPI fluorescent signal was then analysed by fluorescence microscopy.

Retrieval buffer (10mM Tris Base, 1mM EDTA, 0.05% Tween 20, pH=9)

3.2.23. **Echocardiographic analysis**

This study was performed by Dr. Sun J at Columbia University, New York to evaluate the heart parameters observed morphologically. Briefly, anesthetized animals were placed on a mouse bed in a shallow left lateral decubitus position. Transthoracic echocardiography was performed using a pediatric broad band 6–15 MHz linear array ultrasound transducer (Agilent Sonas 5500; Agilent Technologies, Palo Alto, USA). The ultrasound beam depth was set at 2 cm and frame rate at 150 frames/s. The two dimensional parasternal short-axis views were obtained at the level of LV papillary muscles.

3.2.24. **Histological analysis**

Hearts were arrested in diastole with PBS/20 mM KCl solution and pressure fixed at 20 mmHg with 10% neutral buffered formalin. Paraffin-embedded tissues were sectioned (6-µm thick) and stained with hematoxylin and eosin for light microscopy. Paraffin sections were also analyzed with Masson trichrome staining and visualized with a polarized light microscope to evaluate the myocardial collagen distribution.

4. Results

4.1. Wnt signaling expression in an experimental Pulmonary Hypertension

In the present study we utilized the animal model of Monocrotaline (MCT)-induced pulmonary hypertension in rats. To evaluate the possible involvement of the Wnt signaling pathway in pathogenesis of MCT-induced PAH, the mRNA and protein expression profile of the Wnt molecules was first determined. Two time points, 3 and 5 weeks after MCT injection were analyzed to obtain both the early and late stage of the disease.

4.1.1. mRNA expression profile of Wnt signaling in experimental Pulmonary Hypertension

The mRNA expression profile of the main extracellular and intracellular regulators of Wnt signaling was measured from healthy rats, and rats with MCT-induced PAH 3 and 5 weeks after injection. We focused on well-known canonical (Wnt1, Wnt3A) and non-canonical (Wnt5A) Wnt signaling ligands. Other targets were the Wnt ligand receptors like Frizzled 1 (facilitating both pathways), canonical Frizzled 2 and the extracellular Wnt modulator sFRP-1. Real-time PCR demonstrated a trend to progressive decrease in a well known canonical Wnt1 and Wnt3A ligands, while mRNA level of non-canonical Wnt5A was increased both 3 and 5 weeks after MCT injection. Not significant upregulation tendency in the Frizzled 1 and the sFRP-1 expression was also observed in MCT-PAH rat lungs (Figure 4.1.).

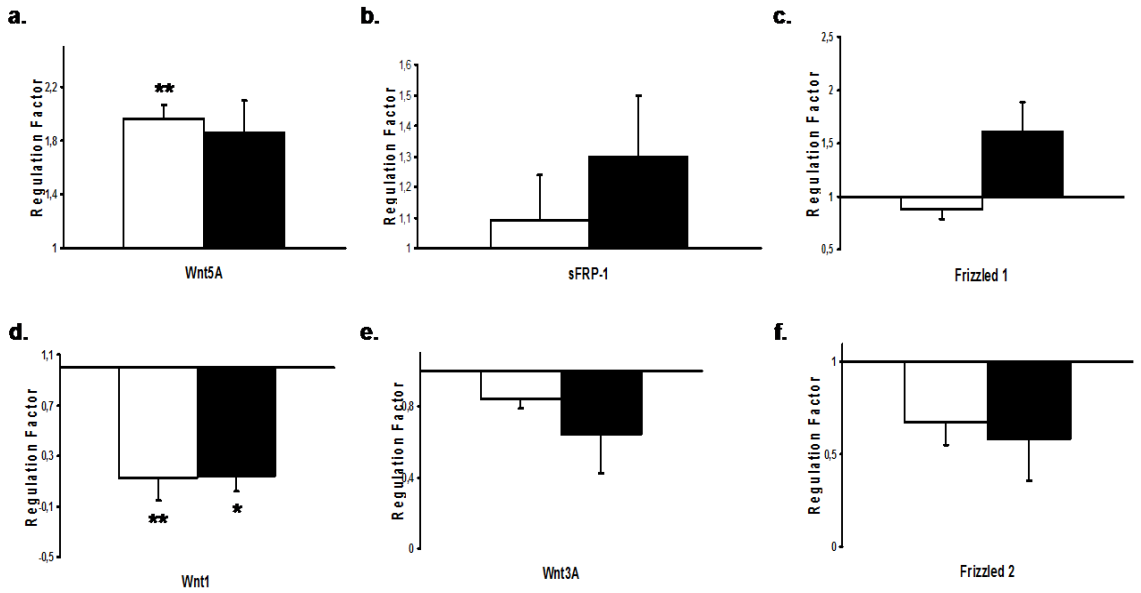

Figure 4.1: Expression of Wnt signaling ligands and receptors in lung tissues of control and MCT-induced PAH rats
mRNA expression of Wnt1, Wnt3a, Wnt5a, Frizzled 1, Frizzled2 and sFRP-1 in lung homogenates from control and after 3 weeks (white bar) and 5 weeks (black bar) of MCT-induced PAH rats, as analyzed by quantitative real-time PCR. All values were given as the mean ± SEM (n=3) and were normalized to PBGD. Values were presented significant as *P < 0.05, **P < 0.01 *vs* control lungs. All values were expressed as mean ± SEM (n=3). Healthy controls were set as 1 on X axis and expression profile from 3 and 5 weeks MCT were presented as fold of gene regulation.

The mRNA expression profile of the principle downstream effectors of canoncal Wnt signaling dependent genes Axin 1, GSK3β and β-Catenin were investigated in pulmonary hypertensive rat lungs after 3 weeks and 5 weeks of MCT injury. Real-time PCR demonstrated a significant increase in mRNA expression of all three targets in MCT-PAH rat lungs (Figure 4.2.) following 5 weeks of MCT injury.

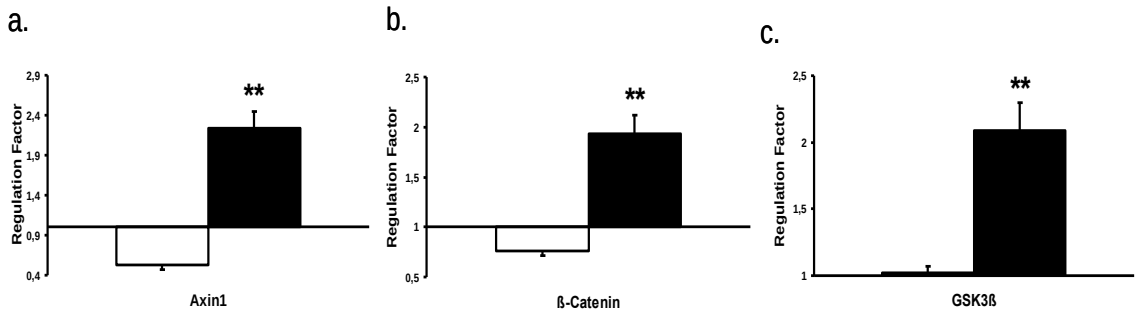

Figure 4.2: Expression of the Wnt signaling intracellular effectors in lung tissues of control and MCT-induced PAH rats
The mRNA expression of Axin1, GSK3β and β-Catenin in lung homogenates from control and MCT-induced PAH rats after 3 weeks (white bar) and 5 weeks (black bar) of MCT injury, as analyzed by quantitative real-time PCR. All values are given as the mean ± SEM (n=4) and were normalized to PBGD. Values are presented significant as **P < 0.01 *vs* control lungs. All values were expressed as mean ± SEM (n=3). Healthy controls were set as 1 on the X axis and the expression profile from 3 and 5 weeks of MCT were presented as fold of gene regulation.

4.1.2. **Protein expression profiling of the Wnt signaling intracellular effectors in an experimental Pulmonary Hypertension**

Protein expression profile of GSK3β and β-Catenin was investigated in pulmonary hypertensive rat lungs after 3 weeks and 5 weeks of MCT injury. Western blotting analysis and subsequent quantification normalized to GAPDH housekeeping control demonstrated a remarkable upregulation of ß-Catenin in 3 weeks MCT-PAH rat lungs and a significant time-

dependent upregulation of GSK3ß in both the 3 and 5 week time point in the MCT-PH rat lungs (Figure 4.3.).

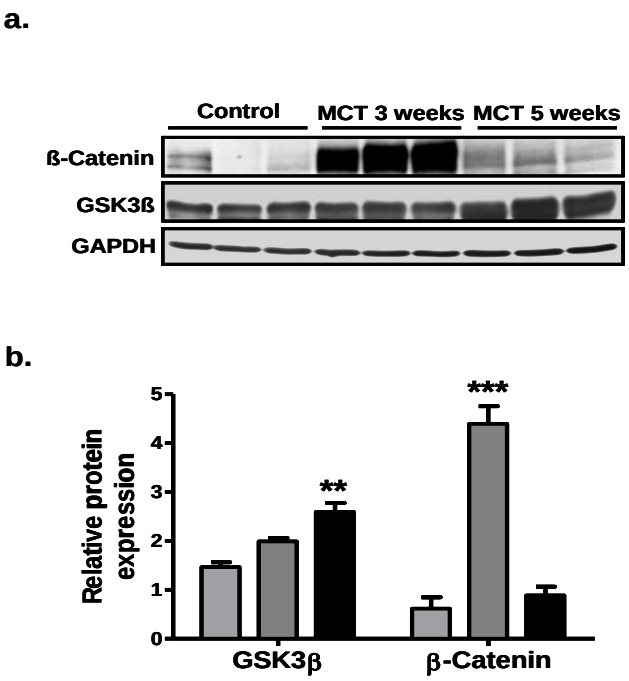

Figure 4.3. Expression of GSK3ß/ß-Catenin signaling molecules in the lung tissue of control and MCT-induced PAH rats
(a.) Protein expression as analyzed by western blotting and subsequent (b.) densitometric quantification of GSK3ß and ß-Catenin in control (light grey bar) and after 3 weeks (dark grey bar) and 5 weeks (black bar) of MCT-induced PAH in rats. GAPDH was used as a loading control. Values were presented significant as **P < 0.01, ***P < 0.001 *vs* control lungs. All values were expressed as mean ± SEM (n=3).

4.1.3. **Wnt signaling expression in PASMC's**

To estimate expression levels of the Wnt signaling pathway we isolated PASMC's from the lungs of MCT injected rats and observed the basal expression of the Wnt signaling dependent genes. Interestingly, we observed a significant decrease in the mRNA expression of the upstream canonical Wnt1, Frizzleds receptors 1 and 2 without changes in Wnt5A expression and the extracellular inhibitor sFRP-1 (Figure 4.4.).

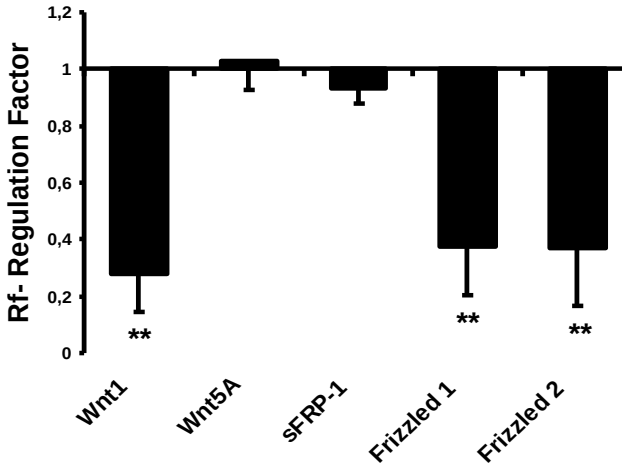

Figure 4.4. Expression of Wnt signaling in primary pulmonary arterial smooth muscle cells isolated from control and MCT-induced PAH rats
mRNA expression of Wnt1, Wnt5a, Frizzled 1, Frizzled2 and sFRP-1 in primary control PASMC's and PASMC's from MCT-induced PAH rats, as analyzed by quantitative real-time PCR. Control values were set as 1. All values were normalized to PBGD and determined as regulation factor compared with a control set as 1. Values were presented significant as **P < 0.01 *vs* control PASMC's. All values were expressed as mean ± SEM (n=4).

4.1.4. **GSK3β/β-Catenin signaling axis protein expression in PASMC's of MCT-induced Pulmonary Hypertension**

Western blot analysis of GSK3ß, phospho-GSK3ß (ser 9) and ß-Catenin in primary PASMC revealed an increase in the total protein expression of ß-Catenin, GSK3ß and a significant increase in GSK3ß phosphorylation at the serine 9 residue (pGSK3ß ser 9) after 5 weeks of the MCT injection (Figure 4.5. a-b).

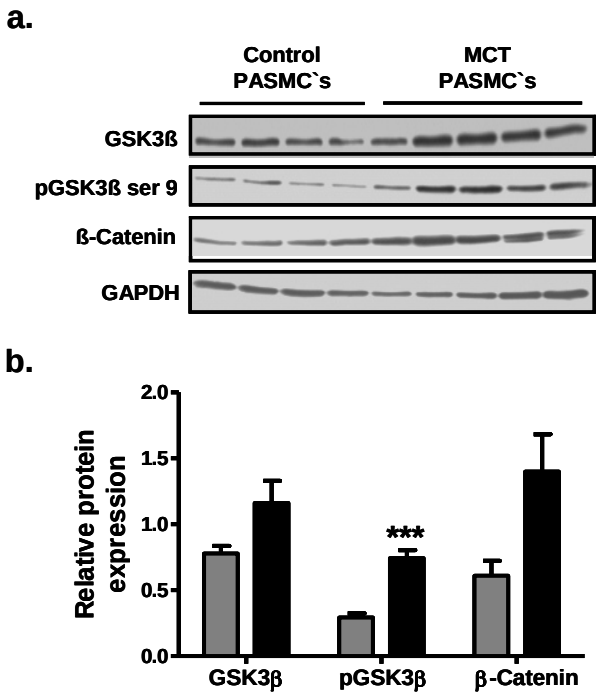

Figure 4.5. Regulation of GSK3ß/ß-Catenin signaling molecules in primary PASMC's isolated from control and MCT-induced PAH rats
(a.) Protein expression as analyzed by western blotting and subsequent (b.) densitometric quantification of total GSK3ß/GAPDH, phosphorylation of GSK3ß at serine 9 residue (pGSK3ß S9/total GSK3ß) and ß-Catenin/GAPDH in primary PASMCs isolated from control (grey bar) and MCT-induced PAH rats (black bar). GAPDH was used as a loading control. All values were expressed as mean ± SEM (Control PASMCs, n=4; MCT-PASMCs n=5). Values were presented significant as ***P < 0.001 *vs* control PASMC's.

4.2. The role of GSK3β/β-Catenin signaling axis in PDGF-BB mitogenic signaling in MCT-PASMC

The role of growth factors, tyrosine/serine-threonine kinase receptors in PAH has been extensively studied at the cellular, preclinical and clinical level. Accumulation of growth factors such as platelet derived growth factor (PDGF), epidermal growth factor (EGF), fibroblast growth factor (FGF) and vascular endothelial growth factor (VEGF) and pro-survival factors like survivin in the pulmonary vasculature has suggested categorizing this disease as a pseudo-malignant proliferatory disorder (206-210).

4.2.1. Phosphorylation of GSK3β by PDGF-BB mitogen in MCT-PASMC's

We evaluated the response of the GSK3β/β-Catenin system to PDGF-BB, which is known to play a critical mitogenic role in PASMC's in PAH. Therefore, we stimulated the MCT-PASMC's with PDGF-BB for 24 hrs. PDGF-BB induced a significant increase in

PASMC proliferation rate (4.6. a), which interestingly correlated with sustained and increased phosphorylation status of GSK3ß at serine 9 (Figure 4.6. b) without any change in the expression level of β-Catenin.

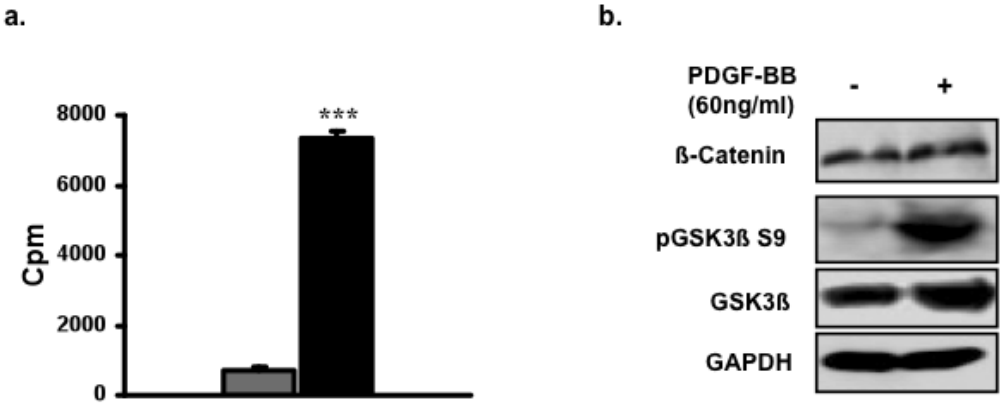

Figure 4.6. Increased phosphorylation of GSK3ß in primary PASMCs after stimulation with PDGF-BB.
(a.) Proliferation of PASMCs after stimulation with PDGF-BB (60ng/ml) (black bar) versus 0.1%FCS (white bar) for 24 hrs as assessed by [^{3}H]-thymidine incorporation (a.). All values were expressed as mean ± SEM (n=4). ***P < 0.001 *vs* 0.1% FCS. (b.) Protein expression as analyzed by western blotting of ß-Catenin, GSK3ß and its phosphorylation status at the serine 9 residue (pGSK3ß S9) in MCT-PASMCs after stimulation with PDGF-BB (60ng/ml) for 24 hrs.

4.2.2. **GSK3β/β-Catenin system is differentially regulated by PDGF-BB and Wnt3A signaling pathways in MCT-PH PASMC's**

Inactivation of GSK3β is usually associated with β-Catenin accumulation so therefore we wondered whether GSK3β may have additional functions in the pathogenic PDGF signaling pathway. To rule out the possibility that sustained up to 24h effect of inactivation of GSK3β we asked if transcriptional response of ß-Catenin does not appear earlier during the PDGF treatment. To investigate this issue MCT-PASMCs were stimulated with PDGF-BB (60ng/ml) or Wnt3A (50ng/ml) for 6 hrs and expression and phosphorylated status of upstream regulators of GSK3ß and ß-Catenin was elucidated. Untreated and stimulated cells were nuclear fractionated and subjected to western blotting with AKT, GSK3ß, ß-Catenin, phospho-AKT and two sites of GSK3ß phosphorylation at serine 9 residue and tyrosine 216 residue (pGSK3ß S9 and Y216). Interestingly, both PDGF-BB and Wnt3A stimulation for 6 hrs caused a significant increase in phospho-AKT and phospho-GSK3ß (serine 9) and a decrease in Axin 1 levels (Figure 4.7. b). In contrast, only Wnt3A stimulation caused nuclear accumulation of ß-Catenin (Figure 4.7. b) suggesting an individual role of GSK3ß in growth factor signaling which is not correlated with ß-Catenin nuclear translocation. Most

interestingly, PDGF-BB and Wnt3A had opposite effect on GSK3ß phosphorylation status at tyrosine 216 residue which contrary to no change induced by Wnt3A, was decreased after PDGF-BB stimulation (Figure 4.7. b).

4.2.3. **Phosphorylation status of GSK3β by PDGF-BB mitogen in MCT-PH PASMC's is restored by Imatinib treatment.**

To verify the specificity of PDGF-BB mediated signaling, PASMCs were also simultaneously treated with PDGF-BB and Imatinib. The proliferation rate induced by PDGF-BB at the 24 hrs of treatment was successfully and significantly decreased upon Imatinib pretreatment (Figure 4.7. a). To determine the early response of the GSK3β/β-Catenin system to PDGF-BB, MCT-PASMC's were stimulated with PDGF-BB alone and pretreated with Imatinib for 6 hrs. Imatinib treatment significantly prevented PDGF-BB-induced phosphorylation changes of AKT and GSK3ß at both of the tested phosphorylation residues observed at 6 hrs after stimulation with PDGF-BB (Figure 4.7. b).

a.

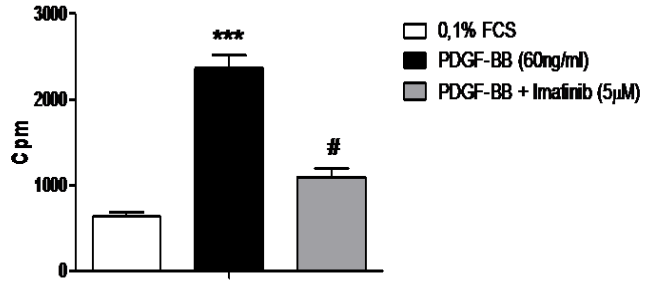

b.

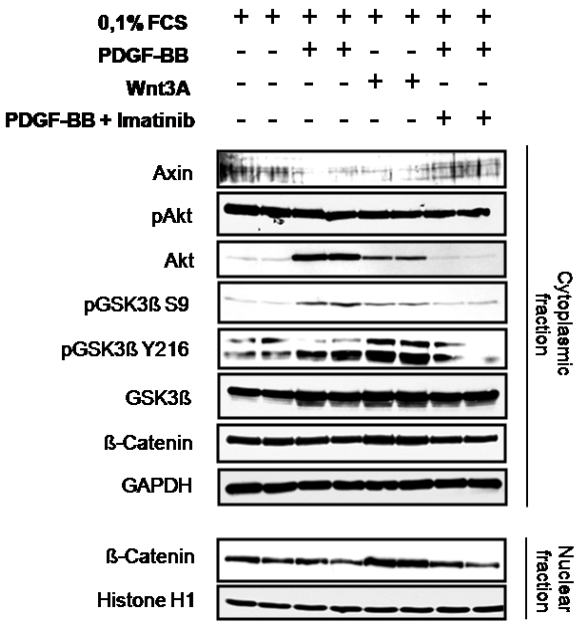

Figure 4.7. GSK3ß/β-Catenin axis is differentially regulated by PDGF-BB and Wnt3A stimulation in primary PASMCs.
(a.) Proliferation of PASMCs after stimulation with PDGF-BB (60ng/ml) for 24hrs in the absence or presence of the PDGF-BB inhibitor Imatinib (Gleevec=STI571) (5µM) as assessed by [^{3}H]-thymidine incorporation. All values were expressed as mean ± SEM (n=4). ***P < 0.001 *vs* 0.1% FCS and #P<0.01 vs PDGF-BB (60ng/ml). (b.) Protein expression analyzed by western blotting and subsequent densitometric quantification of Axin1, AKT, phospho-AKT (pAKT), GSK3ß and its phosphorylation status at serine 9 residue (pGSK3ß S9) and at tyrosine 216 residue (pGSK3ß Y216) and ß-Catenin in both cytoplasmic and nuclear fractions in MCT-PASMCs. Cells were stimulated with PDGF-BB (60ng/ml) in the absence or presence of the PDGF-BB inhibitor Imatinib (Gleevec=STI571) (5µM) or Wnt3a (50ng/ml) for 6hrs. GAPDH was used as a loading control for the cytoplasmic fraction and histone H1 was used as a loading control for the nuclear fraction.

4.2.4. **The generation of human GSK3β constructs with point mutations at the main functional phosphorylation residues.**

GSK3β has two splice isoforms GSKB1 (420 aa) and GSKB2 (433 aa) which are present among all human tissues (Figure 4.8. a). They differ by 13 amino acid (aa). In human lung homogenates using we were able to detect both of them but in human lung PASMC's only one isoform (GSKB1) was detected (Figure 4.8. b,c). For the subsequent overexpression experiment in primary MCT-PASMC's we used human GSKB1 as a template to generate GSK3 β constructs.

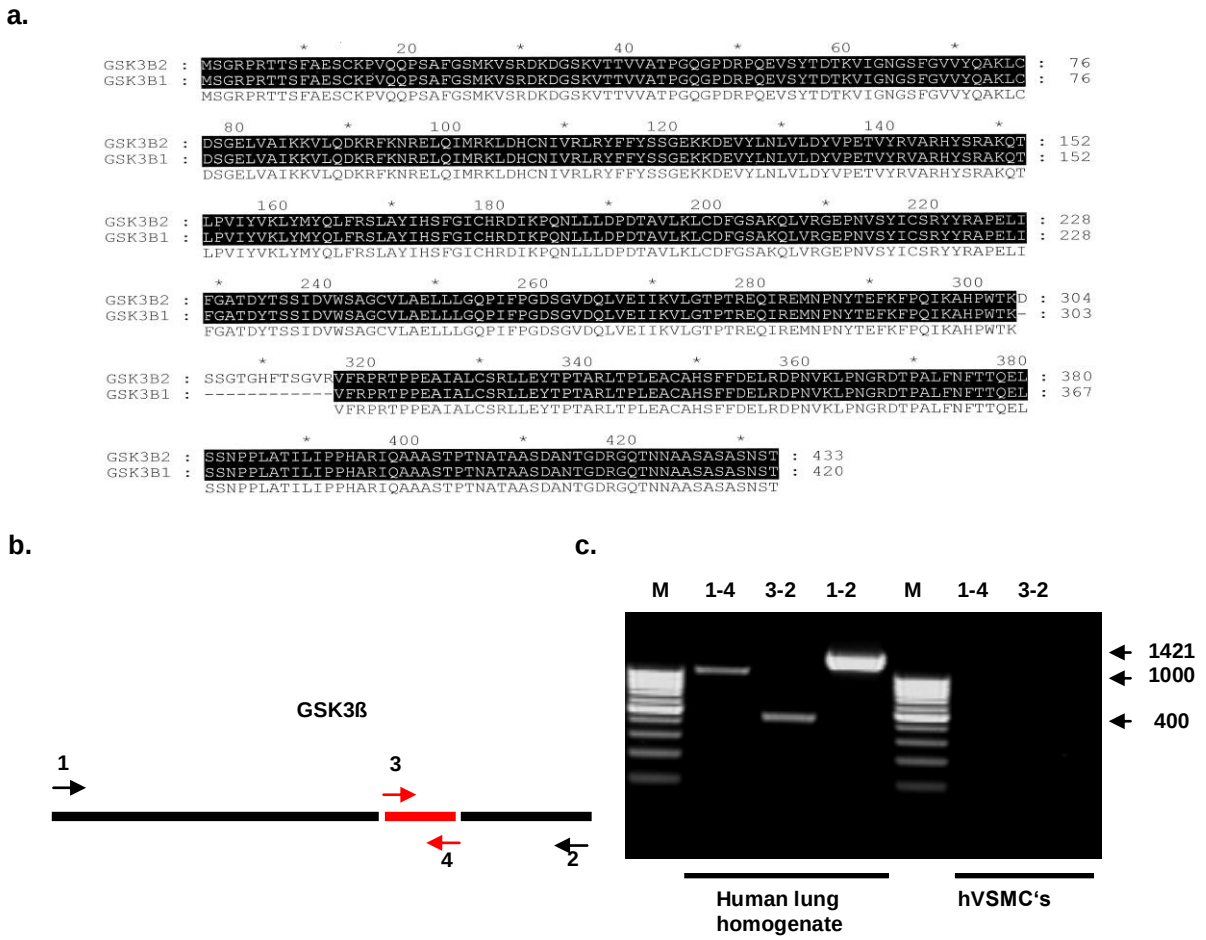

Figure 4.8. Detection of two GSK3ß splice variants in human lungs.
(a.) Sequence alignment of two GSK3β isoforms (GSKB1- 420aa, GSKB2- 433aa) (b.) A schematic picture of the experimental design to detect both isoforms by missing 13aa region (red line) in the GSKB1 isoform with the usage of specific primers: 1- to amplify the sequence starting at 5' end of human GSK3β, 2- to amlify sequence starting at the 3' end of human GSKβ, 3- to amplify 13aa fragment present only in the GSKB2 isoform starting at the 5' end, 4- to amplify the 13aa fragment present only in the GSKB2 isoform starting at the 3' end (c.) Detection of the GSK3β isoforms (GSKB1 and GSKB2) in the human lung homogenate and human lung PASMC's using primers combination 1-4 by semi-quantitative PCR.

To further evaluate the contribution of GSK3ß to the MCT-PASMCs mitogenic response, we generated pcDNA 3.1 TOPO-cloning constructs carrying the human sequence of GSK3ß wild type cDNA. Additionally using site-directed mutagenesis method we performed point mutations on the main functional phosphorylation sites of GSK3ß, which was constitutively active GSK3ß S9A (serine at residue 9 is replaced to alanine) and GSK3ß Y216D (tyrosine at 216 residue is replaced to aspartic acid). The Y216 was mutated to negatively charged aspartic acid (D) created to simulate phosphorylation at this residue. Sequence analysis performed on each construct confirmed the intended point mutation at specific sites in GSK3ß S9A and GSK3ß Y216D (Figure 4.9. a, b).

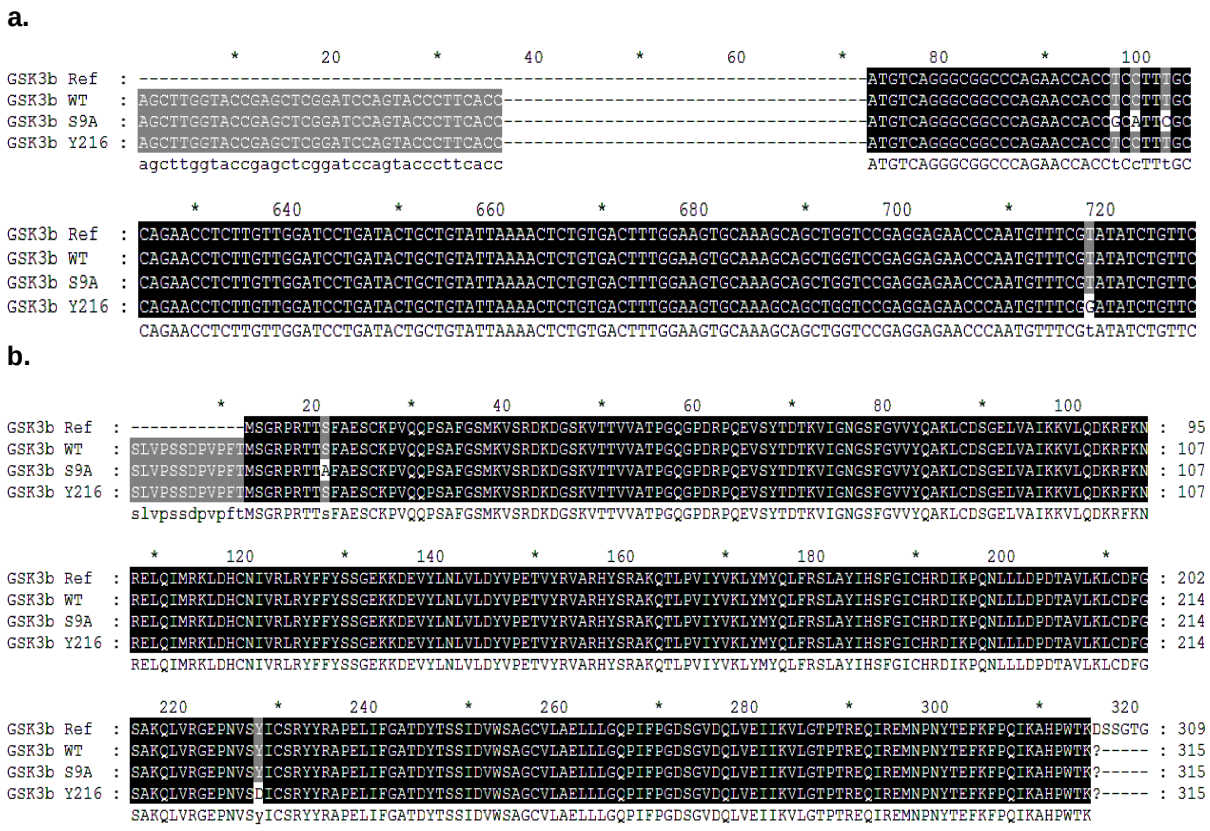

Figure 4.9. Sequence alignment of human GSK3β constructs designed for overexpression in primary PASMC's.
(a.) Nucleotide and (b) amino acid sequence alignment of human GSK3ß (GSK3ß Ref; GenBank accession number NM_002093), wild type GSK3ß (GSK3ß WT) and GSK3ß after site directed mutagenesis at serine 9 to alanine (GSK3ß S9A) and tyrosine 216 to aspartic acid. The non-identical residue corresponds to the mutation, S9A where wild type codon TCC encodes Serine <S>, the mutated codon GCA encodes Alanine <A>. and Y216D where the wild type codon TAT encodes the tyrosine <Y>, the mutated codon GAT encodes the aspartic acid <D>.

4.2.5. **Overexpression of human wild type GSK3β and point mutated variants influences PASMC's proliferation**

Transient overexpression of GSK3ß and its mutated variants GSK3ß S9A GSK3ß Y216D in MCT-PASMCs resulted in significantly enhanced total GSK3ß expression 48h post transfection. Empty vector (EV) transfection resulted in no change in GSK3ß protein expression (Figure 4.10. a). Importantly, FCS stimulation did not lead to any phosphorylation in the GSK3ß S9A mutant overexpressing cells (Figure 4.10. a). Unfortunately the loss of the 216 residue phosphorylation was not observed by western blot analysis (Figure 4.10. a) but further sequence analysis of the GSK3β Y216D construct confirmed the correct mutation. A problem could occur secondary to antibody specificity or other tyrosine residues, which are present at residue 221 and 222. The gain of GSK3ß expression was coupled to a significant

increase in [^{3}H]-thymidine uptake as compared to EV expressing cells 24h post serum stimulation. On the other hand, GSK3ß S9A and Y216D mutations decreased [^{3}H]-thymidine uptake, suggesting that GSK3ß phosphorylation is involved in PASMC proliferation (Figure 4.10. b).

Transiently transfected MCT-PASMC's overexpressing wild type and point mutated forms of the GSK3ß were also treated with PDGF-BB and proliferation rate of these cells was assessed. Similar to 10% FCS stimulated MCT-PASMC's the gain of wild type expressed GSK3ß was coupled to a significantly increased [^{3}H]-thymidine uptake as compared to EV expressing cells 24h post serum stimulation (Figure 4.10. c). On the other hand, only the GSK3ß Y216D mutant expression but not S9A had significant effect and decreased PDGF-induced [^{3}H]-thymidine uptake, suggesting that GSK3ß tyrosine phosphorylation is involved in PDGF-BB mediated PASMC proliferation (Figure 4.10. c).

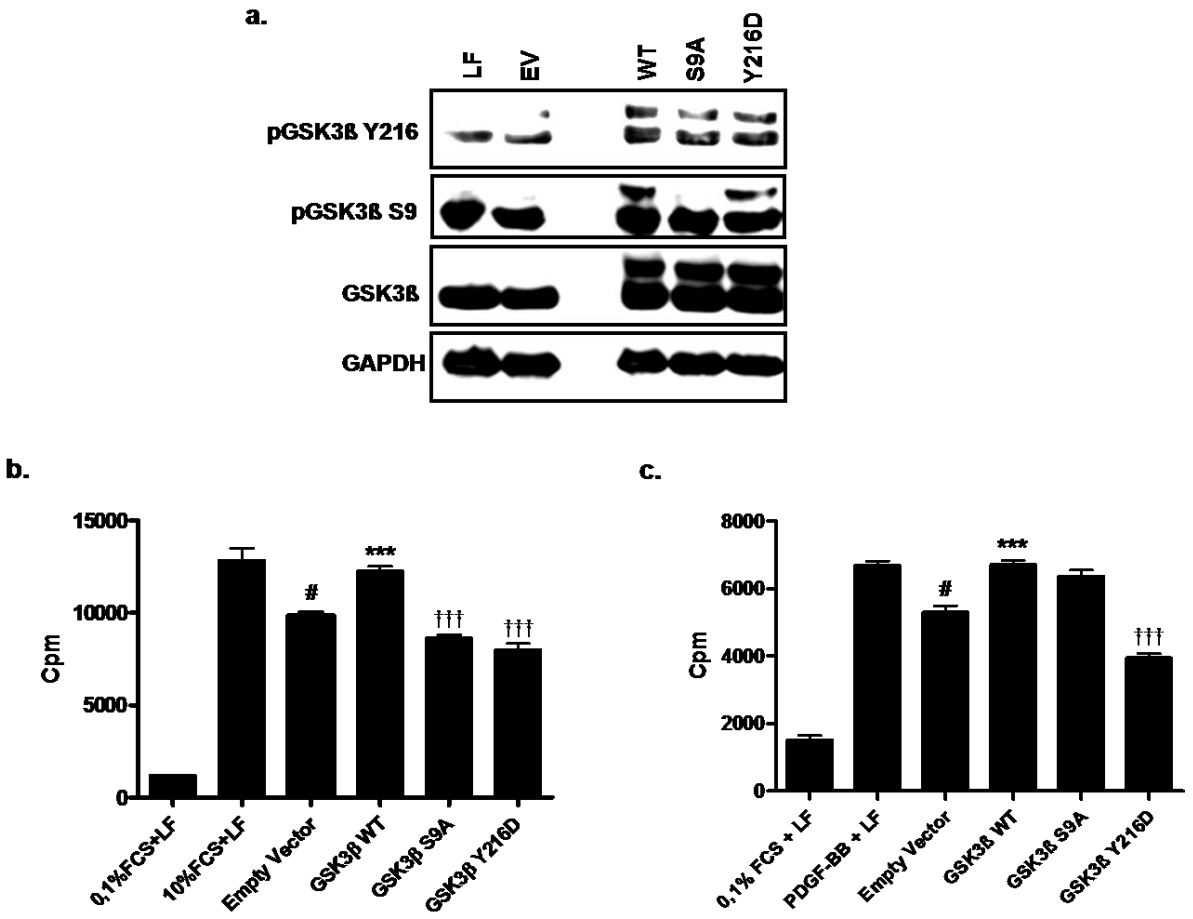

Figure 4.10. Transient transfection of wild type and mutants of GSK3ß influences MCT-PAH PASMCs proliferation

(a.) Primary rat MCT-PAH PASMCs were transiently transfected with GSK3ß wild type (GSK3ß WT), constitutively active GSK3ß (GSK3ß S9A) and GSK3ß Y216D, empty vector

(pcDNA3.1 TOPO) (EV) or with no DNA (only lipofectamine, LF). 24 hrs post transfection, expression and phosphorylation of GSK3ß (GSK3ß, pGSK3ß S9 and pGSK3ß Y216D) were analyzed by western blotting. Additionally MCT-PAH PASMCs transiently transfected with GSK3ß wild type (GSK3ß WT), constitutively active GSK3ß (GSK3ß S9A) and GSK3ß Y216D, empty vector (pcDNA3.1 TOPO) (EV) or with no DNA (only lipofectamine, LF) and proliferation of MCT-PAH PASMCs after stimulation with (b.) 10% FCS or (c.) with PDGF-BB (60ng/ml) for 24 hrs was assessed by [^{3}H]-thymidine incorporation. All values are expressed as mean ± SEM (n=4). Data were expressed as cpm. ***P < 0.001 *vs* 0.1% EV transfected cells and ††† p<0.001 *vs* GSK3ß WT transfected cells and # P<0,01 *vs* 10% FCS + LF (b.) or PDGF-BB + LF (c.)

To further evaluate the influence of GSK3ß on the cell signaling transduction, primary rat MCT-PAH PASMCs were transiently transfected with GSK3ß wild type (GSK3ß WT), constitutively active GSK3ß (GSK3ß S9A) and GSK3ß Y216D. Western blot analysis was performed on β-Catenin and Extracellular Regulated Kinase (ERK). Interestingly, the transient overexpression of wild type GSK3ß increased ERK1/2 phosphorylation as compared to EV transfection and Lipofectamine treatment (with no DNA). In contrary, GSK3ß S9A and Y216D variants decreased serum-induced ERK1/2 phosphorylation in MCT-PASMCs (Figure 4.11.). The overexpression of GSK3ß Y216D had much more prominent effect on ERK phosphorylation as compared to the S9A mutation as demonstrated by a greater reduction of ERK phosphorylation in serum conditions.

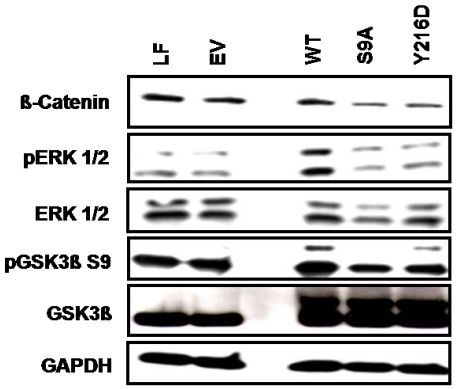

Figure 4.11. Transient transfection of wild type and constitutively active GSK3ß influences ERK phosphorylation
Primary rat MCT-PAH PASMCs were transiently transfected with GSK3ß wild type (GSK3ß WT), constitutively active GSK3ß (GSK3ß S9A) and GSK3ß Y216D, empty vector (pcDNA3.1 TOPO) (EV) or with no DNA (only lipofectamine, LF). 48 hrs post transfection, protein expression of ß-Catenin, ERK1/2 and phospho-ERK1/2 were analyzed by western blotting. As experimental control we used GSK3ß total and GSK3ß S9A and GAPDH was used as loading control.

4.3. **Upregulation of GSK3β in human lungs of IPAH**

To further evaluate the possible relationship of the GSK3β/β-catenin axis to the pathogenesis of human PAH we isolated protein from lung homogenates of human healthy subjects and iPAH patients (n=4). Interestingly protein expression analysis revealed a significant upregulation of total GSK3β with a trend to a decrease in β-catenin accumulation (Figure 4.12. a,b). This is exactly the same expression profile situation observed in the late stage of the experimental MCT-induced PAH in rats.

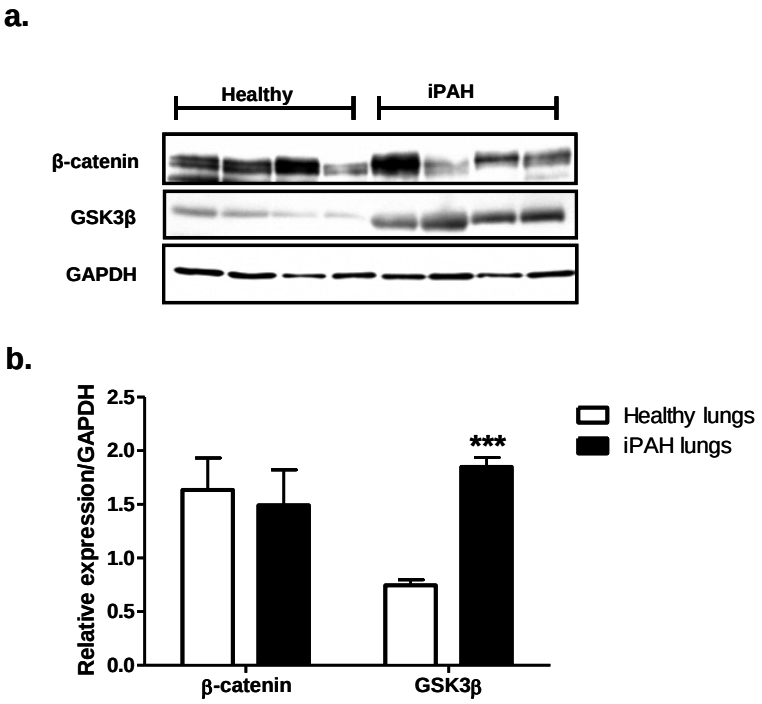

Figure 4.12. Expression of GSK3ß/ß-Catenin signaling molecules axis in human lungs of healthy and iPAH patients
(a.) Protein expression as analyzed by western blotting and subsequent (b.) densitometric quantification of GSK3ß and ß-Catenin in in human lungs of healthy and iPAH patients. GAPDH was used as a loading control. Values were presented significant as ***P < 0.001 *vs* control lungs. All values were expressed as mean ± SEM (n=4).

This result together with significant *in vivo* upregulation of GSK3β collectively suggests that this multi tasking kinase may be of future interest for therapeutical strategies to reverse abnormal PASMC proliferation and possibly benefit the reversing of the vascular remodeling in PAH.

4.4. Canonical Wnt signaling in PASMC's of MCT-induced Pulmonary Hypertension

To further evaluate the effect of translocation of the β-Catenin to the nucleus MCT-PASMC's were stimulated with Wnt3A, potent activator of canonical Wnt signaling pathway. MCT-PASMC's were stimulated with Wnt3A alone and in combinations with 10% FCS and PDGF-BB. Stimulation with Wnt3A alone did not alter proliferation rate of MCT-PASMC's (Figure 4.13. a) but did in combination with FCS and PDGF-BB (Figure 4.13. b,c), Wnt3A significantly decreased serum and the PDGF-BB-induced proliferation rate of these cells.

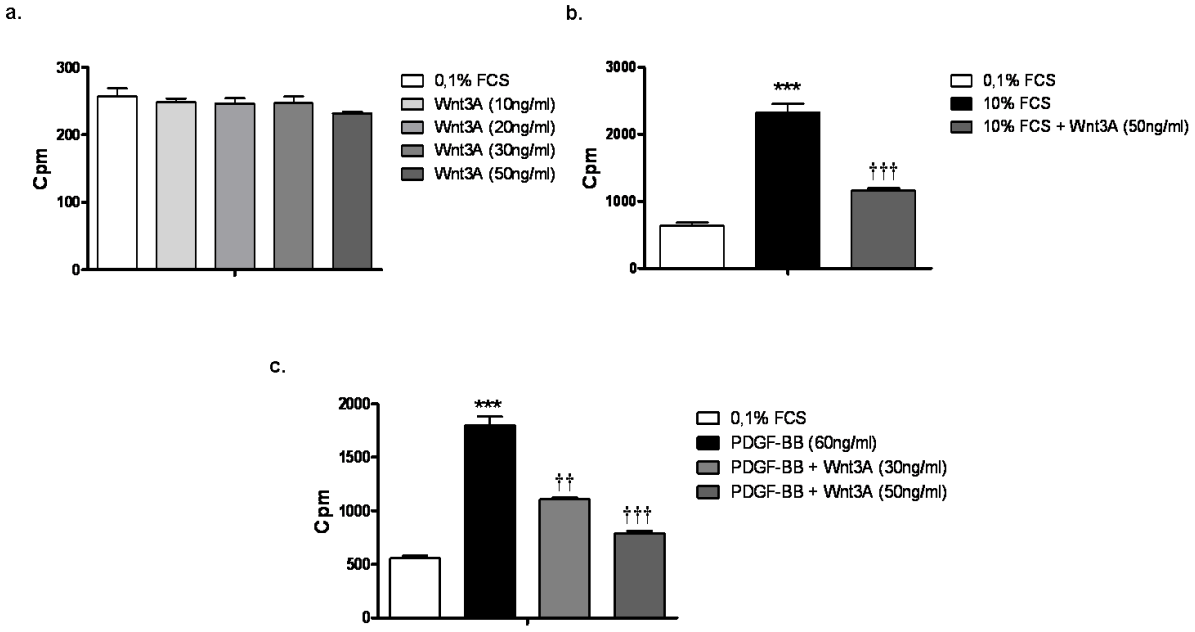

Figure 4.13. Canonical Wnt3A decreases MCT-PAH PASMCs proliferation
Primary rat MCT-PAH PASMCs were starved 24 hrs in 0,1% FCS and further stimulated for 24 hrs with (a.) Wnt3A (10-50ng/ml), (b.) 10% FCS alone and pretreated with (c.) Wnt3A and PDGF-BB alone and pretreated with Wnt3A (30-50ng/ml) and proliferation of MCT-PAH PASMCs was assessed by [^{3}H]-thymidine incorporation. All values are expressed as mean ± SEM (n=4). Data were expressed as cpm.***P < 0.001 *vs* 0.1% FCS cells and †† p<0.01; ††† p<0.001 versus 10% FCS or PDGF-BB stimulated cells.

To confirm this result MCT-PASMC's were stimulated by other Wnt activator. Canonical signaling pathway was induced by stimulation with Lithium Chloride (LiCl), a well accepted in the literature as an activator of the Wnt/β-Catenin pathway. Serum induced proliferation of MCT-PASMC's was in a dose dependent portion abolished by LiCl (Figure 4.14.) consistent with previous results.

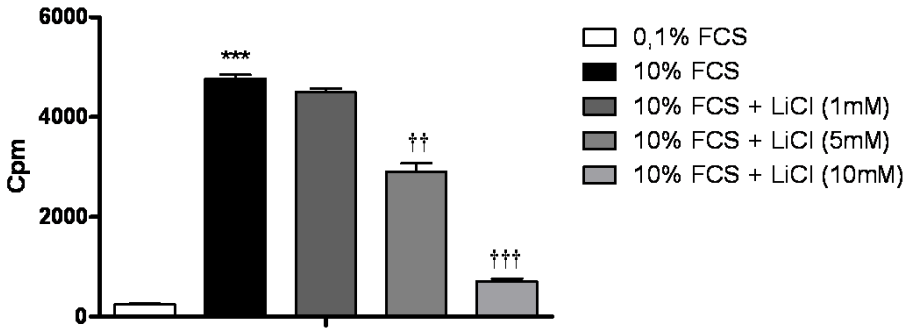

Figure 4.14. Lithium Chloride decreases serum-induced MCT-PAH PASMCs proliferation
Primary rat MCT-PAH PASMCs were starved for 24 hrs in 0,1% FCS and further stimulated for 24 hrs with 10% FCS alone or pretreated with LiCl (1-10mM) and the proliferation of the MCT-PAH PASMCs was assessed by [^{3}H]-thymidine incorporation. All values are expressed as mean ± SEM (n=4). Data were expressed as cpm. ***P < 0.001 *vs* 0.1% FCS cells, †† p<0.01 and ††† p<0.001 *vs* 10% FCS stimulated cells.

4.5. Wnt signaling in cardiac remodeling. Cardiac phenotype of sFRP-1 KO mice

To determine the influence of the Wnt canonical pathway in the heart *in vivo*, sFRP-1 knock-out (KO) mice were studied. Deletion of this gene in theory should lead to activation of the canonical Wnt pathway. To determine the role of sFRP-1 gene in heart function, we characterized the sFRP-1 KO mice over one year of age.

4.5.1. Pattern of sFRP-1 expression in normal mice hearts

To determine the role of sFRP-1 in the heart, the localization study of sFRP-1 in the heart muscle of the WT adult mice during life was performed. Very interestingly immunohistochemical staining revealed that sFRP-1 is abundantly present in mouse heart at 3, 6 and 12 months (n=3, Figure 4.15.) of age predominantly in the cardiomyocytes (Figure 4.15. a-f) but also is highly expressed in the endothelial cells (Figure 4.15. g-l). This strongly suggests the need for this factor for the maintenance of the heart and that the lack of sFRP-1 can be implicated in pathological heart condition.

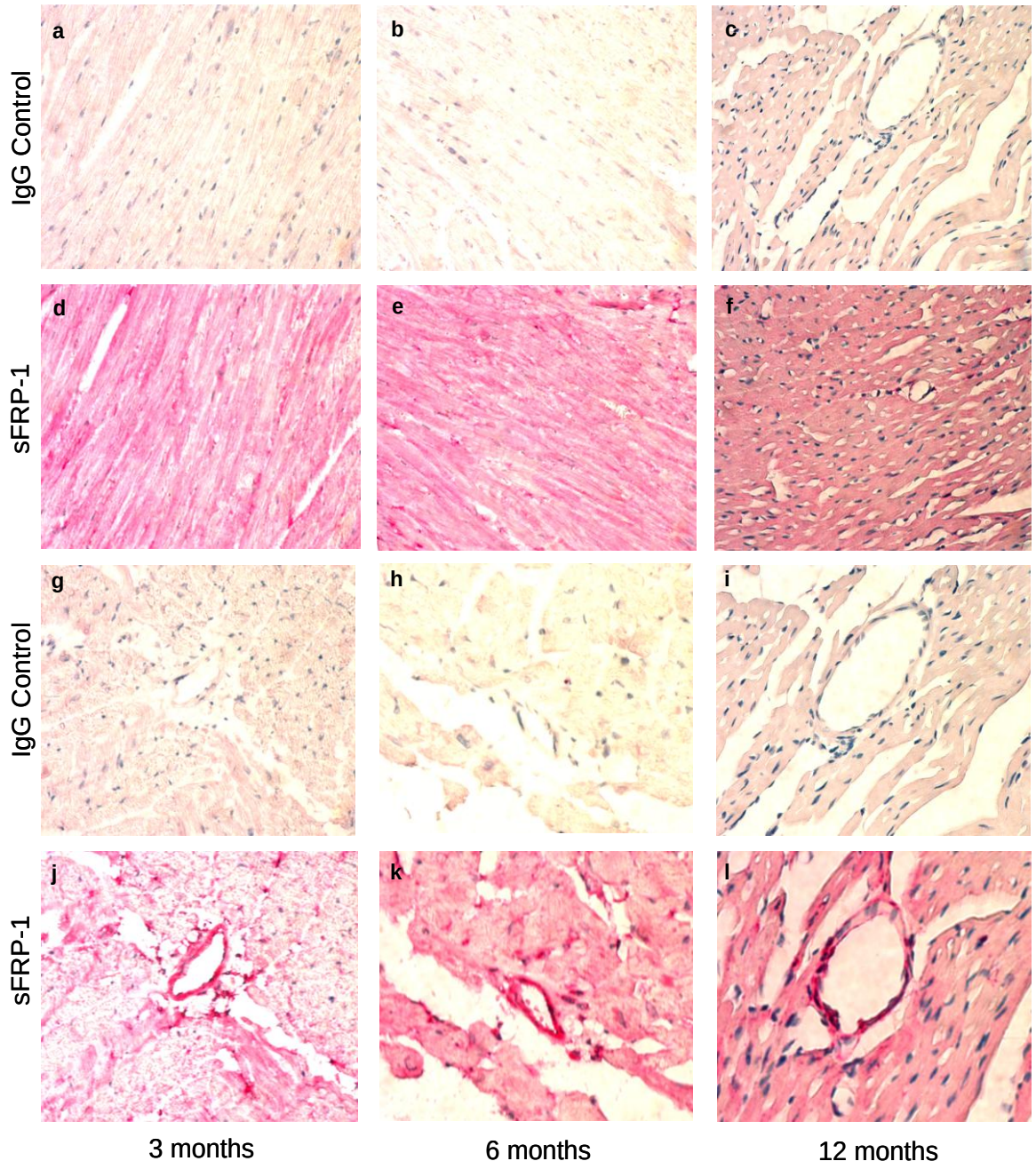

Figure 4.15. The abundant expression of sFRP-1 in the normal heart during mice adult life.
Immunohistochemical staining of sFRP-1 in heart sections at 3 months (d,j), 6 months (e,k) and 12 months (f,l) with IgG controls respectively (a,g), (b,h), (c,i). Sections were counterstained with hematoxylin. Magnification is 40x.

4.5.2. **sFRP-1 KO mice increase heart size**

To determine the role of sFRP-1 in heart function, we characterized the cardiac phenotype of sFRP-1 KO mice over one year of their life. The KO mice grossly appeared to be normal at birth and over 3 months of their life. There was no significant difference in

survival at one year of age between the KO and WT mice. However, at the 6 months time point the KO mice began to develop hypertrophic changes in the heart compared to WT littermates with an increase in the heart/body weight ratio (n=5, Figure 4.16. b). At one year of age the sFRP-1 KO mice interestingly develop a marked increase in heart size (Figure 4.16. a) with an age dependent significant progression of the heart/body weight ratio (Figure 4.16. b).

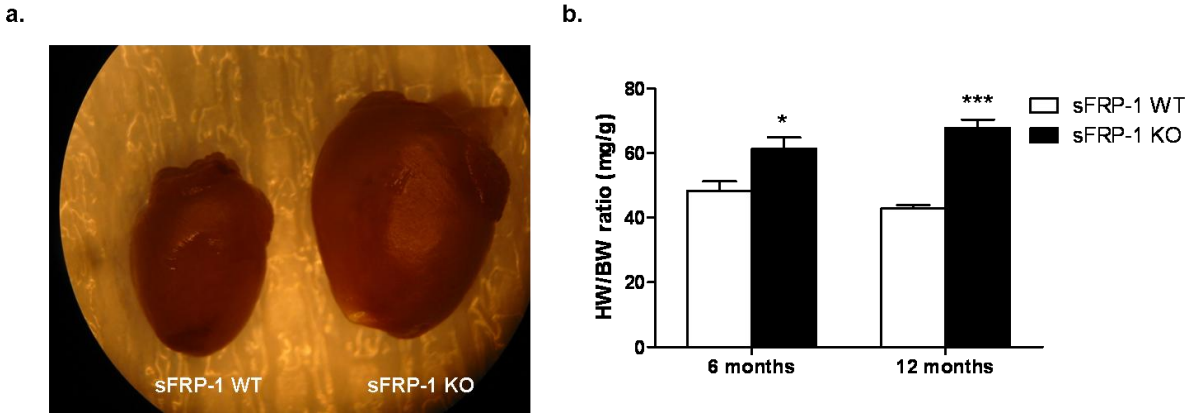

Figure 4.16. sFRP-1 KO mice develop heart hypertrophy at 12 months of age.
(a.) Representative picture of whole hearts of WT and sFRP-1 KO mice at 12 months of age (n=3) (b.) Heart weight/body weight ratio of the sFRP-1 KO mice at 6 months compared to 12 months of age (n=5). Values were presented significant as *P < 0.05, ***P < 0.001 *vs* control litermates hearts. All values were expressed as mean ± SEM.

Although no or little changes were found in heart parameters at 3 and 6 months of age in the sFRP-1 KO mice, at the 12 months time point a significant phenotype was observed. Following the observation of increase heart size, histological analysis using hematoxylin and eosin (H&E) staining of the sFRP-1 KO hearts showed an increased in Left Ventricular End Diastolic Dimension (LVEDD) size compared with wild type hearts (n=3, Figure 4.17. a. i-ii) at one year of age. Furthermore echocardiographic analysis of the heart of sFRP-1 KO and wild-type littermates was performed and confirmed that the KO mice developed LV chamber dilation compared with WT mice. We were able to observe significant increase in LVEDD (KO/n=7, vs WT/n=3, Figure 4.17. b) in sFRP-1 KO mice at 12 months of age with a significant increase in LV Posterior Wall thickness (PW) above the increase already seen at 6 months of age (KO/n=7, vs WT/n=3) and sustained until 12 months of age (KO/n=7 vs WT/n=3, Figure 4.17. c). Significant decrease in fractional shortening (FS, KO/n=7 vs

WT/n=3, Figure 4.17. d) was also observed in sFRP-1 KO mice at 12 months of age showing decrease in normal LV function.

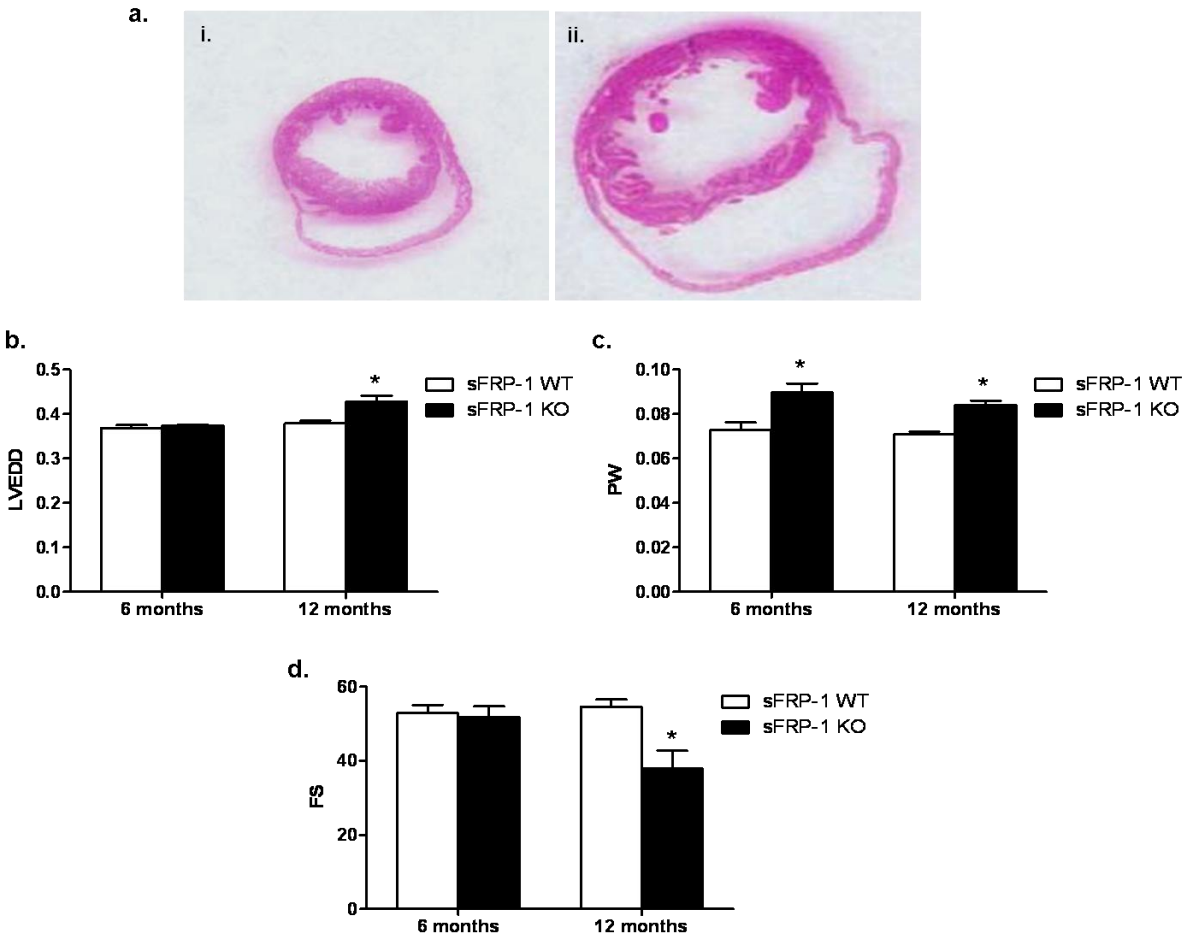

Figure 4.17. **Development of cardiac remodeling with worsened LV parameters**.
(a.) Histological analysis using hematoxylin and eosin (H&E) staining of the sFRP-1 (i) WT and (ii) sFRP-1 KO hearts (n=3). Echocardiographic analysis of the sFRP-1 WT and KO mice hearts representing; (b.) LV end diastolic dimension (LVEDD) (c.) LV posterior wall thickness (PW) (d.) Fractional Shortening, (FS). Values were presented significant as *P < 0.05 *vs* control litermates hearts. All values were expressed as mean ± SEM

4.5.3. **sFRP-1 KO mice increase forming fibrotic lesions in heart myocardium**

Trichrome staining was performed on the histological sections of the heart at 6 and 12 months time points. No fibrosis was observed in the sFRP-1 KO mice at 6 months (n=3, Figure 4.18. a,b) of age however, we were able to show an increase in interstitial and perivascular fibrosis in the KO hearts at the 1 year time point compared with WT littermates (n=3, Figure 4.18. c,d). These results taken together with the above hemodynamic

observations suggest that sFRP-1 plays an important role in maintaining normal cardiovascular function. The absence of sFRP-1 leads to cardiac remodeling with increased fibrosis content.

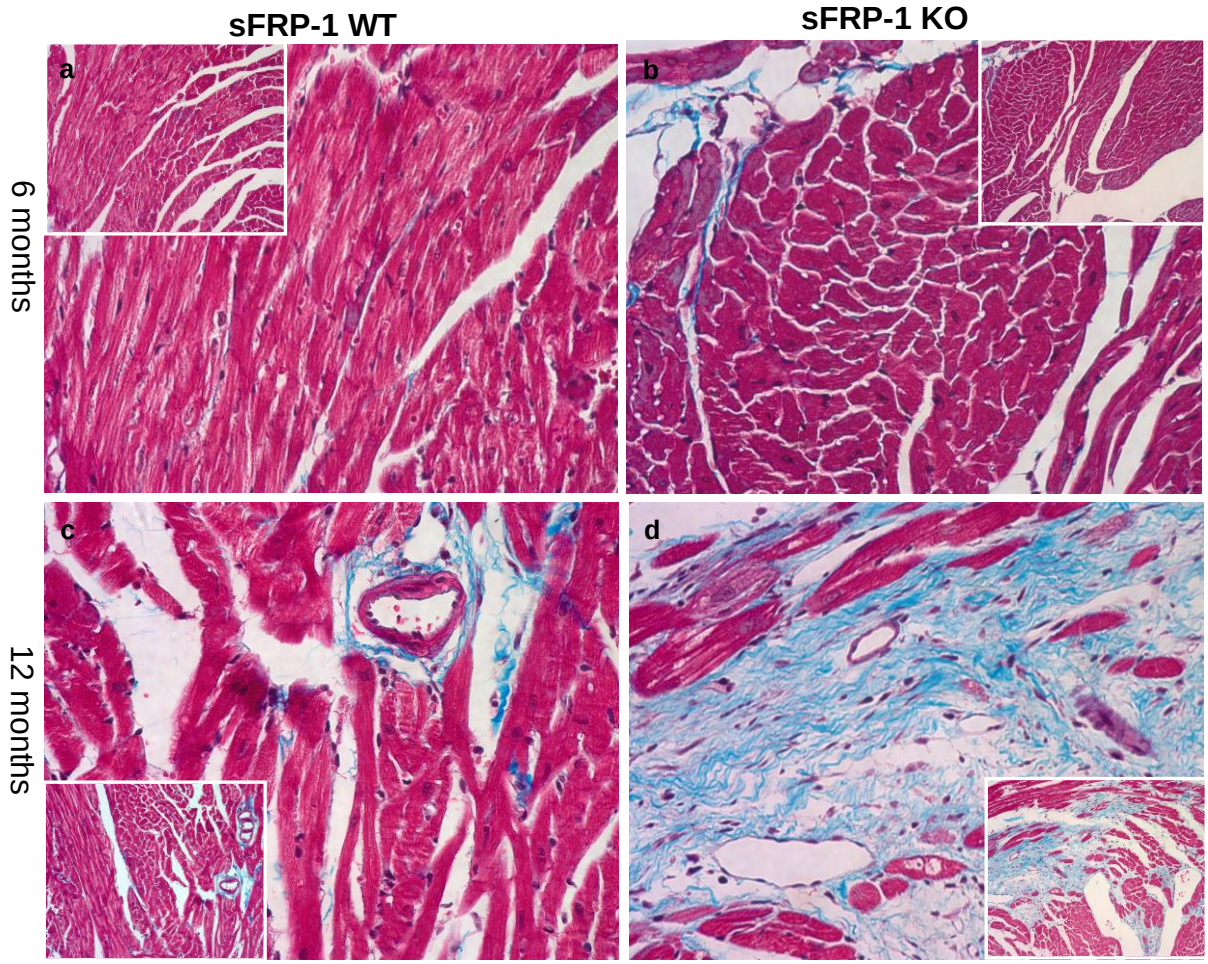

Figure 4.18. Fibrotic lesions formation in myocardium of sFRP-1 KO hearts.
Representative pictures for Masson staining (Trichrome) for collagen deposition. (a-b.) Trichrome staining in sFRP-1 KO hearts (b.) versus sFRP-1 WT hearts (a.) at 6 months of age. (c-d) Trichrome staining in sFRP-1 KO hearts (d.) versus sFRP-1 WT hearts (c.) at 12 months of age. Magnification is 40x and 20x (small in the corners).

4.5.4. **Dysregulation of Wnt signaling pathway in sFRP-1 KO hearts**

Considering the importance of sFRP-1 in heart function based on the above results we examined the molecular mechanism underlying dilated cardiac phenotype of the mice lacking sFRP-1. Since sFRP-1 is one of the main Wnt signaling extracellular modulators we tried to determine how its loss would affect Wnt signaling that is known to participate in normal heart development and cardiac regeneration?

To examine the changes in the Wnt mediated signaling pathway in the sFRP-1 KO hearts versus sFRP-1 WT mice (n=3, Figure 4.19.). A mouse Wnt Signaling pathway PCR array was performed and analysed (Figure 4.19. a,b). Interestingly, we found a significant increase in the Wnt molecules belonging to the Frizzled 2 signaling pathway such as Wnt3, Wnt7b, Wnt8b and Wnt16 (Figure 4.19. c) suggesting activation of the Wnt/Frizzled pathway. Additionally in the sFRP-1 KO remodeled hearts we were able to observe a significant increase in the Wnt components responsible for collagen deposition, cell growth and proliferation like Wnt induced secreted protein 1 (Wisp1), Fibroblast growth factor 4 (Fgf4), Wnt3 and an incease in several of the Wnt transcription factors such as Lef1, Brachyura and Foxn1 (Figure 4.19. c).

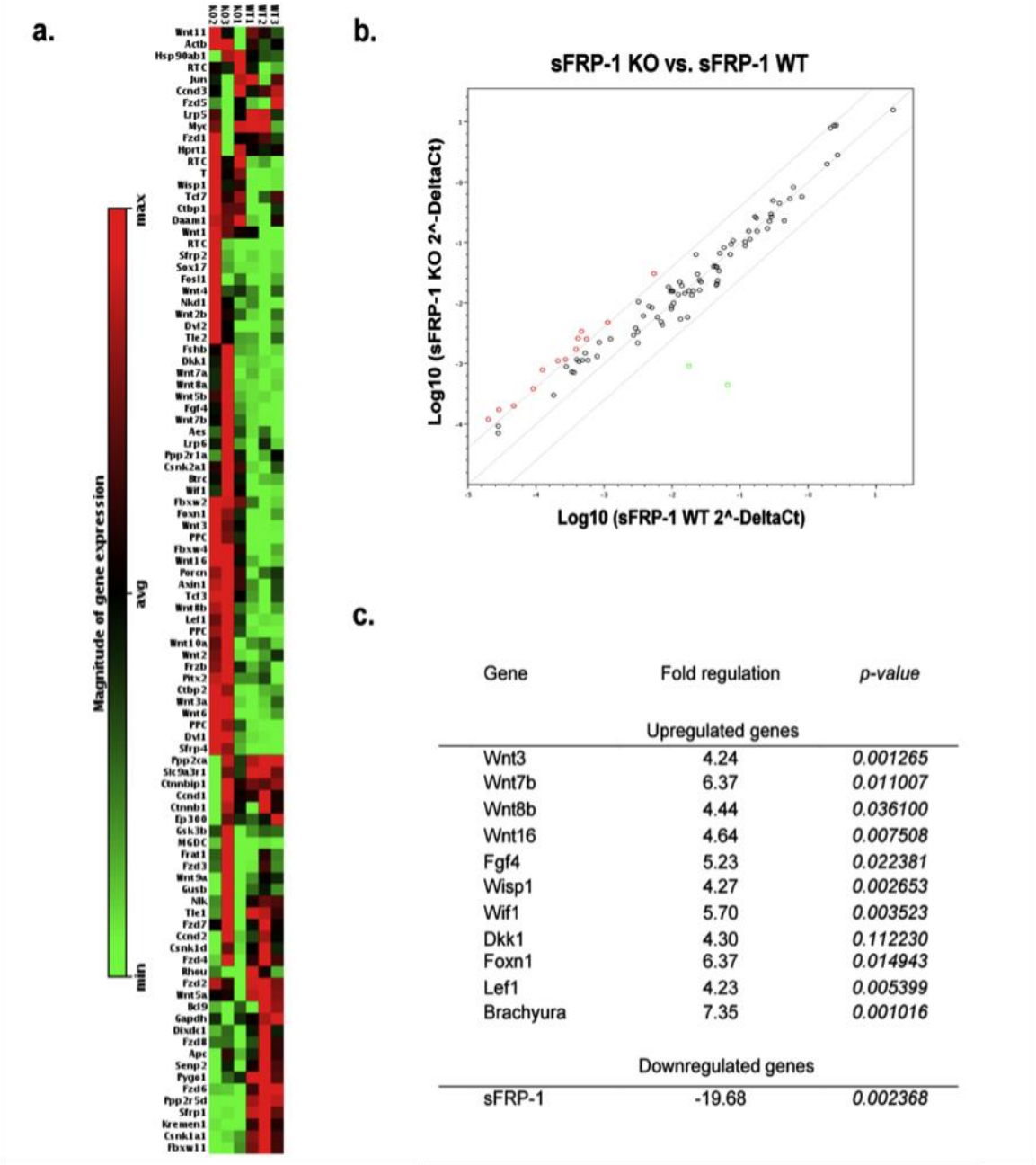

c.

Gene	Fold regulation	*p-value*
	Upregulated genes	
Wnt3	4.24	*0.001265*
Wnt7b	6.37	*0.011007*
Wnt8b	4.44	*0.036100*
Wnt16	4.64	*0.007508*
Fgf4	5.23	*0.022381*
Wisp1	4.27	*0.002653*
Wif1	5.70	*0.003523*
Dkk1	4.30	*0.112230*
Foxn1	6.37	*0.014943*
Lef1	4.23	*0.005399*
Brachyura	7.35	*0.001016*
	Downregulated genes	
sFRP-1	-19.68	*0.002368*

Figure 4.19. Wnt Signaling Real-Time based mRNA expression profile
(a.) Clusterdiagram of 96-well Real-Time PCR based SuperArray targeting Wnt signaling pathway (SABiosciences). (b.) Scatter blot of Wnt PCR Array presenting statistically significant (4-fold and more) Wnt pathway genes which were up or downregulated in the whole heart extracts from the sFRP-1 KO versus WT littermates. (c.) Fold of regulation and statistical significance given as p value of Wnt-regulated genes (4-fold and more) disregulated in sFRP-1 KO hearts. Genes presented: Frizzled 2 pathway (Wnt3, Wnt7b, Wnt8b, Wnt16), negative regulators of Wnt receptor signaling pathway (Dkk1), regulators of growth and proliferation (Wisp1, Wif1, Fgf4), transcription factors (Foxn1, Lef1, Brachyura)

4.5.5. **Increased protein expression profile of the main canonical Wnt signaling molecules in the sFRP-1 KO hypertrophy model**

To determine whether the canonical Wnt signaling pathway mediated through β-catenin was the cause of the dilated cardiomyopathy in the sFRP-1 KO mice, protein expression of the key Wnt canonical molecules like Frizzled 2, Dishevelled-2, β-catenin and GSK3β phosphorylation was examined in sFRP-1 KO hearts at 6 months and 1 year of age. We were able to observe an increased protein levels of the upstream Wnt signaling effectors like disheveled-2 and Frizzled 2 receptor at both time points as compared to sFRP-1 WT hearts (6 months n=3, 12 months n=4 Figure 4.20. a,b) which was consistent with PCR array data showing an increase in Frizzled 2 pathway. We did not observe any significant change in GSK3β phosphorylation in the sFRP-1 KO hearts (6 months n=3, 12 months n=4, Figure 4.20. a,b). Very interestingly, we found a significant accumulation of β-catenin in the heart homogenates of sFRP-1 KO mice at 6 months (n=3, Figure 4.20. a) as well as at one year of age (n=4, Figure 4.20. b).

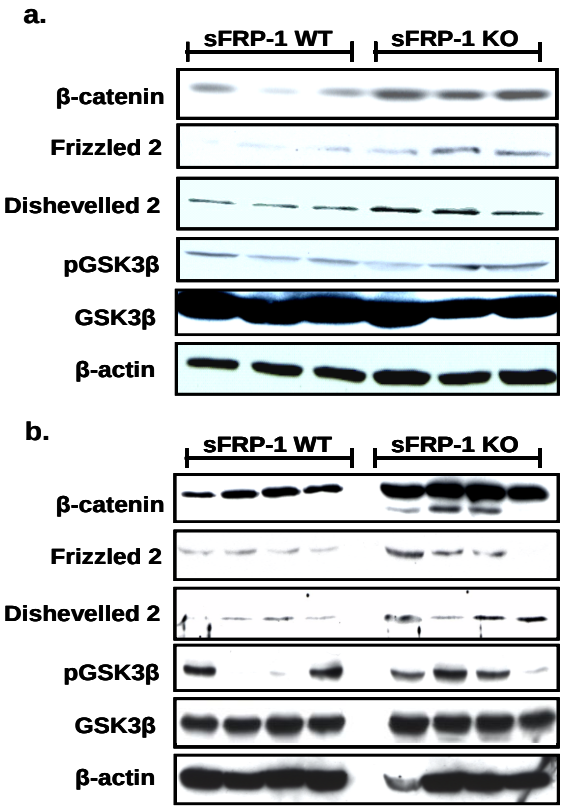
a.
sFRP-1 WT
sFRP-1 KO
β-catenin
Frizzled 2
Dishevelled 2
pGSK3β
GSK3β
β-actin
b.
sFRP-1 WT
sFRP-1 KO
β-catenin
Frizzled 2
Dishevelled 2
pGSK3β
GSK3β
β-actin

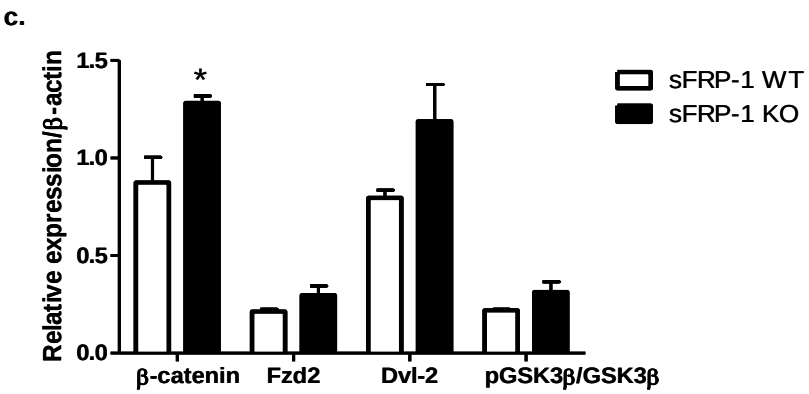
c.
Relative expression/β-actin
1.5
1.0
0.5
0.0
*
β-catenin
Fzd2
Dvl-2
pGSK3β/GSK3β
sFRP-1 WT
sFRP-1 KO

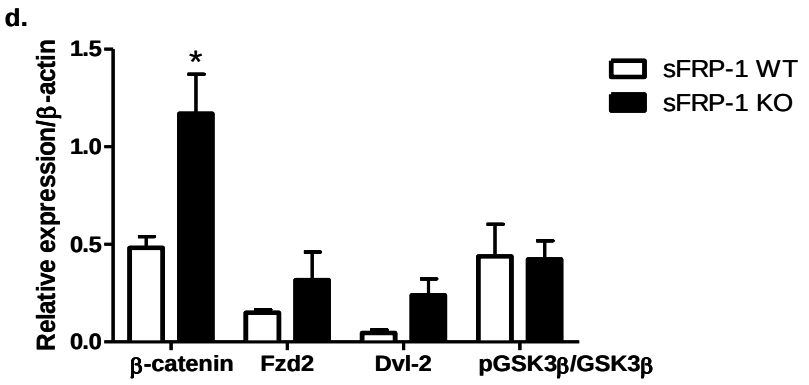
d.
Relative expression/β-actin
1.5
1.0
0.5
0.0
*
β-catenin
Fzd2
Dvl-2
pGSK3β/GSK3β
sFRP-1 WT
sFRP-1 KO

Figure 4.20. Main canonical Wnt signaling molecules are upregulated in sFRP-1 KO heart homogenates.
Protein expression as analyzed by western blotting of GSK3ß phosphorylation status at serine 9 (pGSK3ß S9), Frizzled 2 receptor (Fzd-2), Dishevelled 2 (Dvl-2) and ß-Catenin in control sFRP-1 WT hearts versus sFRP-1 KO hearts after (a.) 6 months and (b.) 12 months of age. Subsequent densitometric quantification of western blots (c.) for 6 months and (d.) 12 months. ß-Actin was used as a loading control. Values were presented significant as *P < 0.05 *vs* control sFRP-1 WT hearts. All values were expressed as mean ± SEM (6 months, n=3; 12 months, n=4).

4.5.6. **An increase in β-catenin accumulation in the intercalated disks of sFRP-1 cardiomyopathic hearts**

To further evaluate the changes in β-catenin expression immunohistofluorescent studies were performed to localize β-catenin. We were able to confirm a marked increase in β-catenin expression in sFRP-1 KO cardiomyopathic hearts in the myocardium at 6 months (n=3, Figure 4.21. a,b) as well as at one year of age (n=3, Figure 4.21. c,d). Interestingly and consistent with the downregulation of canonical Wnt signaling downstream targets we did not observe the translocation of β-catenin to the nucleus in the sFRP-1 KO hearts at any time point. At 6 months of age we did observe disperse staining suggesting co-localization of β-catenin to the cytoplasm but never to nucleus. Interestingly there was a clear accumulation of this protein in the intercalated disks of the myocardium of the sFRP-1 KO hearts at one year of age which probably is a crucial mechanism leading to increased wall stiffness in the cardiomyopathic hearts.

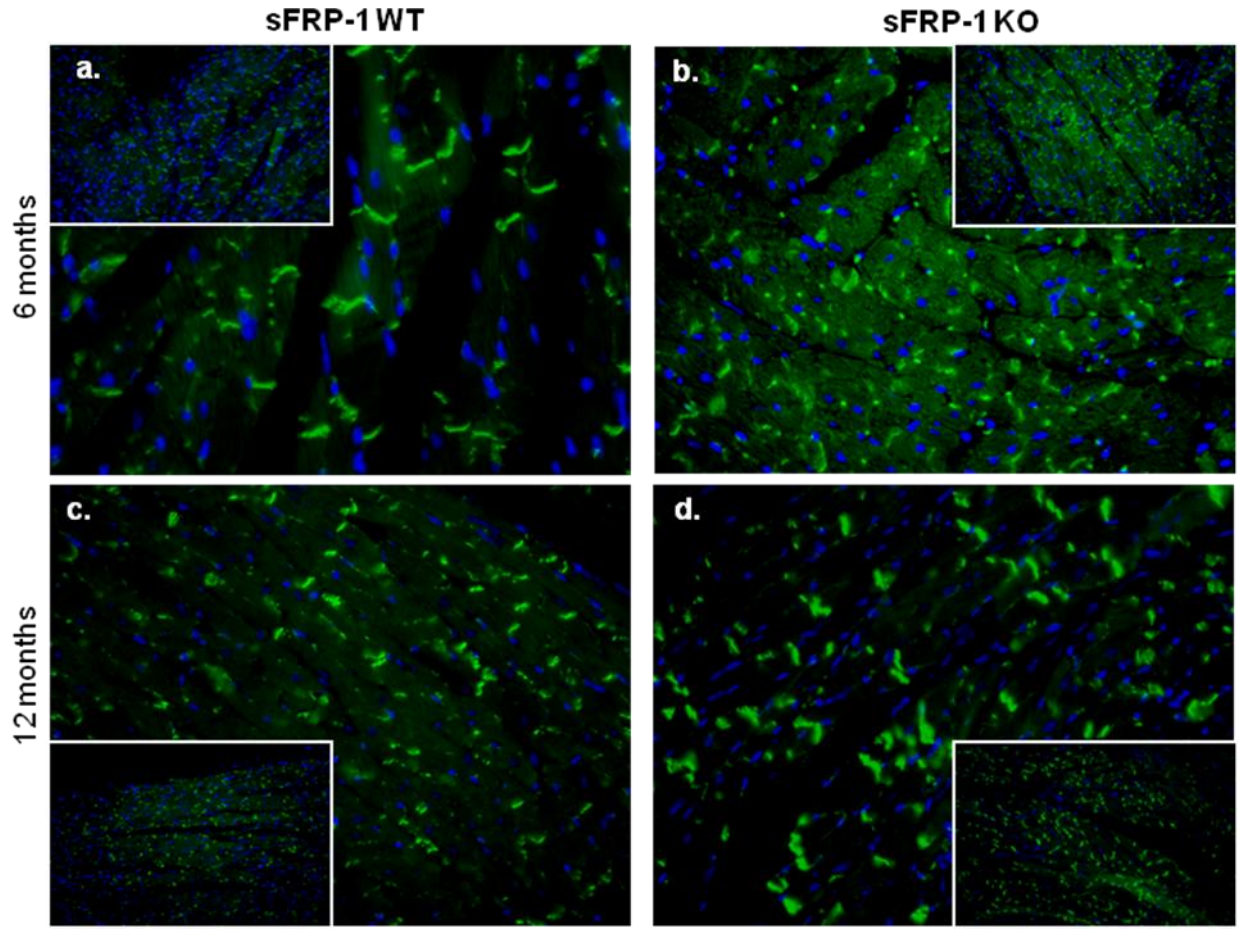

Figure 4.21. β-Catenin accumulates in the intercalated disks of sFRP-1 KO cardiomyopathic hearts.
Representative immunofluorescent staining for β-Catenin merged with DAPI in the myocardium of sFRP-1 KO vs WT hearts. At 6 and 12 months of age. (a-b.) β-Catenin localization in sFRP-1 KO (b.) versus sFRP-1 WT (a.) at 6 months of age, (c-d.) β-Catenin localization in sFRP-1 KO (d.) versus sFRP-1 WT (c.) at 12 months of age. Magnification is 40x.

4.5.7. **Suppression of canonical Wnt transcriptional activity in sFRP-1 KO hearts**

Protein expression of main targets and effectors of Wnt/β-catenin signaling like cyclin D and cMyc was measured. No significant changes were observed in the sFRP-1 KO hearts at 6 months of age (n=3, Figure 4.22. a) versus the WT littermates. However we found a significant decrease in the expression of cyclin D and cMyc in sFRP-1 KO hearts at one year of age (n=4, Figure 4.22. b) suggesting a decrease in the canonical Wnt transcriptional activity.

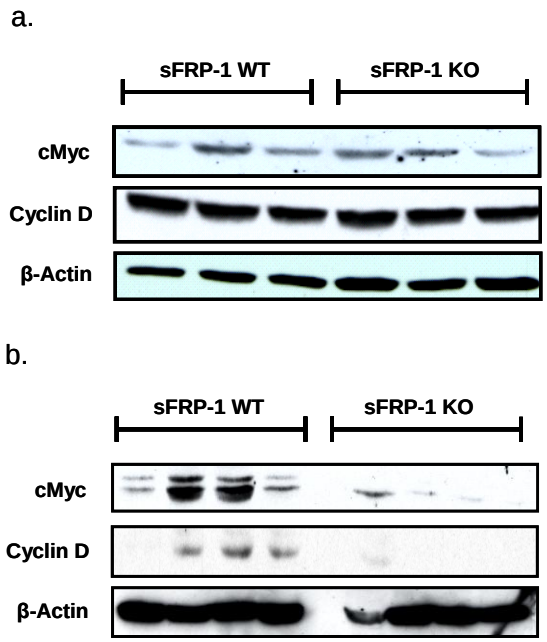

Figure 4.22. Loss of sFRP-1 in hearts leads to age dependent loss of canonical Wnt signaling transcriptional activity
Protein expression as of main transcriptional targets of β-catenin, cMyc and cyclin D analyzed by western blotting in control sFRP-1 WT hearts versus sFRP-1 KO hearts at 6 (a.) and 12 (b.) months of age. ß-Actin was used as a loading control.

These studies demonstrate that the loss of sFRP-1 expression in mice hearts age dependently suppress the activity of the canonical Wnt pathway suggesting its great importance in maintenance of normal heart function in adult life.

4.5.8. **Decreased expression of Connexin43 in sFRP-1 KO remodeled hearts**

Gap junctions channels composed of Connexin43 are essential for normal heart formation and function. To determine if the loss of sFRP-1 can also alter Connexin43 expression, immunohistochemical staining was performed to localize and estimate changes in connexin43 levels in the sFRP-1 KO remodeled hearts. Interestingly, we were able to show that Connexin43 localized in the myocytes junctions in the sFRP-1 WT hearts significantly decreased in an age dependent fashion in the sFRP-1 KO mice at 6 months (n=3, Figure 4.23. a,b) as well as at one year of age (n=3, Figure 4.23. c,d).

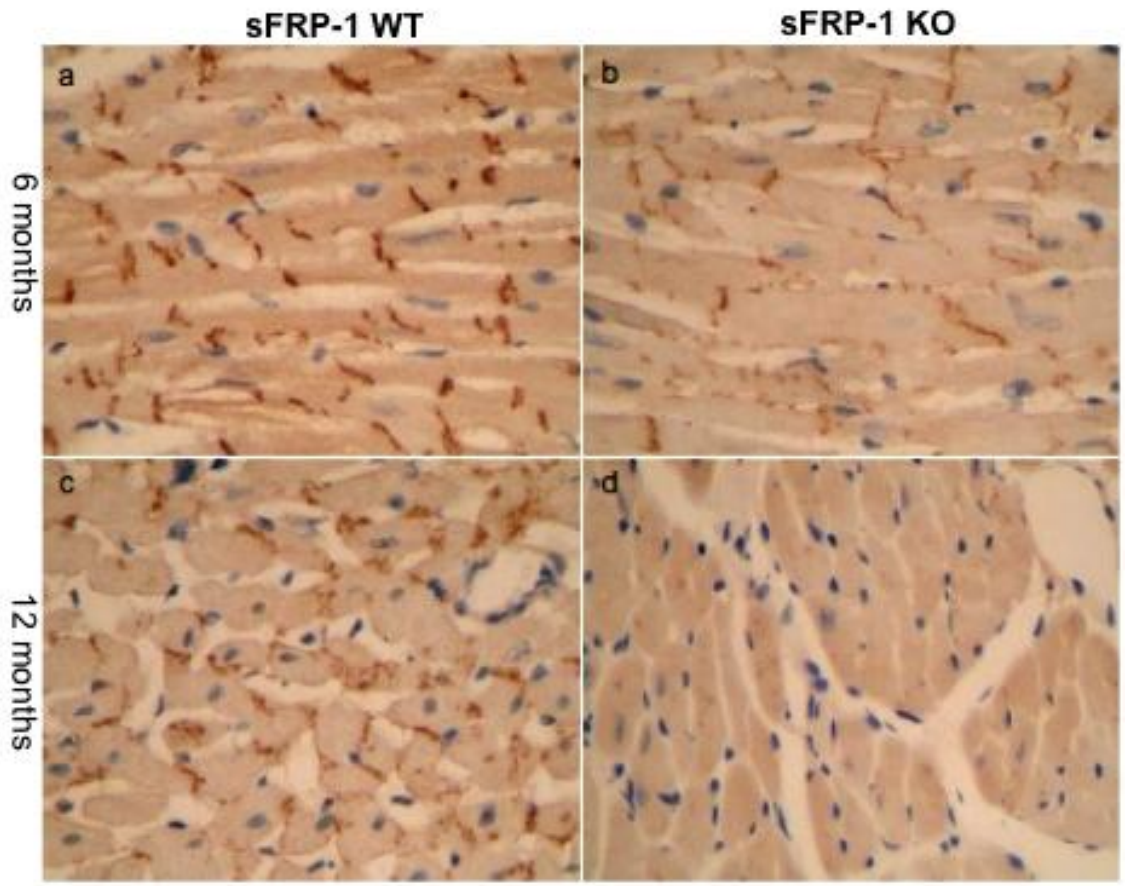

Figure 4.23. Loss of sFRP-1 leads to downregulation of Connexin43 in heart myocardium.
Immunohistochemical staining of Connexin43 in heart sections at 6 months (a,b) and 12 months (c,d) of age. Sections were counterstained with hematoxylin. Magnification is 40x.

5. Discussion

5.1. Dysregulation of Wnt signaling pathway in experimental Pulmonary Hypertension

Wnt growth factors act via the Frizzled receptors affecting cellular proliferation, differentiation, apoptosis and migration by modulating both cellular and transcriptional events (178). Based on studies in mice, Wnts function during mammalian development, but Wnt signaling is also commonly altered in human cancers. The signaling cascades defined for Wnt/Frizzleds are distinct from other receptor-mediated pathways, but their diversity of cellular outputs still presents a challenge to our understanding of how Wnts work.

Recent data suggest a role for Wnt signaling in vessel development and pathology. Although not yet investigated, several Wnt ligands (Wnt1, Wnt2, Wn5a and Wnt10b), its Frizzled receptors (Fzd1, Fzd2, Fzd5) and Wnt antagonists (sFRP-1, sFRP-3) have been identified in the cells of blood vessels *in vivo* and *in vitro* (179). Excessive Wnt signaling resulting from Wnt overexpression, mutations in β-catenin or inactivation of the β-catenin phosphorylation complex (GSK3β with Axin) was reported to directly cause cell transformation, abnormal proliferation and lead to cancer (180). Stabilization of the downstream signaling component β-catenin in blood vessels (in neovascular endothelium and in neointimal smooth muscle) has been demonstrated in several developmental and pathologic states, further supporting the idea that Wnt signaling plays an important regulatory role in the vasculature. Activation of the Wnt signaling pathway may lead to angiogenesis or vessel remodeling, whereas inhibition of Wnt signaling may lead to vessel stability or even regression (179).

PAH is characterized by structural changes in pulmonary arteries resulting from the abnormal increase in the proliferation of vascular cells. Recently wide gene expression analysis of pulmonary arterial resistant vessels revealed differentially regulated canonical and non-canonical Wnt genes in PAH (165). It was also shown that the recruitment of both canonical and non-canonical Wnt molecules is required in BMP-2-mediated angiogenesis (175)leaving the door open to investigate a possible role of this signaling in the vascular remodeling in PAH and led us to evaluate the possible involvement of the canonical Wnt signaling in vascular remodeling and heart hypertrophy.

In rat lung homogenates after MCT-induced PAH we observed a profound change in Wnt signaling. A significant upregulation of Wnt5A and the main intracellular canonical Wnt effectors like β-catenin, Axin1 and GSK3β on mRNA level was consistent with results

obtained in IPAH human lungs and laser microdissected pulmonary arteries from IPAH patients (165). In this report, Laumanns et al. suggested that these findings are in line with the concept of coactivation of the canonical and non-canonical Wnt pathway in IPAH. At the same time the authors report that Wnt11-induced PCP pathway is operational in the IPAH. In line, with this notion, aberrant ß-catenin/GSK3ß signaling was recently implicated in various vascular- and fibro-proliferative diseases (193-195).

Despite downregulation of the well-known canonical Wnt ligands (Wnt1, Wnt3A) in mRNA level, GSK3β and β-Catenin gene expression is induced in MCT-PAH. It may suggest that this induction is dependent on other Wnt ligand. Wnt5a, upregulated in MCT-PAH also is known to induce Wnt/β-catenin signaling depending on the Frizzled receptor complex (181). More interestingly, highly upregulated Wnt11 in human pulmonary resistance arteries in IPAH can also induce the Wnt/β-catenin pathway alone (182-183) or through the complex formation with Wnt5A (184-185). Additionally, in human IPAH, Rho-kinases or calcium signaling deregulation both thought to be downstream targets of ambiguous non-canonical pathway (119,165,186), discovered Wnt-independently are already known to significantly contribute to PASMC's pathogenesis and have a therapeutical potential in vasodilaton as well as reversing vascular remodeling (187-192,196). In the present study we could observe a decrease in β-catenin protein level in the late stage time course of MCT-PAH induction with a significant increase in GSK3β along with observed trend to increase in mRNA levels of sFRP-1 and Frizzled 1 (both canonical and non-canonical receptor) and decrease in Frizzled 2 expression. This may suggest that control on GSK3β/β-Catenin signaling pathway could have been taken over by the non-canonical pathway (196), which needs to be evaluated in the future.

Signaling pathways, involved in pathogenesis of PAH, like growth factors signaling (64-66,208), can also regulate the GSK3β/β-catenin axis. Several reports in the literature implicate growth factors signaling in the regulation of GSK3β/β-catenin axis in EMT (198) and airway SMC mitogenic signaling (199). Recently it was shown that Wnt7b/ß-Catenin signaling is involved in regulating PDGFRß expression and proliferation of VSMC *in vivo* and *in vitro* (200). In a very sophisticated manner using loss-and-gain of function *in vivo* models (Wnt7b ^{lacZ} and SM22α-cre β-catenin $^{flox/flox}$ mutants) authors were able to show that loss of Wnt/ß-Catenin signaling leads to dramatic reduction in PDGFRß expression. On the other hand gain of this signaling leads to significant increase in PDGFRß expression and proliferation of PDGFRß positive VSMC precursors. Knowledge that PDGFRß is highly upregulated in the lungs and remodeled arteries in experimental as well as human iPAH (64-

65) combined with our expression profile of the GSK3β/β-catenin axis in MCT-induced PAH could potentially explain the discrepancy between the time course of ß-Catenin and GSK3ß accumulation during experimental PAH development. A significant upregulation of ß-Catenin in the early stages of disease could suggest the induction of PDGFRß positive SMC precursor cell proliferation in the vascular wall. In the later stages of disease progression, highly increased PDGF-BB in both experimental models of PAH as well as in human IPAH (65) could possibly take over the control of PASMC proliferation through the induction of the receptor tyrosine kinase pathway. This involves the activation of ERK1/2 kinase (64) also shown to be involved in the Wnt signaling pathway (253).

MCT-PASMCs show increased proliferation capability as compared to healthy PASMC. MCT-PASMCs show decreased expression canonical Wnt1 and Frizzled receptors. However the subtypes of Wnt and Frizzled receptors involved in VSMC proliferation have remained ill-defined. Frizzled 1 and 2 receptors are both downregulated *in vivo,* 1 and 4h after arterial injury and in proliferative VSMC's *in vitro* suggesting a negative relationship to proliferation (197).

Significant GSK3ß phosphorylation and not significant ß-Catenin upregulation observed in primary PASMCs isolated from MCT-PAH rats highlights that aberrant inactivation of GSK3ß signaling potentially independent of ß-Catenin may trigger the proliferative phenotype of MCT-PASMCs. GSK3ß-Wnt independent signaling controls proliferation in many types of cancer (171-173,201-203) along with its significant inactivation in MCT-PASMC presents a possible crucial role for GSK3ß in the pathogenesis of PASMCs.

GSK3ß expression increased in a time dependent fashion with disease progression in the MCT-induced PAH model and also in explanted IPAH patient lungs suggesting a role for GSK3ß in disease progression. Recently a crucial role for GSK3ß in systemic vascular remodeling was reported (174,204). Authors demonstrated for the first time *in vivo* that active GSK3ß gene transfer results in a significant reduction in neointima formation in the atherosclerosis model of balloon injury in rat carotid arteries. These effects were attributable, at least in part to the ability of GSK3ß to inhibit smooth muscle proliferation and to promote sustained apoptosis. This concept was extended to demonstrate that GSK3ß plays a significant role in VSMCs proliferation and apoptosis in vascular remodeling after balloon injury (174). Inactivation of GSK3β in MCT-PASMC shows that therapeutic introduction of active GSK3β could also be potentially beneficial for vascular remodeling in experimental PAH. Another interesting finding was the discovery that systemic vascular remodeling is induced by the Akt/GSK3ß/NFAT axis (204). Earlier on the same group published that the activated NFAT

transcription factor is highly increased in the circulating leukocytes in IPAH patients, Inhibition of NFATc2 by VIVIT or cyclosporine restored Kv1.5 expression and decreased proliferation and increased apoptosis *in vitro*. *In vivo*, cyclosporine decreased the established rat MCT-induced PAH (153). In addition to Wnt5a/Ca^{2+} signaling, GSK3ß is one of the major regulators of NFAT activation (205).

PDGF-BB is a very important factor for PAH, it is known to regulate GSK3ß in systemic circulation (204). Constant increase in GSK3β in MCT-PAH and its significantly increaed phosphorylation in MCT-PASMCs at basal conditions as well as after PDGF-BB stimulation suggest that GSK3β have potential role in crosstalk between Wnt and PDGF signaling during PAH progression. Therefore we needed to further evaluate the role of GSK3β in PDGF and Wnt signaling crosstalk.

5.2. Contribution of the GSK3β/β-catenin pathway to growth factors induced signaling in MCT-PASMC

Interestingly, our results demonstrate that PDGF causes GSK3ß phosphorylation at the serine 9 residue. GSK3ß inactivation was not synchronized with the accumulation of ß-catenin after 24 hours in MCT-PASMC along with a significant increase in proliferation rate of MCT-PASMC. This observation reflects that GSK3ß is inactivated in diseased PASMCs as compared to healthy cells. Regulation of GSK3ß by Wnt signaling pathways as an integration point in hypertrophic signaling could possibly be important in the crosstalking between Wnt and growth factor signaling.

Early stimulation of MCT-PASMC showed that PDGF-BB could not exert any effect on ß-catenin nuclear translocation in comparison to Wnt3A treatment even though both factors exhibited a downstream effect on the phosphorylation of Akt and GSK3ß at serine 9 residue. Induction of Akt phosphorylation was reported before in response to an anti-apoptotic stimulus in MC3T3-E1 cells (211) but still the mechanism remains poorly understood. An alternative report demonstrates that Wnt3A mediates proliferation of fibroblasts NIH3T3 cells through activation of the Akt pathway (212). In the present studies PDGF and Wnt3A could both induce the Akt pathway and both have the ability to degrade Axin, a protein strictly involved in the Wnt signaling pathway. Axin potentially has other functions. For instance, during the stimulation of epithelial cells by PDGF, Axin is displaced from ß-catenin allowing the cells to undergo the EMT process (198). Additionally overexpression of Axin is associated negatively with the progression of astrocytomas and

induces cell death and reduces cell proliferation, partially by activating the p53 pathway in astrocytoma cells (213). Degradation of Axin in MCT-PASMC after PDGF stimulation potentially could be correlated with data recently published showing that Axin inhibits cellular proliferation and ERK activation induced by epidermal growth factor, indicating a role for Axin in the regulation of growth induced by ERK activation. This potentially could be crucial for vascular remodeling in MCT-induced PAH (64).

The signaling pathways induced by PDGF-BB and Wnt3A act via AKT act similarly to GSK3ß phosphorylation at the serine 9 residue yet only Wnt3A can translocate β-catenin to the nucleus is extremely interesting. Questions raised were; How these two pathways can regulate downstream targets of GSK3ß? And, Is GSK3ß a regulatory protein in this process that can diversify cellular response of these two growth factors? Indeed we were able to observe that the response of MCT-PASMC to Wnt3A and PDGF differs at GSK3ß, which could be the point of integration. Interestingly PDGF decreased phosphorylation of GSK3ß at Y216 residue.

The Y216 residue recently was thought to be unaffected in response to growth factors. Additionally, the literature suggested that Y216 phosphorylation participated only in its autophosphorylation process having nothing to do with the kinase activity. Protein kinases related to GSK3β, such as CDK2, p38 and ERK2, require the phosphorylation of residues in their activation loops (T-loops) as a prerequisite for activity (214-215). A phosphothreonine is used by all three related kinases to align the key β-strand and α-helical domains. The phosphorylation of a T-loop tyrosine is also required by p38g and ERK2 to open up the catalytic site for substrate access. The T-loop of GSK3β is tyrosine phosphorylated at Y216 but not threonine phosphorylated. Y216 phosphorylation could play a role in forcing open the substrate-binding site, but there appears to be no constraints preventing the open conformation in the unphosphorylated state (150). Thus, T-loop tyrosine phosphorylation of GSK3β might facilitate substrate phosphorylation but is not strictly required for kinase activity (150). However, GSK3β transfected into HEK-293 cells became phosphorylated at Tyr216, but the catalytically inactive mutants did not (216) which demonstrates the involvement of Y216 in kinase activity. Recently exciting data reported that increased Y216 phosphorylation activates GSK3β and facilitates FGF-2 induced apoptosis in cancer cells (217). Additionally, GSK3β autophosphorylates Y216 as a chaperone-dependent transitional intermediate possessing intramolecular tyrosine kinase activity and displaying different sensitivity to small-molecule inhibitors compared to mature GSK3β. After autophosphorylation, mature GSK3β is then an intermolecular serine/threonine kinase no

longer requiring a chaperone. This represents that autoactivating kinases have developed different molecular ways for autophosphorylation and for kinases such as GSK3β.

The evaluation of the role of GSK3ß in PDGF-induced proliferation of MCT-PASMC is one of the salient features of our study. For this purpose we used Imatinib mesylate, an inhibitor of tyrosine receptor kinases like PDGFRβ, c-Kit and BCR-Abl to treat certain types of cancer like chronic myeloid leukemia and gastrointestinal stromal tumors. The use of Imatinib increased drastically in other diseases and it was found to delay atherosclerosis in mice with diabetes. Recently Imatinib was shown to be extremely effective in reversing vascular remodeling and improving lung function in animal models of PAH (64) and patients with iPAH (89) by blocking ERK activation. However, the precise molecular mechanism remains to be elucidated.

In our study PDGFRβ inhibition in MCT-PASMC blocked Axin degradation and Akt phosphorylation with no effect on β-catenin nuclear translocation. Most importantly PDGFRβ inhibition significantly blocked the proliferation rate of MCT-PASMC. Interestingly our results showed that PDGF, acting via PI3-kinase-dependent activation of Akt, causes GSK3ß inactivation (increased S9 and decreased Y216 phosphorylation) that was reversed by Imatinib. The fact that PDGFRβ inhibition regulates the phosphorylation of GSK3ß suggests that this multi tasking kinase is implicated in the pathogenesis of MCT-PASMC (Figure 5.1.). The importance of GSK3ß in vascular remodeling was recently emphasized by targeting Akt pathway in restenosis (204). Authors showed that proproliferative and antiapoptotic states are characterized by a metabolic (glycolytic phenotype and hyperpolarized mitochondria) and electric (downregulation and inhibition of plasmalemmal potassium channels) remodeling involving the activation of the Akt pathway which most importantly phosphorylates and inactivates GSK3ß. Using dehydroepiandrosterone (DHEA) a naturally occurring and clinically used steroid known to inhibit the Akt axis in cancer this group found that orally available, nontoxic, inexpensive DHEA effectively reverses vascular remodeling after carotid injury in vivo or exposure to growth factors like PDGF *in vitro* (204).

Considering the essential role of PDGF receptor inhibition in reversing pulmonary vascular remodeling and GSK3ß activity modulation by PDGF indicates the importance of GSK3ß in the pathogenesis of PAH. Imatinib in the MCT-PASMC blocked PDGF-induced inactivation of GSK3ß, which collectively suggest possible crucial role for GSK3ß in mediating Imatinib-induced reversal of MCT-induced PAH in rats (64) (Figure 5.1.).

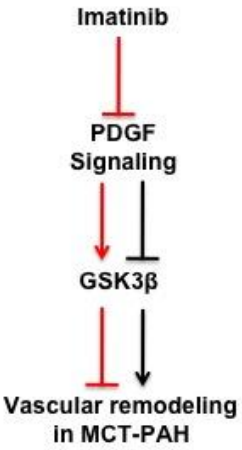

Figure 5.1. Possible role for GSK3β in Imatinib-induced reversal of vascular remodeling in MCT-PAH. Hypothetical scheme representing implication of GSK3β in PDGF signaling pathway that highly contributes to vascular remodeling in PAH (Black arrows) and inhibition of PDGF signaling by Imatinib (Red arrows), (Author's scheme).

5.3. Individual role of GSK3β in regulation of MCT-PASMC proliferation

To evaluate the properties of GSK3ß in PAH our approach was to overexpress three different variants of human GSK3ß. GSK3ß WT and two mutated variants (S9A and Y216D) were introduced to MCT-PASMC.

In the present study we show that GSK3ß is implicated in PASMC proliferation. This effect can be due to the GSK3ß phosphorylation of a diverse group of substrates or by inhibition of transcription factor activation such as p53, CREB and ß-Catenin (218-220). In addition, GSK3ß, which is constitutively active, has also exhibited direct effects on cyclin D1 expression, independent of ß-Catenin (221). Here we show that the overexpression of wild-type GSK3ß and its constitutively active mutants can regulate the MCT-PASMC proliferation rate speculatively via ERK phosphorylation (Figure 5.2.). In a recent study by Wang et al., it was shown that inhibition of GSK3ß by specific inhibitors increased phosphorylation of ERK in human colon cancer cells (222).

Induction of proliferation in GSK3ß WT transfected MCT-PASMC which could be correlated with increased levels of total GSK3ß in MCT-induced as well as human IPAH was accompanied by an increase in ERK phosphorylation (Figure 5.2. black arrows). Constitutive activation of GSK3ß both by serine or tyrosine substitution inhibited the phosphorylation of ERK1/2 and caused a significant decrease in serum-induced proliferation rate of MCT-PASMC (Figure 5.2.). Interestingly, when tyrosine residue 216 was substituted to aspartic acid (D) ERK phosphorylation was abolished as compared to the S9A overexpression. Y216D

effectively inhibited PDGF induced proliferation of the MCT-PASMC as compared to S9A (Figure 5.2. red arrows), which suggests that GSK3ß might regulate PDGF-induced ERK phosphorylation via Y216 residue. It has been reported that GSK3β directly interacts with ERK1/2 (224). In the hepatoma cell line, ERK/ GSK3β association "primes" GSK3β for its subsequent phosphorylation at serine 9 by tyrosine 216. This process is regulated by MEK1/2 (225). In resting cells, ERK1/2 is mainly kept in the cytoplasm by the microtubule cytoskeleton, which serves as a major docking matrix (223). ERK1/2 and GSK3β association is important for cytoplasmic retention of ERK1/2 because disruption of the ERK1/2 and GSK3β complex by specific dominant negative proteins, or down-regulation of GSK3β by siRNA promotes nuclear translocation of phosphorylated ERK1/2 (224). Hydrogen peroxide and ethanol are oxidative stress inducers enhance both FGF2-stimulated phosphorylation of GSK3β (Y216) and ERK/ GSK3β association which potentiates FGF2-induced cytoplamic retention of ERK1/2 and subsequent SK-N-MC cell death.

The results suggest that PDGF-dephosphorylation of GSK3β at Y216 and phosphorylation at Ser 9 in MCT-PASMC possibly allows ERK to be phosphorylated and thereby promotes PDGF-BB induced proliferation. Yet when we mimic phosphorylation of GSK3β at the tyrosine residue by aspartic acid (Y216D) we observed a decrease in ERK phosphorylation and inhibition of PDGF-BB induced proliferation of MCT-PASMC. Constitutively active GSK3β (S9A) is known to reduce vascular remodeling in the balloon injury model of atherosclerosis (174). MCT-PASMC overexpressing active GSK3β (S9A) mutant significantly decreased serum-induced proliferation but not proliferation induced by PDGF-BB (Figure 5.2.). The fact that the S9A mutant of GSK3β did not effectively block PDGF-induced comparing to Y216D has to be more extensively studied in the future in the aspects of the PDGF-BB signaling.

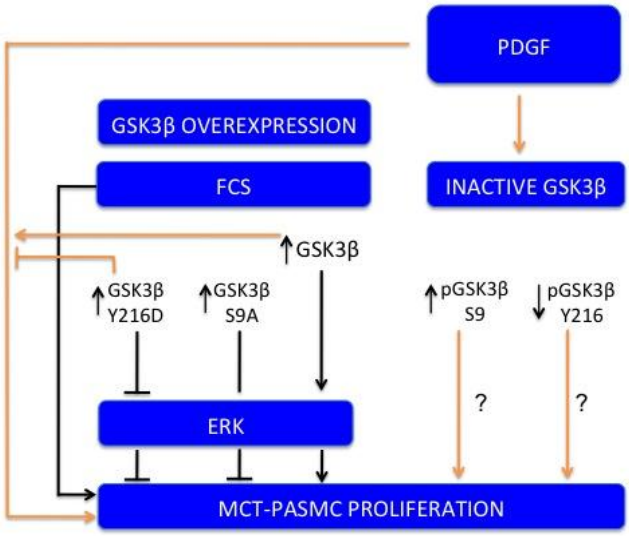

Figure 5.2. Speculative role for GSK3β overexpression on proliferation of MCT-PASMC's (Author's scheme**). PDGF-BB signaling condition (orange arrows), FCS condition (black arrows)**

To our knowledge this is the first study to demonstrate a role for GSK3ß in the pathogenesis of experimental PAH and the regulatory role for GSK3ß in pulmonary arterial smooth muscle cell proliferation. This study supports a possible role for GSK3ß in the lung vascular remodeling.

5.4. Canonical Wnt signaling and its potential role in regulating PASMC proliferation

Canonical Wnt/β-catenin signaling was previously described in development as well as being pro-mitogenic and pro-oncogenic in many cancer types. In the present study we observed a significant downregulation of canonical Wnt ligands during experimental PAH progression. The upregulation of β-catenin on protein level early in experimental PAH progression suggests that upregulation of β-catenin could play a role in the development of PAH but its function is still not very well understood. A recent study by Cohen et al. (200) provides a possible explanation for this induction. The authors describe that the activation of the Wnt/β-catenin signaling pathway in SM22α-cre β-catenin $^{flox/flox}$ mice that lead to a significant increase in the expression of PDGFRß and furthermore proliferation of the PDGFRß positive VSMC precursors. Thus increased upregulation of β-catenin on the protein level in the early stages of MCT-induced PAH might induce an upregulation of PDGFRß followed by enhancement of PDGF-BB signaling, which needs to be studied in the future.

In MCT-PASMC a significant phosphorylation of GSK3β was observed while changes in β-catenin levels were not significantly increased. Considering the fact that PDGF-BB is not affecting β-catenin accumulation we decided to determine role of Wnt/β-catenin signaling in proliferation of MCT-PASMCs. Very interestingly, the activation of the canonical Wnt pathway by Wnt3A or LiCl without additional growth factor stimulation did not exert any changes in the proliferation rate but together with the serum or PDGF stimulation it significantly decreased proliferation of these cells. This result correlates with mRNA time-dependent downregulation of well-known canonical Wnt signaling ligands such as Wnt1 or Wnt3A during experimental PAH progression. In PAH more studies are needed to estimate exact role of β-catenin induction in vascular remodeling.

5.5. Role of Wnt signaling in heart failure. Loss of sFRP-1 leads to cardiac remodeling and loss of heart function

Profound changes in the pulmonary vasculature in PAH are followed by heart hypertrophy and heart failure at the last stages of disease. Some components of Wnt signaling pathway were also implicated to cardiac syste maintenance, such as GSK3ß or sFRP-1. GSK3ß is an essential negative regulator of cardiac development (176) as well hypertrophy and its inhibition by Wnts and growth factors hypertrophic stimuli (177) is an important mechanism contributing to the development of cardiac hypertrophy. sFRP-1 is a potent modulator of Wnt signaling being antagonist and agonist depending on its concentration. sFRP-1 levels were shown to have beneficial effect in heart rupture and affects ischemic heart diseases (245-246). To further evaluate the role of Wnt signaling pathway in cardiac remodeling we investigated sFRP-1 KO mice.

sFRP-1, an inhibitor of the Wnt signaling pathway, is present during both heart development and adult life and participates in the regulation of cell growth and death in various disease states. sFRP-1 is abundantly expressed in the mouse heart during adult life, however, the exact function of sFRP-1 in the heart is not well described. In this study, we demonstrated that the loss of sFRP-1 expression results in the development of cardiac remodeling which progresses to dilated cardiomyopathy via the suppression of the canonical Wnt/β-catenin mediated signaling pathway. These studies identify a novel role for the Wnt signaling pathway in the development of cardiac remodeling.

The Wnt signaling pathway has recently been described to play an important role in cardiovascular development and pathophysiology. As it was shown by van de Schans et al.

interruption of Wnt signaling attenuates pressure overload-induced cardiac hypertrophy in Dvl-1 KO animals by destabilizing of β-catenin (257). Furthermore other studies show that suppression of canonical Wnt/β-catenin signaling recapitulates the phenotype of arrhythmogenic right ventricular hypertrophy (243). Additionally overexpression of FrzA (sFRP-1) after MI (myocardial infarction) reduced cardiac rupture and infarct size, and improved cardiac function (226). However, using the transgenic mouse overexpressing FrzA in cardiomyocytes (α-MHC promoter) under a conditional transgenic expression approach (tet-off system), FrzA transgenic mice resulted in a larger infarct size and worse cardiac function compared with control littermates after PC (227). The authors contribute the difference in their findings by the diffuse versus the cardiomyocyte specific localization of FrzA expression. We for the first time we used sFRP-1 KO animal model to examine the effect of sFRP-1 in cardiac structure maintenance. We found that mice lacking sFRP-1 expression appeared normal until 3 months of age. However, sFRP-1 KO mice starting from 6 months of age exhibit an increase in heart size confirmed by heart to body weight ratio followed by a very significant increase at 1 year of age. Our results suggest that loss of this protein leads to mild cardiac hypertrophy, cardiac dilation and deterioration of heart function in the adult mice at one year of age measured as fractional shortening (FS). This animal model provides new insights into the importance of the Wnt signaling pathway in the pathophysiology of heart failure and genetic predispositions to heart disorders and establishes the significant role of this protein in cardiovascular disease.

Our attempt was to determine mechanism, which could contribute to the cardiac phenotype in the sFRP-1 KO mice. Numerous models have demonstrated the relevance of apoptosis in the development of cardiac hypertrophy and dilated cardiomyopathy (228-229). Furthermore, studies have described sFRP1 in tumorigenesis where upregulation of this gene leads to increased apoptosis (230-231), and downregulation leads to cancer via constitutive activation of the Wnt pathway (232-234). In the heart, the role of sFRP-1 is not clearly defined. Overexpression of FrzA reduced the degree of apoptosis after MI, however, an opposing cardiac phenotypic effect was observed with preconditioning and MI with FrzA overexpression in cardiomyocytes (α-MHC promoter) under a conditional transgenic expression approach (226-227). *In vitro* studies have demonstrated that overepression of sFRP-1 reduced the resistance of cells to apoptotic stimuli (134). There was no change in the degree of apoptosis in the sFRP-1 KO mice compared with control littermates over the time course of 1 year of age. This finding suggests that the development of cardiac remodeling in

the sFRP-1 KO mice occurs through a novel mechanism which prevents cardiomyocytes from undergoing programmed cell death.

Next, we determined whether matrix remodeling, which has been well described in cardiac hypertrophy and dilated cardiomyopathy played a role in the cardiac phenotype of the sFRP-1 KO mice. The Wnt signaling pathway regulates fibrosis in the liver, lung and skin (236-238). However, the role of Wnt, sFRP-1 and fibrosis in the heart is not well defined. Duplaa et al. demonstrated that overexpression of sFRP-1 resulted in improvement of heart function and scar size with increased collagen deposition in the scar in the transgenic mice post-MI (226). We found that there was a significant increase in interstitial and perivascular fibrosis and collagen deposition in the sFRP-1 KO mice compared to their littermates at one year of their age. Interestingly PCR Array analysis performed on heart homogenates of sFRP-1 KO versus WT littermates demonstrated an upregulation of Wnt target genes crucial for proliferation, cell growth (Fgf4, Lef1, Wnt3) as well as the profibrotic gene Wisp1 which was shown to be an extremely potent pro-mitogenic (239), pro-hypertrophic and most importantly pro-fibrotic growth factor for cardiomyocytes *in vitro* (240). (Figure 5.3.) This finding demonstrates that sFRP-1 plays an important role in regulation of Wnt signaling molecules responsible for cardiac function and development of fibrosis.

Cytoplasmic β-catenin translocates to the nucleus and forms a complex with transcription factors of the Tcf/Lef family and regulates expression of specific target genes (241). Recent evidence has shown that downregulation of β-catenin is required for adaptive cardiac remodeling (242,244). Additionally, β-catenin overexpression in a rat MI model resulted in a significant decrease in infarct size and decreased apoptosis (247). Overexpression of FrzA in MI resulted in decreased cytosolic accumulation of β-catenin (226). In human dilated cardiomyopathy and coronary artery disease decreased expression of β-catenin was observed (235). Additionally GSK3β, previously described as a crucial factor for cardiac hypertrophy (176) was dysregulated in heart hypertrophy of the MCT-induced PAH. In the present study sFRP-1 KO animals developed cardiac remodeling changes with no significant changes in the phosphorylation status of GSK3β suggesting different molecular mechanism of sFPR-1 heart disorder than observed in MCT-induced PAH in rats. However, we observed an increase in the accumulation of β-catenin in the sFRP-1 KO heart homogenates. Interestingly protein expression of the main transcriptional targets of canonical Wnt/β-catenin signaling pathway, cyclin D and cMyc was downregulated in sFRP-1 KO hearts at one year of age. This provides a conclusion that the loss of sFRP-1 leads to

significant loss of canonical Wnt signaling activity (Figure 5.3.). To support this finding recent report show that suppression of canonical Wnt signaling in heart of plakoglobin deficient mice was associated with arrhythmogenic right ventricular cardiomyopathy (ARVC) and an increase in fibrosis in the heart (243). The authors attempt to link an essential role of the Wnt/β-catenin signaling in regulating transcriptional switch between myogenesis versus adipogenesis (243) and the occurrence of fibrosis in the myocardium.

As a support to our finding of canonical Wnt inactivation, fluorescent staining was performed showing that β-catenin accumulation is marked and clearly located in intercalated disks but not translocated to the nucleus in the myocardium of sFRP-1 KO mice hearts at one year of age (Figure 5.3.). Interestingly, accumulation of β-catenin in the intercalated disks was demonstrated in hamster and human cardiomyopathic hearts where it is mainly implicated in mediating cell to cell adhesion and shapening of cardiomyocytes rather than transcription of Wnt target genes and this accumulation could increase myocardial wall stiffness and left ventricular end diastolic pressure in human cardiomyopathic hearts (248).

In patients with end-stage congestive heart failure or idiopathic dilated cardiomyopathy, the most prominent feature of remodeling involve the downregulation of Connexin43 (Cx43) and reduction in gap junction plaque size (249) (Figure 5.3.). Connexin43 was previously shown to be decreased in cardiomyopathies and the diseased myocardium (250-251). Interestingly it has been published that the induction of the canonical Wnt signaling pathway by LiCl or Wnt1 clearly correlated with an increase in the transcript levels of Cx43 in rat cardiomyocytes. The authors suggest that the upregulation of Cx43 is likely to result in nuclear translocation of β-catenin and the subsequent transcriptional transactivation, which is dimished in our sFRP-1 KO cardiomyopathic hearts. In the transgenic model of cardiomyopathy due to the conditionally expressed diphtheria toxin A in cardiomyocytes the authors observed a decrease in Cx43 and β-catenin in the diseased heart. Our results indicate that loss of sFRP-1 leads to suppression of β-catenin transcriptional activity through the loss of cyclin D and cMyc expression leading to an age dependent decrease in Cx43 (Figure 5.3.). A positive regulation and association of Connexin43 with β-catenin signaling in the cardiomyocytes as well as a correlation of Connexin43 with idiopathic dilated cardiomyopathy has been reported (248,252).

Our results suggest that the loss of sFRP-1 suppressed Wnt/β-catenin signaling leading to an age dependent downregulation of Cx43 expression, which positively correlates, with normal heart function. Loss of Connexin43 supports the idea that sFRP-1 is crucial for cardiac

maintenance and its loss is clearly associated with the development of cardiac remodeling in adult mouse (Figure 5.3.).

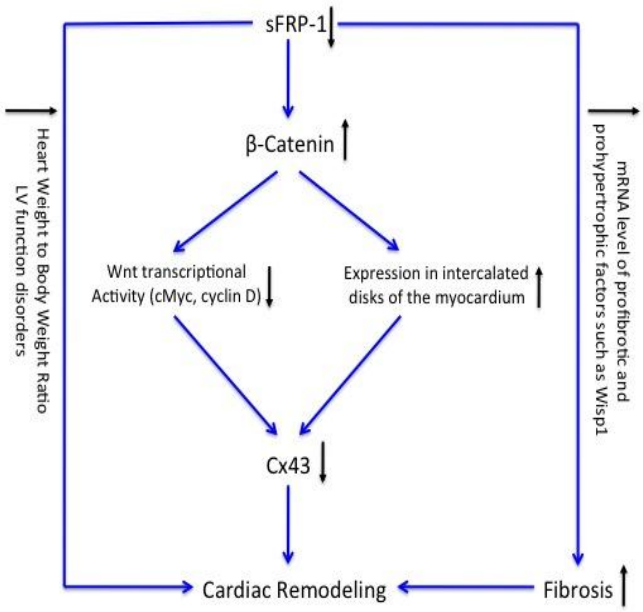

Figure 5.3. Potential mechanism of sFRP-1 KO-induced cardiac remodeling in mice. (Author's scheme)

Sudden cardiac death accounts for approximately 300,000 deaths in the United States each year, most of these are caused by cardiac arrhythmias and are commonly seen in dilated cardiomyopathy. The development of new therapies has been hindered by the limited knowledge of the molecular mechanisms underlying these arrhythmias. The role of sFRP-1 and Wnt in the induction of cardiac arrhythmia in the transgenic animal model is unknown. The sFRP-1 KO mice did not exhibit increased mortality compared to control littermates after one year which means that sFRP-1 does not play a significant role in the sudden death in this model of idiopathic dilated cardiomyopathy. In conclusion, we describe sFRP-1 as a critical factor in maintaining normal cardiovascular function and loss of this gene as a novel mechanism of cardiac remodeling which progresses to dilated cardiomyopathy via the loss of the Wnt mediated canonical signaling pathway. In addition, loss of sFRP-1 leads to inactivation of the canonical Wnt signaling pathway and an increase in interstitial and perivascular fibrosis, which may implicate a novel potential mechanism for dilated cardiomyopathy which is unique to the Wnt signaling pathway. Further studies elucidating the role of sFRP-1 in the heart and how it regulates the Wnt signaling pathway needs to be performed and may bring forth new insight into novel therapeutic targets in the management of heart failure patients.

5. Outlook

Our study in MCT-PAH presents potential role of PDGF/GSK3β Wnt independent signaling in vascular remodeling in PAH as well as Wnt signaling in cardiac maintenance but also highlights areas that require addressing and further studies needs to be performed.

To further consider the role of Wnt/GSK3β signaling in pathogenesis of MCT-PASMC several experiment need to be performed to improve our understanding in this issue, such as:

1. Non-canonical Wnt5A was observed to be upregulated on mRNA level in lung tissues of MCT-induced PAH comparing to healthy controls. To further elucidate this observation would be of interest. MCT-PASMC should be stimulated with different concentrations of Wnt5A and the effect on proliferation and downstream cellular signaling should be investigated according to its potential to manipulate Wnt signaling canonical as well as non-canonical Wnt pathway.
2. To further evaluate role of GSK3β in pathogenesis of MCT-PASMC we should try to investigate the effect of its modulation by amino-acid substitutions on broader variety of PASMC effector molecules since we know that it potentially has influence on a wider spectrum of downstream targets like: cyclin D, NFATc and Kv channels all of which shown to be crucial factors in PAH pathogenesis
3. Additionally next step we should take is to test apoptotic abilities of Wnt3A which blocked proliferation induced by growth factors and GSK3β variants like: wild type, S9A, Y216D and double S9A/Y216D mutant on MCT-PASMC.
4. To complete GSK3β study in PAMSC use of siRNA would be of our interest to see how loss of GSK3β would infuence cellular signaling and most importantly functional parameters of MCT-PASMC like proliferation or apoptosis.
5. The role of β-catenin is still not well understood. Induction of canonical Wnt signaling by Wnt3A and LiCl has inhibitory effect on proliferation rate of these cells. Overexpression of active and dominant negative β-catenin in MCT-PASMC could potentially give important insights to the role of canonical Wnt signaling in PASMC pathogenesis.

Finally and most importantly the concept will need to be proven our *in vivo* in experimental animal models of PAH. To evaluate our hypothesis *in vivo* several approaches can be elucidated such as:

1. To evaluate role of GSK3β in experimental model of MCT-induced PAH different variants of GSK3β could be overexpressed in rats using adenoviral vectors potentially as a preventive therapy or applied during the disease progression 3 or 5 weeks after monocrotaline injection. Results could be evaluated by messuring PAP, RVSP and muscularization degree.
2. To test our hypothesis *in vivo,* the best way would be to approach our concepts genetically using transgenic mice and usage of already established in mice hypoxia-induced Pulmonary Hypertension. To do this first we need to evaluate expression profile of our system in this model. If it is simarly regulated like in MCT-induced PAH in rats several type of mice can be used. To prove involvement of GSK3β in vascular remodeling and PASMC pathogenesis *in vivo* would be extremely interesting to use different variants GSK3β (WT, S9A, Y216D) knock-in mice where GSK3β is conditionally expressed under control of alpha SM22 promoter for induction of PH by hypoxia. Effect of GSK3β could be measured by PAP, RVSP, and assessment of muscularization degree. Additionally cellular signaling and proliferation ability could be evaluated in PASMC isolated from these animals.
3. Induction of canonical Wnt signaling *in vitro* by stimulation of MCT-PASMC with Wnt3A or LiCl inhibited proliferation response of these cells. Treatment of MCT-induced PAH at very late stages of disease when Wnt signaling is switched off around 4 to 5 weeks post MCT injection would be of interest. Results could be evaluated by messuring PAP, RVSP and muscularization degree.

Cardiac phenotype observed in sFRP-1 KO mice at one year of age provided us very interesting insights into loss of heart function induced via suppression of Wnt signaling and decrease of connexin43 expression. Yet there are still many interesting questions to address like:

1. To further evaluate the concept that loss of sFRP-1 disturb maintenance of heart function further hemodynamics study shoul be performed to estimate LV systolic and diastolic function by estimation of such parameters like Left Ventricular Systolic Pressure (LVSP) or Left Ventricular End Diastolic Pressure (LVEDP)
2. sFRP-1 expressed in endothelial cells serving potentially as angiogenic factor could potentially contributes to PAH. Role of sFRP-1 in hypoxia-induced Pulmonary Hypertension can be expressed by measuring such parameters like Right Ventricle Systolic Pressure (RVSP), PAP, and muscularization degree in sFRP-1 KO mice exposed to hypoxia comparing to not exposed.

7. Summary

Pulmonary Arterial Hypertension is a complex disease associated with a poor prognosis. Many therapeutical strategies have been introduced to PAH patients. All approved therapies targeting vasodilation are effective by improving hemodynamics, exercise capacity and give small improvements in survival in PAH patients (78), however, they failed to reverse the disease. Therefore the focus of the treatment in recent years has changed from vasodilators to anti-proliferative agents and new signaling pathways are needed to be evaluated for future therapies.

In our studies we focused on the Wnt signaling pathway, which was recently implicated to many cancerous diseases. In addition it has been shown that this pathway is crucial for cardiovascular diseases. In our study we observed downregulation of well-known canonical Wnt signaling ligands in experimental PAH in rats. GSK3ß and ß-Catenin, which are downstream targets of canonical Wnt signaling, are upregulated in lungs as well as in PASMCs from MCT-induced PAH rats compared to controls on protein level. Further, stimulation of MCT-PASMCs with both PDGF-BB and Wnt3a induced inactivation of GSK3ß, whereas only Wnt3a regulated ß-Catenin accumulation in PASMCs. Constitutive activation of GSK3ß by amino acid substitution S9A (9th serine replaced to alanine) or Y216D (tyrosine replaced to aspartic acid) inhibited serum-induced PASMC proliferation influencing ERK phosphorylation. PDGF-BB-induced proliferation was inhibited by Y216D mutant, which seems to be implicated in PDGF signaling in experimental PAH.

The fact that PDGF-induced MCT-PASMC proliferation could be significantly decreased by GSK3ß amino acid residues modulation, collectively indicate the importance of GSK3ß in the pathogenesis of PAH. Significant upregulation of GSK3ß in lung explants of patients with iPAH support a concept that this protein plays a role in development of PAH.

Profound changes in pulmonary vasculature in PAH are followed by heart hypertrophy and heart failure. Wnt signaling was previously reported to play crucial role in cardiovascular maintenance and one of our candidate genes was sFRP-1, an extracellular Wnt signaling modulator. We found that sFRP-1 is abundantly expressed in normal mice hearts at 3, 6 and 12 months of age and predominantly localized in cardiomyocytes and endothelial cells suggesting that it may play a significant role in heart function maintenance. To evaluate the role of sFRP-1 in adult hearts we used sFRP-1 KO mice up to 12 months of age. No significant phenotype was observed in these mice up to 6 months of age. At one year of age, sFRP-1 KO mice exhibited significant increase in heart size with age-dependent increase in

heart weight to body weight ratio. Additionally to this phenotype, an increase in left ventricular dimensions, posterior wall thickness, and a decrease in fractional shortening occurred in sFRP-1 KO mice at 1 year of age. Increased formation of fibrotic lesions in myocardium of 1-year-old mice collectively suggest that loss of sFRP-1 leads to cardiac hypertrophy and finally cardiomyopathy. Determination of wide mRNA expression profile showed that parts of Wnt signaling in heart of 1-year-old mice are significantly upregulated mainly the Frizzled 2 pathway and pro-hypertrophic, pro-fibrotic Wnt dependent genes like Fgf4, WIF1 and already well described Wisp1. Increased β-catenin expression and its accumulation in intercalated disks suggested a decrease in Wnt/β-catenin transcriptional activity that was confirmed by significant down regulation of cyclin D and cMyc. Suppression of canonical Wnt signaling is possible mechanism of downregulation of connexin43 and loss of heart function both described in human idiopathic and dilated cardiomyopathies.

In conclusion, we describe that sFRP-1 is a critical factor in maintaining normal cardiovascular function and loss of this gene induces cardiac remodeling which progresses to dilated cardiomyopathy. The mechanism is a supression of Wnt mediated canonical signaling pathway followed by decrease in connexin 43 expression, protein that is very important in heart function and its contraction ability. Yet more studies needs to be done to elucidate and propose final role of Wnt signaling in mainaining cardiovascular system function.

8. Zusammenfassung

Die pulmonale arterielle Hypertonie (PAH) ist eine Erkrankung der Lungengefäße, die mit einer sehr schlechten Prognose assoziiert ist. Die zur Therapie zugelassenen Medikamente umfassen Endothelin-Rezeptor Antagonisten, Prostanoide und Phosphodiesterase 5 Hemmstoffe, alles gefäßerweiternde Medikamente, die zwar die Belastbarkeit der Patienten erhöhen, aber die Erkrankung nicht heilen können. Daher ist es notwendig, neue Signalwege für zukünftige Therapien zu evaluieren.

In unseren Untersuchungen haben wir uns auf den Wnt Signalweg fokussiert, der bei vielen malignen Erkrankungen eine Rolle spielt. Zusätzlich wurde gezeigt, dass dieser Signalweg auch bei anderen kardiovaskulären Erkrankungen involviert ist. In unserer Studie zeigen wir die Abnahme der Liganden des Wnt Signalweges bei experimenteller pulmonaler Hypertonie im Rattenmodell (Monocrotalin (MCT) Injektion). GSK3β und β-Catenin, die nachgeschalteten Ziele des Wnt Signalweges, waren auf Protein-Ebene erhöht, sowohl in Lungen als auch in pulmonalarteriellen glatten Muskelzellen (PASMCs) von MCT Ratten im Vergleich zur gesunden Tieren. Die Behandlung von MCT-PASMCs mit dem Wachstumsfaktor PDGF-BB oder mit Wnt3a führte zu einer Inaktivierung von GSK3β, wobei nur Wnt3a die β-Catenin Akkumulation in PASMCs regulierte. Um die Rolle von GSK3β näher zu untersuchen, generierten wir konstitutiv aktive Mutanten bei denen die Aminosäure S9A (9tes Serin mit Alanin ersetzt) oder Y216D (Tyrosin mit der Aminosäure Aspartat ersetzt) ersetzt wurden. Eine Überexpression dieser GSK3 Mutanten in PASMCs inhibierte die Serum-induzierte Proliferation wobei die extrazellulär regulierte Kinase (ERK) als nachgeschalteter Signalweg identifiziert wurde. Untersuchungen an humanem Lungengewebe von Patienten mit PAH zeigten eine signifikante Erhöhung von GSK3β und unterstützen die Theorie, dass dieses Protein eine Rolle in der Entwicklung der PAH spielt.

Profunde Veränderungen der pulmonalen Gefäßstruktur bei PAH führen zu Herzhypertrophie und Herzversagen. Es wurde bereits erwähnt, dass der Wnt Signalweg eine entscheidende Rolle bei der Aufrechterhaltung der kardiovaskulären Funktion spielt, und eines unserer untersuchten Gene war sFRP-1, ein extrazellulärer Modulator des Wnt Signalweges. Wir konnten zeigen, dass sFRP-1 in normalen Mausherzen im Alter von 3, 6 und 12 Monaten exprimiert wird und v.a. in Kardiomyozyten und Endothelzellen lokalisiert ist, so dass man vermuten kann, dass es eine signifikante Rolle in der Aufrechterhaltung der Herzfunktion spielt. Um die Rolle von sFRP-1 in erwachsenen Herzen zu untersuchen,

wurden sFRP-1 KO Mäuse im Alter von bis zu 12 Monaten untersucht. Dabei konnte kein signifikanter Unterschied im Phänotyp bei den Mäusen im Alter von bis zu 6 Monaten beobachtet werden. Im Alter von einem Jahr zeigten sFRP-1 KO Mäuse eine Zunahme der Herzgröße mit einer altersabhängigen Zunahme des Verhältnisses von Herzgewicht zu Körpergewicht. Darüberhinaus trat bei den sFRP-1 KO Mäusen im Alter von einem Jahr eine Zunahme der linksventrikulären Herzdimensionen, der hinteren Herzwanddicke und eine Abnahme des Fractional Shortening (FS) auf. Die vermehrte Entstehung von fibrotischen Läsionen im Myokard von ein Jahr alten Mäusen lässt vermuten, dass ein Verlust von sFRP-1 zu kardialer Hypertrophie führt, die eine dilatierte Kardiomyopathie zur Folge hat. Die Bestimmung eines weitläufigen mRNA Expressionsprofils hat gezeigt, dass Teile des Wnt Signalweges im Herzen signifikant erhöht sind, dabei v.a. der Frizzled 2 Signalweg und prohypertrophische, profibrotische und Wnt abhängige Gene wie Fgf4, WIF1 und das bereits gut beschriebene Wisp1. Die erhöhte β-Catenin-Expression läßt eine Abnahme der transkriptionellen Aktivität von Wnt/β-Catenin vermuten. Die Suppression des bewährten Wnt Signalweges ist ein möglicher Mechanismus zur Senkung von Connexin 43 und zum Verlust der Herzfunktion, die beide in menschlischer idiopathischer und dilatativer Kardiomyopathie beschrieben werden.

Abschließend beschreiben wir, dass sFRP-1 ein kritischer Faktor in der Aufrechterhaltung der kardiovaskulaeren Funktion ist und ein Verlust dieses Gens ein kardiales Remodelling induziert, das zu dilatativer Kardiomyopathie führt. Der Mechanismus besteht aus der Suppression des Wnt vermittelten, bewährten Signalweges, gefolgt von einer Abnahme der Connexin 43 Expression, eines Proteins, das sehr wichtig fuer die Herzfunktion und ihre Kontraktionsfähigkeit ist. Es müssen noch mehr Studien erfolgen, um die endgültige Rolle des Wnt Signalweges in der Aufrechterhaltung der Funktion des kardiovaskulären Systems aufzuklären.

9. Appendix

Gene	Primers	Anealing [°C]	Product size
	Real-Time PCR		
Wnt1	F:CTACGTTGCTACTGGCACTGAC	60	121bp
	R:AGACTCTTGGAATCTGTCAGCAG		
Wnt3A	F: ATTTGGAGGAATGGTCTCTCG	60	172bp
	R: GCAGGTCTTCACTTCGCAAC		
Wnt5A	F: GCCACTTGTATCAGGACCACA	60	200bp
	R: GGCATTTACCACTCCAGCAG		
sFRP-1	F:GCTAGAGAGGAGCCCTGAAAAT	60	136bp
	R:TGCACTGTATCCCTCTATCTTGC		
Frizzled1	F:CGTACTGAGTGGAGTGTGTTTTG	60	188bp
	R:TGAGCTTTTCCAGTTTCTCTGTC		
Frizzled2	F: TACCTGTTCATCGGCACATC	60	143bp
	R: GTGTAGAGCACGGAGAAGACG		
Axin1	F:GAGGAAGAAGAAAAGAGAGCAA	60	123bp
	R:CCACAGAAATAGTAGGCCACAAC		
GSK3ß	F: ACTTTGTGACTCAGGAGAACTGG	60	141bp
	R:TCGCCACTCGAGTAGAAGAAATA		
ß-catenin	F:TCAGATCTTAGCTTACGGCAA	60	134bp
	R:TTGTTGCTAGAGCAGACAGAC		
	Cloning and Mutagenesis		
GSK3ß	F:CCTAACACCCCAACATAAAGACA	58	1420bp
UTR	R:GTAACTGGTGGTTTTTCCTGTGC		
GSK3ß WT	F:CCTAACACCCCAACATAAAGACA	58	1299bp
TOPO	R: GTAACTGGTGGTTTTTCCTGTGC		
GSK3ß S9A	F:ggcccagaaccaccgcattcgcggagagctgcaa	58	6813bp
Mutagenesis	R:ttgcagctctccgcgaatgcggtggttctgggcc		
GSK3ß Y216D	F:gaacccaatgtttcggatatctgttctcggtac	58	6813bp
Mutagenesis	R:gtaccgagaacagatatccgaaacattgggttc		

Table 1.App List of primers used for PCR amplification

Sequencing		
Sequence	**Primers**	**Plasmid**
T7	F: taatacgactcacattaggg	pGEM-T Easy
SP6	R: tatttaggtgacactatag	pGEM-T Easy
T7	F: taatacgactcacattaggg	pcDNA 3.1 TOPO
BGH	R: tagaaggcacagtcgagg	pcDNA 3.1 TOPO

Table 2.App List of primers used for PCR fragments sequencing

GSK3β splice variant detection		
Primer name	**Sequence**	**Description**
1	CCTAACACCCCAACATAAAGACA	GSK3β full length
2	GTAACTGGTGGTTTTTCCTGTGC	GSK3β full length
3	ATTCGTCAGGAACAGGACATTT	GSK3β 13aa forward
4	CCCGCACTCCTGAGGTGAAAT	GSK3β 13aa reverse

Table 3.App List of primers used for PCR GSK3β splice variant detection

Primary Antibody	Source	Dilution WB	Dilution IHC/IHF	Company
ß-catenin	Rabbit	1:1000	1:100	BD Transduction
pGSK3ß S9	Rabbit	1:1000		Cell Signaling
GSK3ß Y216	Mouse	1:1000		BD Transduction
GSK3ß total	Rabbit	1:1000		Cell Signaling
Axin1	Rabbit	1:500		Santa Cruz
GAPDH	Mouse	1:1000		Novus
H1	Rabbit	1:500		Santa Cruz
pAKT	Rabbit	1:1000		Cell Signaling
AKT total	Rabbit	1:1000		Cell Signaling
pERK ½	Mouse	1:1000		Santa Cruz
ERK ½ total	Mouse	1:1000		Santa Cruz
Frizzled 2	Rabbit	1:1000		Cell Signaling
Dvl-2	Rabbit	1:1000		Cell Signaling

Cylin D	Rabbit	1:1000		Cell Signaling
cMyc	Rabbit	1:1000		Cell Signaling
Connexin 43	Rabbit		1:100	Cell Signaling
sFRP-1	Rabbit		1:200	Santa Cruz

Table 4.App List of primary antibodies used

Secondary Antibody	Dilution WB	Company
HRP-conjugated anti-mouse IgG	1:30000	Sigma
HRP-conjugated anti-rabbit IgG	1:30000	Sigma
Alexaflur anti-rabbit 488 antibody	1:500	Molecular Probes

Table 5.App List of secondary antibodies used

10. **References**

(1) Humbert, M., Morrell, N. W., Archer, S. L., Stenmark, K. R., MacLean, M. R., Lang, I. M., Christman, B. W., Weir, E. K., Eickelberg, O., Voelkel, N. F., Rabinovitch, M., **Cellular and molecular pathobiology of pulmonary arterial hypertension**. *J. Am. Coll. Cardiol.* 2004

(2) Simonneau, G., Galie, N., Rubin, L. J., Langleben, D., Seeger, W., Domenighetti, G., Gibbs, S., Lebrec, D., Speich, R., Beghetti, M., Rich, S., Fishman, A., **Clinical classification of pulmonary hypertension**. *J. Am. Coll. Cardiol.*

(3) McLaughlin, V. V., Shillington, A., Rich, S., **Survival in primary pulmonary hypertension: the impact of epoprostenol therapy.** *Circulation* 2002

(4) D'Alonzo, G. E., Barst, R. J., Ayres, S. M., Bergofsky, E. H., Brundage, B. H., Detre, K. M., Fishman, A. P., Goldring, R. M., Groves, B. M., Kernis, J. T. **Survival in patients with primary pulmonary hypertension. Results from a national prospective registry**. *Ann. Intern. Med.* 1991

(5) Zaiman, A., Fijalkowska, I., Hassoun, P. M., Tuder, R. M., **One Hundred Years of Research in the Pathogenesis of Pulmonary Hypertension.** *Am. J. Respir. Cell. Mol. Biol.* 2005

(6) Cournand, A., Ranges, H. A., **Measurement of cardiac output in man using the technique of catheterization of the right auricle or ventricle.** *J. Clin. Invest.* 1945.

(7) Hatano, S., Strasser, T., **World Health Organization 1975 primary pulmonary hypertension**. *Geneva* 1975

(8) Rubin, L. J., **Primary pulmonary hypertension**. *N. Engl. J. Med.* 1997

(9) Fishman, A. P., **Clinical classification of pulmonary hypertension**. *Clin. Chest. Med.* 2001

(10) Fishman, A. P., **Primary pulmonary arterial hypertension: a look back**. *J. Am. Coll. Cardiol.* 2004

(11) Dresdale, D. T., Schultz, M., Michtom , R. J., **Primary pulmonary hypertension. I. Clinical and hemodynamic study.** *Am. J. Med* 1991

(12) Simonneau, G., Robbins, I. M., Beghetti, M., Channick, R. N., Delcroix, M., Denton, CH. P., Elliott, C. G., Gaine, S. P., Gladwin, M. T., Jing, Z. C., Krowka, M. J., Langleben, D., Nakanishi, N., Souza, R., **Updated Clinical Classification of Pulmonary Hypertension**. *J. Am. Coll. Cardiol.* 2009

(13) Rich, S., **Primary pulmonary hypertension: executive summary.** *Evian, France: World Health Organization* 1998

(14) Jeffery, T.K., Morrell, N.W., **Molecular and cellular basis of pulmonary vascular remodeling in pulmonary hypertension.** *Prog. Cardiovasc. Dis.* 2002

(15) Mandegara, M., Fung, Y. C., Huang, W., Remillarda, C. V., Rubina, L. J., Yuana, J., **Cellular and molecular mechanisms of pulmonary vascular remodeling: role in the development of pulmonary hypertension**. *Microvascular Research* 2004

(16) Barman, S. A., Zhu, S., White, R. E., **RhoA/Rho-kinase signaling: a therapeutic trget for pulmonary hypertension**. *Vascular Health and Risk Menagement* 2009

(17) Hishikawa, K., Nakaki, T., Marumo, T., Hayashi, M., Suzuki, H., Kato, R., Saruta, T., **Pressure promotes DNA synthesis In rat cultured vascular smooth muszle cells**. *J. Clin. Invest.* 1991

(18) Gaine, S. P., Rubin, L. J., **Primary pulmonary hypertension**. *Lancet* 1998

(19) Tuder, R. M., Marecki, J. C., Richter, A., Fijalkowska, I., Flores, s., **Pathology of Pulmonary Hypertension.** *Clin. Chest. Med.* 2007

(20) Archer, S., Rich, S., **Primary Pulmonary Hypertension: A Vascular Biology and Translational Research "Work in Progress**". *Circulation* 2000

(21) Galie, N., Torbicki, A., Barst, R., Dartevelle, P., Haworth, S., Higenbottam, T., Olschewski, H., Peacock, A., Pietra, G., Rubin, L. J., Simonneau, G., **Guidelines on diagnosis and treatment of pulmonary arterial hypertension The Task Force on Diagnosis and Treatment of Pulmonary Arterial Hypertension of the European Society of Cardiology.** *European Heart Journal* 2004
(22) Cool, C. D., Stewart, J. S., Werahera, P., Miller, G. J., Williams, R. L., Voelkel, N. F., **Three-dimensional reconstruction of pulmonary arteries in plexiform pulmonary hypertension using cell specific markers: evidence for a dynamic and heterogeneous process of pulmonary endothelial cell growth.** *Am. J. Pathol.* 1999
(23) Tuder, R. M., Groves, B. M., Badesch, D. B., Voelkel, N. F., **Exuberant endothelial cell growth and elements of inflammation are present in plexiform lesions of pulmonary hypertension**. *Am. J. Pathol.* 1994
(24) Heath, D., Smith, P., Gosney, J., **Ultrastructure of early plexogenic pulmonary arteriopathy.** *Histopathology* 1988
(25) Chazova, I., Loyd, J. E., Newman, J. H., Belenkov, Y., Meyrick, B., **Pulmonary artery adventitial changes and venous involvement in primary pulmonary hypertension**. *Am. J. Pathol.* 1999
(26) Palevsky, H. I., Schloo, B. L., Pietra, G. G., Weber, K. T., Janicki, J. S., Rubin, E., **Primary pulmonary hypertension, vascular structure, morphometry, and responsiveness to vasodilator agents**. *Circulation* 1989
(27) Kurt, R., Stenmark, N. D., Frid, M., Gerasimovskaya, E., Das, M., **Role of the Adventitia in Pulmonary Vascular Remodeling.** *Physiology* 2006
(28) Sartore, S., Chiavegato, A., Faggin, E., Franch, R., Puato, M., Ausoni, S., Pauletto, P., **Contribution of Adventitial Fibroblasts to Neointima Formation and Vascular Remodeling From Innocent Bystander to Active Participant.** *Circulation* 2007
(29) Li, G., Chen, S. J., Oparil, S., Chen, Y. F., Thompson, J. A., **Direct in vivo evidence demonstrating neointimal migration of adventitial fibroblasts after balloon injury of rat carotid artery.** *Circulation* 2000
(30) Short, M., Raphel, A., Nemenoff, W., Zawada, M., Stenmark, K., Das, M., **Hypoxia induces differentiation of pulmonary artery adventitial fibroblasts into myofibroblasts.** *Am. J. Physiol. Cell. Physiol.* 2004
(31) Herve, P., Humbert, M., Sitbon, O., **Pathobiology of pulmonary hypertension: the role of platelets and thrombosis.** *Clin. Chest Med.* 2001
(32) Friedman, R., Mears, J. G., Barst, R. J., **Continuous infusion of prostacyclin normalizes plasma markers of endothelial cell injury and platelet aggregation in primary pulmonary hypertension**. *Circulation* 1997
(33) Pietra, G. G., Capron, F., Stewart, S., **Pathologic assessment of vasculopathies in pulmonary hypertension.** *J. Am. Coll. Cardiol*. 2004
(34) Eisenberg, P. R., Lucore, C., Kaufman, L., **Fibrinopeptide A levels indicative of pulmonary vascular thrombosis in patients with primary pulmonary hypertension**. *Circulation* 1990
(35) Christman, B. W., McPherson, C. D., Newman, J. H., **An imbalance between the excretion of thromboxane and prostacyclin metabolites in pulmonary hypertension.** *N. Engl. J. Med.* 1992
(36) Chaouat, A., Weitzenblum, E., Higenbottam, T., **The role of thrombosis in severe pulmonary hypertension**. *Eur. Respir.* 1996
(37) Morrel, N. W., Adnot, S., Archer, S. L., Dupuis, J., Jones, P. L., MacLean, M., McMurry, I. F., Stenmark, K. R., Thistlethwaitre, P. A., Weissmann, N., Yuan, J., Weir, E. K., **Cellular and Molecular basis of Pulmonary Arterial Hypertension** *J. Am. Coll. Cardiol*. 2009

(38) Adnot, S., **Lessons learned from cancer may help in the treatment of pulmonary hypertension.** *J. Clin. Invest.* 2005
(39) Eddahibi, S., Guignabert, C., Barlier-Mur, A. M., **Cross talk between endothelial and smooth muscle cells in pulmonary hypertension: critical role for serotonin-induced smooth muscle hyperplasia.** *Circulation* 2006
(40) Touyz, R. M., Schiffrin, E. L., **Reactive oxygen species in vascular biology: implications in hypertension**. *Histochem. Cell. Biol.* 2004
(41) Durmowicz, A. G., Parks, W. C., Hyde, D. M., Mecham, R. P., Stenmark, K. R., **Persistence, re-expression, and induction of pulmonary arterial fibronectin, tropoelastin, and type I procollagen mRNA expression in neonatal hypoxic pulmonary hypertension**. *Am. J. Pathol.* 1994
(42) Stenmark, K. R., Mecham, R. P., **Cellular and molecular mechanisms of pulmonary vascular remodeling**. *Ann. Rev. Physiol.* 1997
(43) Desmouliere, A., Chaponnier, C., Gabbiani, G., **Tissue repair, contraction, and the myofibroblast**. *Wound Repair Regen.* 2005
(44) Jones, F. S., Meech, R., Edelman, D. B., Oakey, R. J., Jones, P. L**., Prx1 controls vascular smooth muscle cell proliferation and tenascin-C expression and is upregulated with Prx2 in pulmonary vascular disease.** *Circ. Res.* 2001
(45) Jones, P. L., Rabinovitch, M., **Tenascin-C is induced with progressive pulmonary vascular disease in rats and is functionally related to increased smooth muscle cell proliferation.** *Circ. Res.* 1996
(46) Christman, B. W., McPherson, C. D., Newman, J. H., **An imbalance between the excretion of thromboxane and prostacyclin metabolites in pulmonary hypertension**. *N. Engl. J. Med.* 1992
(47) Tuder, R. M., Cool, C. D., Geraci, M. W., **Prostacyclin synthase expression is decreased in lungs from patients with severe pulmonary hypertension**. *Am. J. Respir. Crit. Care Med.* 1999
(48) Hoshikawa, Y., Voelkel, N. F., Gesell, T. L., **Prostacyclin receptor dependent modulation of pulmonary vascular remodeling**. *Am. J. Respir. Crit. Care Med.* 2001
(49) Geraci, M. W., Gao, B., Shepherd, D. C., **Pulmonary prostacyclin synthase overexpression in transgenic mice protects against development of hypoxic pulmonary hypertension.** *J. Clin. Invest.* 1999
(50) Giaid, A., Saleh, D**., Reduced expression of endothelial nitric oxide synthase in the lungs of patients with pulmonary hypertension.** *N. Engl. J. Med.* 1995
(51) Xu, W., **Increased arginase II and decreased NO synthesis in endothelial cells of patients with pulmonary arterial hypertension**. *FASEB J.* 2004
(52) Rabinovitch, M., **Molecular pathogenesis of pulmonary arterial hypertension**. *J. Clin. Invest.* 2009
(53) Giaid, A., Yanagisawa, M., Langleben, D., **Expression of endothelin-1 in the lungs of patients with pulmonary hypertension.** *N. Engl. J. Med.* 1993
(54) Li, H., **Enhanced endothelin-1 and endothelin receptor gene expression in chronic hypoxia**. *J. Appl. Physiol.* 1994
(55) Geraci, M. W., Moore, M., Gesell, T., **Gene expression patterns in the lungs of patients with primary pulmonary hypertension: a gene microarray analysis**. *Circ. Res.* 2001
(56) Yuan, J. X., Wang, J., Juhaszova, M., Gaine, S. P., Rubin, L. J., **Attenuated K+ channel gene transcription in primary pulmonary hypertension.** *Lancet* 1998
(57) Michelakis, E. D., McMurtry, M. S., Wu, X. C**., Dichloroacetate, a metabolic modulator, prevents and reverses chronic hypoxic pulmonary hypertension in rats: role**

of increased expression and activity of voltage-gated potassium channels. *Circulation* 2002
(58) Moudgil, R., Michelakis, E. D., Archer, S. L.**The role of k+ channels in determining pulmonary vascular tone, oxygen sensing, cell proliferation, and apoptosis: implications in hypoxic pulmonary vasoconstriction and pulmonary arterial hypertension.** *Microcirculation* 2006
(59) McMurtry, M. S., Archer, S. L., Altieri, D. C., Bonnet, S., Haromy, A., Harry, G., Bonnet, S., Puttagunta, L., Michelakis, E., **Gene therapy targeting surviving selectively induces pulmonary vascular apoptosis and reverses pulmonary arterial hypertension.** *J. Clin. Invest.* 2005
(60) Hassoun, P. M., Mouthon, L., Barbera, J. A., Eddahibi, S., Flore, S., Grimminger, F., Jones PL, Maitland ML, Michelakis ED, Schermuly RT, Stenmark KR, Yuan J, Humbert M. **Inflammation, growth factors and pulmonary vascular remodeling.** *J. Am. Coll. Cardiol*. 2009
(61) Barst, R. J., **PDGF signaling in pulmonary arterial hypertension.** *J. Clin. Invest.* 2005
(62) Humbert, M., Monti, G., Fartoukh, M., **Platelet-derived growth factor expression in primary pulmonary hypertension: comparison of HIV seropositive and HIV seronegative patients**. *Eur. Respir. J.* 1998
(63) Eddahibi, S., Humbert,. M, Sediame, S., **Imbalance between platelet vascular endothelial growth factor and platelet-derived growth factor in pulmonary hypertension: effect of prostacyclin therapy.** *Am. J. Respir. Crit. Care Med.* 2000
(64) Schermuly, R. T., Dony, E., Ghofrani, H. A., Pullamsetti, S., Savai, R., Roth, M., Sydykov, A., Lai, Y. J., Weissmann, N., Seeger, W., **Reversal of experimental pulmonary hypertension by pdgf inhibition.** *J. Clin. Invest.* 2005
(65) Perros, F., Montani, D., Dorfmuller, P., Durand-Gasselin, I., Tcherakian, C., Le Pavec, J., Mazmanian, M., Fadel, E., Mussot, S., Mercier, O., **Platelet-derived growth factor expression and function in idiopathic pulmonary arterial hypertension**. *Am. J. Respir. Crit. Care Med.* 2008
(66) Merklinger, S. L., Jones, P. L., Martinez, E. C., Rabinovitch, M., **Epidermal growth factor receptor blockade mediates Smooth muscle cell apoptosis and improves survival in rats with pulmonary hypertension.** *Circulation* 2005
(67) Iziki, M., Guignabert, C., Fadel, E., Humbert, M., Tu, L., Zadique, P., Dartevelle, P., Simmoneau, G., Adnot, S., Maitre, B., Raffestin, B., Eddahibi, S., **Endothelial-derived FGF2 contributes to the progression of pulmonary hypertension in humans and rodents** *J. Clin. Invest.* 2009
(68) Jones, P. L., Cowan, K. N., Rabinovitch, M., **Tenascin-C, proliferation and subendothelial fibronectin in progressive pulmonary vascular disease**. *Am. J. Pathol.* 1997
(69) Okada, Y., Nakanishi, I., **Activation of matrix metalloproteinase 3 and matrixz metalloproteinase 2 by human neutrophil elastase and cathepsin G**. *FEBS Letters* 1989
(70) Jones, P. L., Crack, J., Rabinovitch, M., **Regulation of tenascin-C gene expression by denature type I collagen is dependent upon a β3 integrin-mediated mitogen-activated protein kinase pathway and a 122-base promoter element.** *J. Cell Science* 1999
(71) Cowan, K. N., Jones, P. L., Rabinovitch, M., **Elastase and matrix metalloproteinase inhibitors induce regression and tenascin-C antisense prevents progression of vascular disease.** *J. Clin. Invest.* 2000
(72) Cowan, K. N., Heilbut, A., Humpl, T., Lam, C., Ito, S., Rabinovitch, M., **Complete reversal of fatal pulmonary hypertension in rats by a serine elastase inhibitor** *Nat. Med.* 2000

(73) Lane, K. B., Machado, R, D., Pauciulo, M. W., Thomson, J. R., Philips, J. A., Loyd, J. E., Nichols, W. C., Trembath, R. C., **Heterozygous germline mutation in BMPR2, encoding TGFbeta receptor, cause familial pulmonary Hypertension.** *Nat. Genetics* 2000
(74) Zaiman, A. L., Podowski, M., Medicherla, S., Gordy, K., Xu, F., Zhen, L., Shimoda, L. A., Neptune, E., Higgins, L., Murphy, A., Chakravarty, S., Protter, A., Sehgal, P., Champion, H., Tuder, R. M., **Role of TGF-beta/ Alk5 signaling pathway in monocrotaline-induced Pulmonary Hypertension.** *Am. J. Respir. Crit. Care Med.* 2008
(75) Galie, N., Torbicki, A., Barst, R., Dartevelle, P., Haworth, S., Higenbottam, T., Olschewski, H., Peacock, A., Pietra, G., Rubin, L. J., Simonneau, G., **Guidelines on diagnosis and treatment of pulmonary arterial hypertension.** *Eur. Respir. J.* 2004
(76) McGoon, M., Gutterman, D., Steen, S., Barst, R., McCrory, D. C., Fortin, T. A., Loyd, J. E., **Screening, early detection, and diagnosis of pulmonary arterial hypertension: ACCP evidence-based clinical practice guidelines**. *Chest* 2004
(77) Badesch, D. B., Abman, S. H., Ahearn, G. S., Barst, R. J., McCrory, D. C., Simonneau, G., McLaughlin, V. V., **Medical therapy for pulmonary arterial hypertension: ACCP evidence-based clinical practice guidelines**. *Chest* 2004
(78) Ghofrani, H. A., Voswinckel, R., Reichenberger, F., Weissmann, N., Schermuly, R. T., Seeger, W., Grimminger, F., **Hypoxia- and non hypoxia related pulmonary hypertension-established and new therapies** *Cardiovasc. Res.* 2006
(79) Lee, S. H., Rubin, L. J., **Current treatment strategies for pulmonary arterial hypertension.** *Journal o Internal Medicine* 2005
(80) Fuster, V., Steele, M., Edwards, W. D., Gersh, B. J., McGoon, M. D., Fry, R. L., **Primary Pulmonary Hypertension: natural history and importance of thrombosis.** *Circulation* 1984
(81) Barst, R. J., Rubin, L. J., Long, W. A., McGoon, M. D., Rich, S., Badesch, D. B., **A comparison of continuous intravenous epoprostenol (prostacyclin) with conventional therapy fo primary pulmonary hypertension.** *N. Engl. J. Med.* 1996
(82) Olschewski, H., Simonneau, G., Galiè, N., Higenbottam, T., Naeije, R., Rubin, L. J., Nikkho, S., Speich, R., Hoeper, M. M., Behr, J., Winkler, J., Sitbon, O., Popov, W., Ghofrani, H. A., Manes, A., Kiely, D. G., Ewert, R., Meyer, A., Corris, P. A., Delcroix, M., Gomez-Sanchez, M., Siedentop, H., Seeger, W., **Inhaled iloprost for severe pulmonary hypertension.** *N. Engl. J. Med.* 2002
(83) Barst, R. J., McGoon, M. D., McLaughlin, V., Tapson, V., Rich, S., Rubin, L., **Beraprost therapy for pulmonary hypertension.** *J. Am. Coll. Cardiol*. 2003
(84) Voswinckel, R., Ghofrani, H. A., Grimminger, F., Olschewski, S. W., **Inhaled treprostinil for treatment of chronic pulmonary arterial hypertension** *Ann. Intern. Med.* 2006
(85) Galie, N., Ghofrani, H. A., Torbicki, A., Barst, R. J., Rubin, L. J., Badesch, D., Fleming, T., Parpia, T., Burgess, G., Branzi, A., Grimminger, F., Kurzyna, M., M.D., Simonneau, G., **Sildenafil Citrate Therapy for Pulmonary Arterial Hypertension.** *N. Engl. J. Med. 2005*
(86) Rubin, L. J., Badesch, D. B., Barst, R. J., Galie, N., Black, C. M., Keogh, A., Pulido, T., Frost, A., Roux, S., Leconte, I., Landzberg, M., Simonneau, G., **Bosentan therapy for pulmonary arterial hypertension**. *N. Engl. J. M.* 2002
(87) Barst, R. J., Langleben, D., Frost, A., Horn, E. M., Oudiz, R., Shapiro, S., **Sitaxentan therapy in Pulmonary Hypertension.** *Am. J. Respir. Crit. Care Med.* 2004
(88) Langleben, D., Brock, T., Dixon, R., Barst, R. J., **STRIDE 1: effects of the selective ETA recptor antagonist, sitaxentan sodium in a patient population with pulmonary hypertension that meets traditional inclusion criteria of previous PAH trials.** *J Cardiovasc. Pharmacol.* 2004

(89) Ghofrani, H. A., Seeger, W., Grimminger, F., **Imatinib for the Treatment of Pulmonary Arterial Hypertension.** *N. Engl. J. Med.* 2005
(90) Ghofrani, H. A., Barst, B. J., Benza, R. L., Champion, H. C., Fagan, K. A., Grimminger, F., Humbert, M., Simonneau, G., Stewart, D. J., Ventura, D. J., Rubin, L. J., **Future Perspectives for the Treatment of Pulmonary Arterial Hypertension.** *J. Am. Coll. Cardiol*. 2009
(91) Klein, M., Schermuly, R. T., Ellinghaus, P., Milting, H., Riedl, B., Nikolova, S., Pullamsetti, S., Weissmann, N., Dony, E., Savai, R., Ghofrani, H. A., Grimminger, F., Busch, A. E., Schäfer, S., **Combined tyrosine and serine/threonine kinase inhibition by sorafenib prevents progression of experimental pulmonary hypertension and myocardial remodeling**. *Circulation* 2008
(92) Rai, P. R., Cool, C. D., Judy, A., King, C., Stevens, T., Burns, N., Winn, R. A., Kasper, M., Voelkel, N. F., **The Cancer Paradigm of Severe Pulmonary Arterial Hypertension.** *Am. J. Respir. Crit. Care Med.* 2008
(93) Voelkel, N. F., Cool, C. D., Lee, S. D., Wright, L., Geraci, M. W., Tuder, R. M., **Primary pulmonary hypertension between inflammation and cancer.** *Chest* 1999
(94) Moon, R. T., Kohn, A. D., De Ferrari, G. V., Kaykas, A., **WNT and beta-catenin signalling: diseases and therapies**. *Nat. Rev. Genet.* 2004.
(95) MacDonald, B. T., Tamai, K., He, X., **Wnt/b-Catenin Signaling: Components, Mechanisms, and Diseases** . *Developmental Cell* 2009
(96) Nusse, R., **Wnt signaling in disease and in development.** *Cell Res.* 2005
(97) Komiya1, Y., Habas, H., **Wnt signal transduction pathways.** *Organogenesis* 2008
(98) Willert, K., Brown, J. D., Danenberg, E., Duncan, A. W., Weissman, I. L., Reya, T., Yates, J. R., Nusse, R. **Wnt proteins are lipid-modified and can act as stem cell growth factors.** *Nature* 2003
(99) Wallingford, J. B., Habas, R., **The developmental biology of Dishevelled: an enigmatic protein governing cell fate and cell polarity**. *Development* 2005
(100**)** Cadigan, K. M., Liu, Y. I., **Wnt signaling: complexity at the surface.** *J. Cell Scie.* 2005
(101) Shimizu, H., Julius, M. A., Giarre, M., Zheng, Z., Brown, A. M., Kitajewski, J., **Transformation by Wnt family proteins correlates with regulation of betacatenin.** *Cell Growth Differ.* 1997
(102) Du, S. J., Purcell, S. M., Christian, J. L., McGrew, L. L., Moon, R. T., **Identification of distinct classes and functional domains of Wnts through expression of wild-type and chimeric proteins in *Xenopus* embryos.** *Mol. Cell. Biol.* 1995
(103) Chienl, A. J., Conradl, W. H., Moon, R. T., **A Wnt Survival Guide: From Flies to Human Disease.** *Journal of Investigative Dermatology* 2009
(104) Lucas, F. R., Salinas, P. C., **WNT-7a induces axonal remodeling and increases synapsin I levels in cerebellar neurons.** *Dev. Biol.* 1997
(105) Maye, P., Zheng, J., Li, L., Wu, D., **Multiple mechanisms for Wnt11- mediated repression of the canonical Wnt signaling pathway.** *J. Biol. Chem.* 2004
(106) Kofron, M., Birsoy, B., Houston, D., Tao, Q., Wylie, C., Heasman, J., **Wnt11/ beta-catenin signaling in both oocytes and early embryos acts through LRP6-mediated regulation of axin.** *Development* 2007
(107) Seifert, J. R., Mlodzik, M., **Frizzled/PCP signalling: a conserved mechanism regulating cell polarity and directed motility.** *Nat. Rev. Genet.* 2007
(108) He, X., Semenov, M., Tamai, K., Zeng, X., **LDL receptor-related proteins 5 and 6 in Wnt/betacatenin signaling: arrows point the way.** *Development* 2004

(109) Marlow, F., Topczewski, J., Sepich, D., Solnica-Krezel, L., **Zebrafish Rho kinase 2 acts downstream of Wnt11 to mediate cell polarity and effective convergence and extension movements.** *Curr. Biol.* 2002
(110) Weiser, D. C, Pyati, U. J., Kimelman, D., **Gravin regulates mesodermal cell behavior changes required for axis elongation during zebrafish gastrulation.** *Genes. Dev.* 2007
(111) Lu, W., Yamamoto, V., Ortega, B., Baltimore, D., **Mammalian Ryk is a Wnt coreceptor required for stimulation of neurite outgrowth**. *Cell* 2004
(112) Lu, X., Borchers, A. G., Jolicoeur, C., Rayburn, H., Baker, J. C., Tessier-Lavigne, M., **PTK7/CCK-4 is a novel regulator of planar cell polarity in vertebrates.** *Nature* 2004
(113) Nishita, M., Yoo, S. K., Nomachi, A., Kani, S., Sougawa, N., Ohta, Y., Takada, S., Kikuchi, A., Minami, Y., **Filopodia formation mediated by receptor tyrosine kinase Ror2 is required for Wnt5a induced cell migration**. *J. Cell Biol.* 2006
(114) Park, T. J., Gray, R. S., Sato, A., Habas, R., Wallingford, J. B., **Subcellular localization and signaling properties of dishevelled in developing vertebrate embryos**. *Curr. Biol.* 2005
(115) Kohn, A. D., Moon, R. T**., Wnt and calcium signaling: beta-catenin-independent pathways**. *Cell Calcium* 2005
(116) Slusarski, D. C., Pelegri, F., **Calcium signaling in vertebrate embryonic patterning and morphogenesis.** *Dev. Biol.* 2007
(117) Sheldahl, L. C., Slusarski, D. C., Pandur, P., Miller, J. R., Kuhl, M., Moon, R. T., **Dishevelled activates Ca2+ flux, PKC, and CamKII in vertebrate embryos.** *J. Cell Biol.* 2003
(118) Kuhl, M., Sheldahl, L. C., Malbon, C. C., Moon, R. T., **Ca(2+)/calmodulin-dependent protein kinase II is stimulated by Wnt and Frizzled homologs and promotes ventral cell fates in Xenopus.** *J. Biol. Chem.* 2000
(119) Slusarski, D. C., Yang-Snyder, J., Busa, W. B., Moon, R. T., **Modulation of embryonic intracellular Ca2+ signaling by Wnt-5A**. *Dev. Biol.* 1997
(120) Dejmek, J., Safholm, A., Kamp, N. C., Andersson, T., Leandersson, K., **Wnt-5a/Ca2+-induced NFAT activity is counteracted by Wnt-5a/Yes-Cdc42-casein kinase 1alpha signaling in human mammary epithelial cells.** *Mol. Cell Biol.* 2006
(121) Safholm, A., Leandersson, K., Dejmek, J., Nielsen, C. K., Villoutreix, B. O., Andersson, T., **A formylated hexapeptide ligand mimics the ability of Wnt-5a to impair migration of human breast epithelial cells**. *J. Biol. Chem.* 2006
(122) Kuhl, M., Sheldahl, L. C., Malbon, C. C., Moon, R. T., **Ca(2+)/calmodulindependent protein kinase II is stimulated by Wnt and Frizzled homologs and promotes ventral cell fates in Xenopus.** *J. Biol. Chem.* 2000
(123) **Wnt11-R signaling regulates a calcium sensitive EMT event essential for dorsal fin development of Xenopus**. *Dev. Biol.* 2007
(124) Robitaille, J., MacDonald, M. L., Kaykas, A., Sheldahl, L. C., Zeisler, J., Dube, M. P., **Mutant frizzled-4 disrupts retinal angiogenesis in familia exudative vitreoretinopathy**. *Nat. Genet.* 2002
(125) Westfall, T. A., Brimeyer, R., Twedt, J., Gladon, J., Olberding, A., Furutani-Seiki, M., **Wnt-5/pipetail functions in vertebrate axis formation as a negative regulator of Wnt/beta-catenin activity**. *J. Cell Biol.* 2003
(126) Topol, L., Jiang, X., Choi, H., Garrett-Beal, L., Carolan, P. J., Yang, Y., **Wnt-5a inhibits the canonical Wnt pathway by promoting GSK-3-independent beta-catenin degradation**. *J. Cell. Biol.* 2003
(127) Weidinger, G., Moon, R. T., **When Wnts antagonize Wnts**. *J. Cell. Biol.* 2003
(128) Torres, M. A., Yang-Snyder, J. A., Purcell, S. M., DeMarais, A. A., McGrew, L. L., Moon, R. T., **Activities of the Wnt-1 class of secreted signaling factors are antagonized by**

the Wnt-5A class and by a dominant negative cadherin in early Xenopus development. *J. Cell Biol.* 1996
(129) Huang, H. C., Klein, P. S., **The Frizzled family: receptors for multiple signal transduction Pathways.** *Genome Biology* 2004
(130) He, X., Semenov, M., Tamai, K., Zeng, X., **LDL receptor-related proteins 5 and 6 in Wnt/beta-catenin signaling: arrows point the way.** *Development* 2004
(131) Van Amerongen, R., Mikels, A., Nusse, R., **Alternative wnt signaling is initiated by distinct receptors**. *Sci. Signal*. 2008
(132) Satoh, W., Matsuyama, M., Takemura, H., Aizawa, S., Shimono, A., **Sfrp1, Sfrp2, and Sfrp5 regulate the Wnt/beta-catenin and the planar cell polarity pathways during early trunk formation in mouse.** *Genesis* 2008
(133) Hoang, B., Moos, M., Vukicevic, S., Luyten, F. P., **Primary structure and tissue distribution of FRZB, a novel protein related to Drosophila frizzled, suggest a role in skeletal morphogenesis**. *J. Biol. Chem.* 1996
(134) Jones, S. E., Jomary, C., **Secreted Frizzled-related proteins: searching for relationships and patterns.** *Bioessays* 2002
(135) Kawano, Y., Kypta, R., **Secreted antagonists of the Wnt signaling pathway**. *J. Cell Science* 2003
(136) Bafico, A., Gazit, A., Pramila, T., Finch, P. W., Yaniv, A., Aaronson, S. A., **Interaction of frizzled related protein (FRP) with Wnt ligands and the frizzled receptor suggests alternative mechanisms for FRP inhibition of Wnt signaling.** *J. Biol. Chem.* 1997
(137) Nelson, W. J., Nusse, R., **Convergence of Wnt, β-catenin, and cadherin pathways**. *Science* 2004
(138) Tolwinski, N. S., Wieschaus, E., **Rethinking WNT signaling**. *Trends Genet.* 2004
(139) Doble, B. W., Woodgett, J. R., **GSK-3: tricks of the trade for a multi-tasking kinase.** *J. Cell Science* 2003
(140) Woodgett, J. R., **Molecular cloning and expression of glycogen synthase kinase-3/factor A**. *EMBO J.* 1990
(141) Hoeflich, K. P., Luo, J., Rubie, E. A., Tsao, M. S., Jin, O., Woodgett, J. R., **Requirement for glycogen synthase kinase-3beta in cell survival and NF-kappaB activation**. *Nature* 2000
(142) Mukai, F., Ishiguro, K., Sano, Y., Fujita, S. C., **Alternative splicing isoform of tau protein kinase I/glycogen synthase kinase 3beta**. *J.Neurochem.* 2002
(143) Woodgett, J. R., **Judging a Protein by More Than Its Name: GSK-3.** *Science* 2001
(144) Frame, S., Cohen, P., **GSK3 takes centre stage more than 20 years after its discovery.** *Biochem. J.* 2001
(145) Fiol, C. J., Williams, J. S., Chou, CH., Wang, Q. M., Roach, P. J., Andrisani, O. M., **A secondary phosphorylation of creb341 at ser129 is required for the camp-mediated control of gene expression. A role for glycogen synthase kinase-3 in the control of gene expression**. *J. Biol. Chem.* 1994
(146) Welsh, G. I., Miller, C. M., Loughlin, A. J., Price, N. T., Proud, C. G., **Regulation of eukaryotic initiation factor eif2b: Glycogen synthase kinase-3 phosphorylates a conserved serine which undergoes dephosphorylation in response to insulin.** *FEBS Letters* 1998
(147) Morisco, C., Seta, K., Hardt, S. E., Lee, Y., Vatner, S. F., Sadoshima, J., **Glycogen synthase kinase 3beta regulates gata4 in cardiac myocytes.** *J. Biol. Chem.* 2001
(148) Van der Velden, J. L., Schols, A. M., Willems, J., Kelders, M. C., Langen, R. C., **Glycogen synthase kinase 3 suppresses myogenic differentiation through negative regulation of NFATc3**. *J. Biol. Chem.* 2008

(149) Canagarajah, B. J., Khokhlatchev, A., Cobb, M. H., Goldsmith, E. J., **Activation mechanism of the MAP kinase ERK2 by dual phosphorylation**. *Cell* 1997
(150) Dajani, R., Fraser, E., Roe, S. M., Young, N., Good, V., Dale, T. C., Pearl, L. H., **Crystal structure of glycogen synthase kinase 3 beta: structural basis for phosphate-primed substrate specificity and autoinhibition.** *Cell* 2001
(151) Steiner, M. R., Holtsberg, F. W., Keller, J. N., Mattson, M. P., Steiner, S. M., **Lysophosphatidic acid induction of neuronal apoptosis and necrosis**. *Ann. N. Y. Acad. Sci.* 2000
(152) Hartigan, J. A., Johnson, G. V., **Transient increases in intracellular calcium result in prolonged site-selective increases in Tau phosphorylation through a glycogen synthase kinase 3b-dependent pathway**. *J. Biol. Chem.* 1999
(153) Bonnet, S., Rochefort, G., Sutendra, G., Archer, S. L., Haromy, A., Webster, L., Hashimoto, K., Bonnet, S. N., Michelakis, E. D., **The nuclear factor of activated T cells in pulmonary arterial hypertension can be therapeutically targeted.** *Proc. Natl. Acad. Sci.* 2007
(154) Hislop, A., Reid, L., **Arterial changes in crotalaria spectabilis-induced pulmonary hypertension in rats.** *Brit. J. Exp. Pathol.* 1974
(155) Mattocks, A. R., **Toxicity of pyrrolizidine alkaloids**. *Nature* 1968
(156) Schermuly, R. T., Kreisselmeier, K. P., Ghofrani, H. A., **Chronic sildenafil treatment inhibits monocrotaline-induced pulmonary hypertension in rats.** *Am. J. Respir. Crit. Care Med.* 2004
(157) Lorenza, K., Schmitta, J. P., Vidala, M., Martin, J., **Lose Cardiac hypertrophy: Targeting Raf/MEK/ERK1/2-signaling.** *The International Journal of Biochemistry & Cell Biology* 2009
(158) Bogaard,H. J., Abe, K., Noordegraaf, A. V., Voelkel, N. F., **Right ventricle under pressure.** *Chest* 2008
(159) Mann, D. L., **Basic mechanisms of left ventricular remodeling: the contribution of wall stress.** *J. Card. Fail* 2004
(160) Janicki, J. S., Brower, G. L., Grdner, J. D., **Cardiac mast cell regulation of matrix metalloproteinase- related ventricular remodeling in chronic pressure or volume overload.** *Cardiovasc. Res.* 2006
(161) Baicu, C. F., Stroud, J. D., Livesay, V., **Changes in extracellular collagen matrix after myocardial systolic performance.** *Am. J. Physiol. Heart. Circ. Physiol.* 2003
(162) Tomanek, R. J., **Response of the coronary vasculature to myocardial hypertrophy.** *J. Am. Coll. Cardiol.* 1990
(163) Sano, M., Minamino, T., Toko, H., **p53-induced inhibition of Hif-1 causes cardiac dysfunction during pressure overload.** *Nature* 2007
(164) Partovian, C., Adnot, S., Eddahibi, S., **Heart and lung VEGF mRNA expression in rats with monocrotaline-induced hypertension.** *Am. J. Physiol.* 1998
(165) Laumanns, I. P., Fink, L., Wilhelm, J., Wolff, J. C., Mitnacht-Kraus, R., Graef-Hoechst, S., Stein, M. M., Bohle, R. M., Klepetko, W., Hoda, M. A., **The non-canonical wnt-pathway is operative in idiopathic pulmonary arterial hypertension**. *Am. J. Respir. Cell. Mol. Biol.* 2008
(166) Goodwin, A. M., D'Amore, P. A., **Wnt signaling in the vasculature.** *Angiogenesis* 2002
(167) Morin, P. J., Sparks, A. B., Korinek, V., Barker, N., Clevers, H., Vogelstein, B., Kinzler, K. W., **Activation of beta-catenin-Tcf signaling in colon cancer by mutations in beta-catenin or APC**. *Science* 1997

(168) Nhieu, J. T., Renard, C. A., Wei, Y., Cherqui, D., Zafrani, E. S., Buendia, M. A., **Nuclear accumulation of mutated beta-catenin in hepatocellular carcinoma is associated with increased cell proliferation**. *Am. J. Pathol.* 1999
(169) Polakis, P., **The oncogenic activation of beta-catenin**. *Curr. Opin.Genet. Dev.* 1999
(170) Waltzer, L., Bienz, M., **The control of beta-catenin and TCF during embryonic development and cancer.** *Cancer Metastasis Rev.* 1999
(171) Wang, X., **A role for the beta-catenin/T-cell factor signaling cascade in vascular remodeling.** *Circ. Res***.** 2002
(172) Cao, Q., **Glycogen synthase kinase-3beta positively regulates the proliferation of human ovarian cancer cells**. *Cell Res*. 2006
(173) Shakoori, A., **Deregulated GSK3beta activity in colorectal cancer: its association with tumor cell survival and proliferation.** *Biochem. Biophys. Res. Commun.* 2005
(174) Park, K. W., **Constitutively active glycogen synthase kinase-3beta gene transfer sustains apoptosis, inhibits proliferation of vascular smooth muscle cells, and reduces neointima formation after balloon injury in rats.** *Arterioscler. Thromb. Vasc. Biol.* 2003
(175) de Jesus Perez, V. A., Alastalo, T. P., Wu, J. C., Axelrod, J. D., Cooke, J. P., Amieva, M., Rabinovitch, M,. **Bone morphogenetic protein 2 induces pulmonary angiogenesis via Wnt-beta-catenin and Wnt-RhoA-Rac1 pathways**. *J. Cell Biol.* 2009
(176) Hardt, S. H., Sadoshima, J., **Glycogen Synthase Kinase-3 A Novel Regulator of Cardiac Hypertrophy and Development.** *Circ. Res.* 2002
(177) Sugden, P. H., Fuller, S. J., Weiss, S. C., Clerk, A., **Glycogen synthase kinase 3 (GSK3) in the heart: a point of integration in hypertrophic signaling and a therapeutic target? A critical analysis.** *British Journal of Pharmacology* 2008
(178) Moon, R. T., Kohn, A. D., De Ferrari, G. V., Kaykas, A., **WNT and beta-catenin signalling: diseases and therapies.** *Nat. Rev. Genet.* 2004
(179) Goodwin, A. M., D'Amore, P. A., **Wnt signaling in the vasculature.** *Angiogenesis* 2002
(180) Morin, P. J., **Beta-catenin signaling and cancer**. *Bioessays* 1999
(181) Mikels, A. J., Nusse, R., **Purified Wnt5a protein activates or inhibits beta-catenin-TCF signaling depending on receptor context.** *P.L.o.S. Biol.* 2006
(182) Tao, Q., Yokota, C., Puck, H., Kofron, M., Birsoy, B.., Yan, D., Asashima, M., Wylie, C. C., Lin, X., Heasman, J., **Maternal wnt11 activates the canonical wnt signaling pathway required for axis formation in Xenopus embryos**. *Cell* 2005
(183) Kofron, M., Birsoy, B., Houston, D., Tao, Q., Wylie, C., Heasman, J., **Wnt11/beta-catenin signaling in both oocytes and early embryos acts through LRP6-mediated regulation of axin.** *Development* 2007
(184) Cha, S. W., Tadjuidje, E., White, J., Wells, J., Mayhew, C., Wylie, C., Heasman, J., **Wnt11/5a complex formation caused by tyrosine sulfation increases canonical signaling activity.** *Curr. Biol.* 2009
(185) Cha, S. W., Tadjuidje, E., Tao, Q., Wylie, C., Heasman, J., **Wnt5a and Wnt11 interact in a maternal Dkk1-regulated fashion to activate both canonical and non-canonical signaling in Xenopus axis formation.** *Development.* 2008
(186) Miller, J. R., Hocking, A. M., Brown, J. D., Moon, R. T., **Mechanism and function of signal transduction by the Wnt/b-catenin and Wnt/Ca2+ pathways.** *Oncogene* 1999
(187) Chen, X. Y., Dun, J. N., Miao, Q. F., Zhang, Y. J., **Fasudil hydrochloride hydrate, Rho-kinas inhibitor suppress 5-hydroxytryptamine-induced pulmonary artery smooth muscle cell proliferation via JNK and ERK1/2 pathway.** *Pharmacology* 2009
(188) Li, F., Xia, W., Yuan, S., Sun, R., **Acute inhibition of Rho-kinase attenuates pulmonary hypertension in patients with congenital heart disease.** *Pediatr. Cardiol.* 2009

(189) Yu, Y., Keller, S. H., Remilliard, C. V., Safrina, O., Nicholson, A., Zhang, S. L, Jiang, W., Vangala, N., Landsberg, J. W., Wang, J. Y., Thistlethwaite, P. A., Channick, R. N., Robbins, I. M., Loyd, J. E., Ghofrani, H. A., Grimminger, F., Schermuly, R. T., Cahalan, M. D., Rubin, L. J., Yuan, J. X., **A functional single-nucleotide polymorphism in the TRPC6 gene promoter associated with iPAH.** *Circulation* 2009
(190) Zhang, S., Dong, H., Rubin, L. J., Yuan, J. X., **Upregulation of Na+/Ca2+ exchanger contributes to the enhanced Ca2+ entry in pulmonary artery smooth muscle cells from patients with iPAH.** *Am. J. Physiol. Cell Physiol.* 2007
(191) Hirenallur-S, D. K., Haworth, S. T., Leming, J. T., Chang, J., Hernandez, G., Gordon, J. B., Rusch, N. J., **Upregulation of vascular calcium channels in neonatal piglets with hypoxia-induced pulmonary hypertension.** *Am. J. Physiol. Lung Cell Mol. Physiol.* 2008
(192) Rossol-Allison, J., Stemmle, L. N., Swenson-Fields, K. I., Kelly, P., Fields, P. E., McCall, S. J., Casey, P. J., Fields, T. A., **Rho-GTPase activity modulates Wnt3a-beta-catenin signaling.** *Cell Signal.* 2009
(193) Wang, X., Xiao, Y., Mou, Y., Zhao, Y., Blankesteijn, W. M., Hall, J. L., **A role for the beta-catenin/t-cell factor signaling cascade in vascular remodeling.** *Circ. Res.* 2002
(194) Bentley, J. K., Deng, H., Linn, M. J., Lei, J., Dokshin, G. A., Fingar, D. C., Bitar, K. N., Henderson, W. R. Jr., Hershenson, M. B., **Airway smooth muscle hyperplasia and hypertrophy correlate with glycogen synthase kinase-3(beta) phosphorylation in a mouse model of asthma**. *Am. J. Physiol. Lung Cell Mol. Physiol.* 2009
(195) Chilosi, M., Poletti, V., Zamo, A., Lestani, M., Montagna, L., Piccoli, P., Pedron, S., Bertaso, M., Scarpa, A., Murer, B., **Aberrant wnt/beta-catenin pathway activation in idiopathic pulmonary fibrosis**. *Am. J. Pathol.* 2003
(196) Humbert, M., Sitbon, O., Simonneau, G., **Treatment of Pulmonary Arterial Hypertension.** *N. Engl. J. Med.* 2004
(197) Mao, C., Malek T-BO, Pueyo, M. E., Steg, P. G., Soubrier, F., **frzb-1 and frizzled receptor fz1 and fz2 genes in the rat aorta after balloon injury.** *Artrerioscler. Thromb. Vasc. Biol.* 2000
(198) Yang, L., Lin, C., Liu, Z. R., **P68 RNA helicase mediates PDGF-induced epithelial to mesenchymal transition by displacing Axin from beta-catenin.** *Cell* 2006
(199) Nunes, R. O., Schmidt, M., Dueck, G., Baarsma, H., Halayko, A. J., Kerstjens, H. A., Meurs, H., Gosens, R., **GSK-3/beta catenin signaling axis in airway smooth muscle: role in mitogenic signaling.** *Am. J. Physiol. Lung Cell Mol. Physiol.* 2008
(200) Cohen, E. D., Ihida-Stansbury, K., Min Lu, M., Panettieri, R. A., Jones, P. L., Morrisey, E. E., **Wnt signaling regulates smooth muscle precursor development in the mouse lung via tenascin C/PDGFR pathway.** *J. Clin. Invest.* 2009
(201) Forde, J. E., Dale, T. C., **Glycogen synthase kinase 3: A key regulator of cellular fate** *Cell Mol. Life Sci.* 2007
(202) Cohen, P., Goedert, M., **GSK3 inhibitors: Development and therapeutic potential.** *Nat. Drug Disc.* 2004
(203) James, R., Woodgett, J., **Judging a Protein by More Than Its Name: GSK-3.** *Science* 2001
(204) Bonnet, S., Paulin, R., Sutendra, G., Dromparis, P., Roy, M., Watson, K. O., Nagendran, J., Haromy, A., Dyck, J., Michelakis, E. D., **Dehydroepiandrosterone reverses systemic vascular remodeling through the inhibition of Akt/GSK3ß/NFAT axis.** *Circulation* 2009
(205) Chow, W., Hou, G., Bendeck, M. P., **Glycogen synthase kinase 3β regulation of NFATc in the vascular smooth muscle cell response to injury.** *Exp. Cell Res.* 2008
(206) Schermuly, R. T., Dony, E., Ghofrani, H. A., Pullamsetti, S., Savai, R., Roth, M., Sydykov, A., Lai, Y. J., Weissmann, N., Seeger, W., **Reversal of experimental pulmonary hypertension by PDGF inhibition.** *J. Clin. Invest.* 2005

(207) Perros, F., Montani, D., Dorfmuller, P., Durand-Gasselin, I., Tcherakian, C., Le Pavec, J., Mazmanian, M., Fadel, E., Mussot, S., Mercier, O., **Platelet-derived growth factor expression and function in idiopathic pulmonary arterial hypertension**. *Am. J. Respir. Crit. Care Med.* 2008

(208) Merklinger, S. L., Jones, P. L, Martinez, E. C, Rabinovitch, M., **Epidermal growth factor receptor blockade mediates smooth muscle cell apoptosis and improves survival in rats with pulmonary hypertension.** *Circulation* 2005

(209) Wedgwood, S., Devol, J. M., Grobe, A., Benavidez, E., Azakie, A., Fineman, J. R., Black, S. M., **Fibroblast growth factor-2 expression is altered in lambs with increased pulmonary blood flow and pulmonary hypertension**. *Pediatr. Res.* 2007

(210) McMurtry, M. S., Archer, S. L, Altieri, D. C., Bonnet, S., Haromy, A., Harry, G., Puttagunta, L., Michelakis, E. D., **Gene therapy targeting survivin selectively induces pulmonary vascular apoptosis and reverses pulmonary arterial hypertension.** *J. Clin. Invest.* 2005

(211) Almeida, M., Han, L., Bellido, T., Manolagas, S. C., and Kousteni, S., **Wnt Proteins Prevent Apoptosis of Both Uncommitted Osteoblast Progenitors and Differentiated Osteoblasts by beta-Catenin-dependent and -independent Signaling Cascades Involving Src/ERK and Phosphatidylinositol 3-Kinase/AKT.** *J. Biol. Chem.* 2005

(212) Kim, S. E., Lee, W. J., Choi, K. Y., **The PI3 kinase-Akt pathway mediates Wnt3a-induced proliferation.** *Cell Signal.* 2007

(213) Zhang, L. Y., Ye, J., Zhang, F., Li, F. F., Li, H., Gu, Y., Liu, F., Chen, G. S., Li, Q**., Axin induces cell death and reduces cell proliferation in astrocytoma by activating the p53 pathway**. *Int. J. Oncol*. 2009

(214) Brown, N. R., Noble, M. E., Endicott, J. A., Johnson, L. N., **The structural basis for specificity of substrate and recruitment peptides for cyclin-dependent kinases**. *Nat. Cell Biol.* 1991

(215) Canagarajah, B. J., Khokhlatchev, A., Cobb, M. H., Goldsmith, E. J., **Activation mechanism of the MAP kinase ERK2 by dual phosphorylation**. *Cell* 1997

(216) Cole, A., Frame, S., Cohen, P., **Further evidence that the tyrosine phosphorylation of glycogen synthase kinase-3 (GSK3) in mammalian cells is an autophosphorylation event**. *Biochem. J.* 2004

(217) Cuiling, Ma., Bower, K. A., Chen, G., Shi, X., Ke, Z. J., Luo, J., **Interaction between ERK and GSK3beta Mediates Basic Fibroblast Growth Factor-induced Apoptosis in SK-N-MC Neuroblastoma Cells.** *J. Biol. Chem.* 2008

(218) Pap, M., Cooper, G. M., **Role of glycogen synthase kinase-3 in the phosphatidylinositol 3-kinase/akt cell survival pathway**. *J. Biol. Chem.* 1998

(219) Sakanaka, C., Weiss, J. B., Williams, L. T., **Bridging of beta-catenin and glycogen synthase kinase-3beta by axin and inhibition of beta-catenin-mediated transcription**. *Proc. Natl. Acad. Sci.* 1998

(220) Fiol, C. J., Williams, J. S., Chou, CH., Wang, Q. M., Roach, P. J., Andrisani, O. M., **A secondary phosphorylation of creb341 at ser129 is required for the camp-mediated control of gene expression. A role for glycogen synthase kinase-3 in the control of gene expression**. *J. Biol. Chem.* 1994

(221) Diehl, J. A., Cheng, M., Roussel, M. F., Sherr, C. J., **Glycogen synthase kinase-3beta regulates cyclin d1 proteolysis and subcellular localization**. *Genes Dev.* 1998

(222) Wang, Q., Zhou, Y., Wang, X., Evers, B. M., **Glycogen synthase kinase-3 is a negative regulator of extracellular signal-regulated kinase.** *Oncogene* 2006

(223) Reszka, A. A., Seger, R., Diltz, C. D., Krebs, E. G., Fischer, E. H., **Association of mitogen-activated protein kinase with the microtubule cytoskeleton.** *Proc. Natl. Acad. Sci.* 1995

(224) Jope, R. S., Johnson, G. V., **The glamour and gloom of glycogen synthase kinase-3**. *Trends Biochem. Sci*. 2004
(225) Takahashi-Yanaga, F., Shiraishi, F., Hirata, M., Miwa, Y., Morimoto, S., Sasaguri, T., **Glycogen synthase kinase-3beta is tyrosine-phosphorylated by MEK1 in human skin fibroblasts.** *Biochem. Biophys. Res. Commun*. 2004
(226) Barandon, L., Couffinhal, T., Ezan, J., Dufourcq, P., Costet, P., Alzieu, P., Leroux, L., Moreau, C., Dare, D., Duplaa, C., **Reduction of infarct size and prevention of cardiac rupture in transgenic mice overexpressing FrzA.** *Circulation* 2003
(227) Barandon, L., Dufourcq, P., Costet, P., Moreau, C., Allieres, C., Daret, D., Dos Santos, P., Daniel Lamaziere, J. M., Couffinhal, T., Duplaa, C., **Involvement of FrzA/sFRP-1 and the Wnt/frizzled pathway in ischemic preconditioning.** *Circ. Res.* 2005
(228) Sawyer, D. B., Siwik, D. A., Xiao, L., Pimentel, D. R., Singh, K., Colucci, W. S., **Role of oxidative stress in myocardial hypertrophy and failure**. *J. Mol. Cell Cardiol*. 2002
(229) Sam, F., Kerstetter, D. L., Pimental, D. R., Mulukutla, S., Tabaee, A., Bristow, M. R., Colucci, W. S., and Sawyer, D. B., **Increased reactive oxygen species production and functional alterations in antioxidant enzymes in human failing myocardium.** *J. Card. Fail* 2005
(230) Melkonyan, H. S., Chang, W.C., Shapiro, J. P., Mahadevappa, M., Fitzpatrick, P.A., Kiefer, M. C., Tomei, L. D., and Umansky, S. R., **SARPs: a family of secreted apoptosis-related proteins.** *Proc. Natl. Acad. Sci.* 1997
(231) Zhou, Z., Wang, J., Han, X., Zhou, J., Linder, S., **Up-regulation of human secreted frizzled homolog in apoptosis and its down-regulation in breast tumors**. *Int. J. Cancer* 1998
(232) Moon, R. T., Kohn, A. D., De Ferrari, G. V., Kaykas, A., **WNT and beta-catenin signalling: diseases and therapies.** *Nat. Rev. Genet.* 2004
(233) Ugolini, F., Charafe-Jauffret, E., Bardou, V. J., Geneix, J., Adelaide, J., Labat-Moleur, F., Penault-Llorca, F., Longy, M., Jacquemier, J., Birnbaum, D., **WNT pathway and mammary carcinogenesis: loss of expression of candidate tumor suppressor gene SFRP1 in most invasive carcinomas except of the medullary type.** *Oncogene* 2001
(234) Suzuki, H., Watkins, D. N., Jair, K. W., Schuebel, K. E., Markowitz, S. D., Chen, W. D., Pretlow, T. P., Yang, B., Akiyama, Y., Van Engeland, M., **Epigenetic inactivation of SFRP genes allows constitutive WNT signaling in colorectal cancer**. *Nat. Genet.* 2004
(235) Schumann, H., Holtz, J., Zerkowski, H. R., Hatzfeld, M., **Expression of secreted frizzled related proteins 3 and 4 in human ventricular myocardium correlates with apoptosis related gene expression.** *Cardiovasc. Res.* 2000
(236) Suzuki, H., Watkins, D. N., Jair, K. W., Schuebel, K. E., Markowitz, S. D., Chen, W. D., Pretlow, T. P., Yang, B., Akiyama, Y., Van Engeland, M., **Epigenetic inactivation of SFRP genes allows constitutive WNT signaling in colorectal cancer.** *Nat. Genet.* 2004
(237) Bayle, J., Fitch, J., Jacobsen, K., Kumar, R., Lafyatis, R., Lemaire, R., **Increased expression of Wnt2 and SFRP4 in Tsk mouse skin: role of Wnt signaling in altered dermal fibrillin deposition and systemic sclerosis**. *J. Invest. Dermatol.* 2008
(238) Cheng, J. H., She, H., Han, Y. P., Wang, J., Xiong, S., Asahina, K., Tsukamoto, H., **Wnt antagonism inhibits hepatic stellate cell activation and liver fibrosis**. *Am. J. Physiol. Gastrointest. Liver Physiol.* 2008
(239) Venkatachalam, K., Venkatesan, B., CHandrasekar, B., **WISP1, a pro-mitogenic, pro-survival Factor, mediates Tumor Necrosis Factor alpha- stimulated cardiac fibroblast proliferation but inhibits TNF-alpha-induced cardiomyocytes death**. *J. Biol. Chem.* 2009
(240) Colston, J. T., de la Rosa, S. D., Koehler, M., Chandrasekar, B., **Wnt-induced secreted protein 1 is a pro-hypertrophic and pro-fibrotic growth factor.** *Am. J. Physiol. Heart Circ. Physiol.* 2007

(241) Hardt, S. E., Sadoshima, J., **Glycogen synthase kinase-3beta: a novel regulator of cardiac hypertrophy and development.** *Circ. Res.* 2002
(242) Baurand, A., Zelarayan, L., Betney, R., Gehrke, C., Dunger, S., Noack, C., Busjahn, A., Huelsken, J., Taketo, M. M., Birchmeier, W., **Beta-catenin downregulation is required for adaptive cardiac remodeling.** *Circ. Res.* 2007
(243) Garcia-Gras, E., Lombardi, R., Giocondo, M. J., Marian, A. J., **Suppression of canonical Wnt/beta-catenin signaling by nuclear plakoglobin recapitulates phenotype of arrhythmogenic right ventricular hypertrophy.** *J. Clin. Invest.* 2006
(244) Zelarayan, L., Gehrke, Ch., Bergmann, M. W., **Role of β-Catenin in Adult Cardiac Remodeling.** *Cell cycle* 2007
(245) Barandon, L., Dufourcq, P., Coster, O., Moreau, C., Allieres, C., Daret, D., Dos Santos, P, Duplaa, C., **Involvement of sFRP-1 and Wnt/Frizzled pathway in ischemic preconditioning.** *Circ. Res.* 2005
(246) Barandon, L., Couffinhal, T., Ezan, J., Dufourcq, P., Costet, P., Moreau, B. S., Duplaa, C., **Reduction of infarct size and prevention of cardiac rupture sFRP-1.** *Circulation 2003*
(247) Hahn, J. Y., Cho, H. J., Bae, J. W., Yuk, H. S., Kim, K. I., Park, K. W., Koo, B. K., Chae, I. H., Shin, C. S., Oh, B. H., **Beta-catenin overexpression reduces myocardial infarct size through differential effects on cardiomyocytes and cardiac fibroblasts**. *J. Biol. Chem.* 2006
(248) Masuelli, L., Bei, R., Sacchetti, P., Scappaticci, I., Francalanci, P., Albonici, L., Coletti, A., Palumbo, C., Minieri, M., Fiaccavento, R., **Beta-catenin accumulates in intercalated disks of hypertrophic cardiomyopathic hearts.** *Cardiovasc. Res.* 2003
(249) Bruce, A. F., Rothery, S., Dupont, E., Severs, N. J., **Gap junction remodeling in human heart failure is associated with increased interaction of connexin43 with ZO-1.** *Cardiovasc. Res.* 2008
(250) Severs, N. J., Dupont, E., Kaba, T. N., Rothery, S., Jain, R., Fry, Ch,. **Alterations in cardiac connexin expression in cardiomyopathies.** *Adv. Cardiol.* 2006
(251) Severs, N. J., Bruce, A. F., Dupont, E., Rothery, S., **Remodeling of gap junctions and connexin expression in diseased myocardium.** *Cardiovasc. Res.* 2008
(252) Ross, S. E., **Inhibition of adipogenesis by Wnt signaling.** *Science* 2000
(253) Yun, M. S., Kim, S. E., Jeon, S. H., Lee, J. S., Choi, K. Y., **Both ERK and beta-catenin are involved in Wnt3A-induced proliferation.** *J. Cell Science* 2005
(254) Bernheim, D., **De l'asystole veineuse dons l'hypertrophie du coeur gauche par stenose concomitante du ventricule droit**. *Rev. Med. (Paris)* 1910
(255) Reeves, J. T., Groves, B. M., **Approach to the patient with pulmonary hypertension.** *Mt Kisco, New York: Futura Publishing Company Inc.* 1984
(256) Voelkel, N. F., Quaife, R. A., Leinwand, L. A., Barst, R. J., McGoon, M. D., Meldrum, D. R., Dupuis, J., Long, C. S., Rubin, L. J., Smart, F. W., Suzuki, Y. J., Gladwin, M., Denholm, E. M., Gail, D. B **Right Ventricular Function and Failure: Report of a National Heart, Lung, and Blood Institute Working Group on Cellular and Molecular Mechanisms of Right Heart Failure.** *Circulation* 2006
(257) van de Schans, V. A., van den Borne, S. W., Strzelecka, A. E., Jansen, B. J., van der Velden, J. L., Langen, R. C., Wynshaw-Boris, A., Smits, J. F., Blankensteijn, W. M., **Interruption of Wnt signaling attenuates the onset of pressure overload-induced cardiac hypertrophy.** *Hypertension* 2007

11. **Curriculum Vitae**

Surname:	**Sklepkiewicz**
Name:	**Piotr Lukasz**
Birthyear:	**1981**
Birthplace:	**Kutno, Poland**
Nationality:	**Polish**

Education

2008-2009	Exchange research work in the laboratory of Prof. Jeanine D'Armiento at the Columbia University in New York, USA **Project:** Wnt signaling suppression via loss of sFRP-1 leads to dilated cardiomyopathy in mice
2006-2010	Research work in the laboratory of Prof. Ralph Schermuly at the Department of Internal Medicine, Justus-Liebig-University Giessen, Giessen, Germany. **Project:** GSK3β/β-Catenin signaling pathway regulates vascular remodeling in Pulmonary Arterial Hypertension
2005	PhD studentship at the International Graduate ProgramMBML of the Justus Liebig University of Giessen, Germany
2005	Master's degree **Project:** "Organisation of short fragment of human DNA into minicircles particles. Recognising topological features of human satellite DNA and DNA of human CpG island"
2003 – 2004	**Socrates Erasmus Student**: one year of International Graduate program at the University of Denis Diderot Paris VI/VII in Paris, France **Experimental work**: Biochemistry of the Chromatin laboratory at the Univerity of Paris, France at Institute Jacques Monod Marie – Curie University VI/VII in Paris, France Research work and Master Thesis in the Laboratory of dr. Ariel Prunell, supervised by

	Prof. Jan Filipski
2002	Practical lab training in the Molecular Genetics Laboratory at the Nicolaus Copernicus University in Torun, Poland
2001	Specialization of Molecular Biology
2000	Started Nicolaus Copernicus University in Torun, Poland Faculty of Biology and Earth Sciences
2000	Maturity Exam and University examinations
1996-2000	J. H. Dabrowski- High School in Kutno, Poland
1988-1996	Primary School in Kutno, Poland

Additional qualifications

Languages	Native Polish, English Fluent (FCE level) French: Basic
Computer Skills	work on PC platforms and MACs, MS Office, Adobe Photoshop, nucleotide and protein sequnces analysis (BLAST, ClustalW, GeneDoc)

Scientific Contributions

Publications

1. Sklepkiewicz Piotr*, Pullamsetti SS*, Xia Tian, Ghofrani HA, Weissmann N, Seeger W, Grimminger F, Schermuly R. Glycogen Synthase Kinase 3ß inactivation contributes to vascular remodeling. Submitted to *AJRCMB*

2. Sklepkiewicz Piotr, Kwon S, Shiomi T, Sun J, Foronjy B, Schermuly RT, D'Armiento J. Loss of sFRP-1 leads to dilated cardiomyopathy in mice via suppression of canonical Wnt signaling. *In preparation*

3. Pullamsetti SS, Kreymborg K, Sklepkiewicz Piotr, Behrendts M, Schluter KD, Janssen W, Helmus K, Weissmann N, Ghofrani HA, Grimminger F, Braun T, Seeger W, Schermuly RT. Effect of Bosentan on myocardial remodeling- Studies in experimental models of right heart hypertrophy. *In preparation*

Poster Presentations

1. Sklepkiewicz Piotr, Pullamsetti SS, Xia Tian, Ghofrani HA, Weissmann N, Seeger

W, Grimminger F, Schermuly R. Role of Glycogen Synthase Kinase 3ß/ß-Catenin signaling system in Pulmonary Arterial Hypertension *DGIM Conference 2007 Wiesbaden, Germany*

2. Sklepkiewicz Piotr, Pullamsetti SS, Xia Tian, Ghofrani HA, Weissmann N, Seeger W, Grimminger F, Schermuly R. Role of Glycogen Synthase Kinase 3ß / ß catenin signaling system in Pulmonary Arterial Hypertension *Annual Congress of the American Thoracic Society (ATS), Toronto, Canada 16-22 May 2008*

3. Pullamsetti SS, Kreymborg K, Sklepkiewicz Piotr, Helmus K, Ghofrani HA, Weissmann N, Seeger W, Schermuly RT. Role of Raf kinases I right ventricular hypertrophy. *Annual Congress of the American Thoracic Society (ATS), Toronto, Canada 16-22 May 2008*

4. Schermuly RT, Pullamsetti SS, Kreymborg K, Behrendts M, Sklepkiewicz Piotr, Helmus K, Braun T, Weissmann N, Seeger W, Ghofrani HA, Grimminger F. Effects of Bosentan on right ventricular hypertrophy: Role of Ras Raf kinases *AHA Meeting 2008*

5. Sklepkiewicz Piotr, Kwon S, Shiomi T, Sun J, Foronjy B, Schermuly RT, D'Armiento J. Canonical Wnt signaling suppression via loss of sFRP-1 leads to dilated cardiomyopathy in mice *WNT SIGNALING Meeting* 2009

Oral presentation

1. Role of Glycogen Synthase Kinase 3ß/ß catenin signaling system in Pulmonary Arterial Hypertension *Molecular Biology and Medicine of the Lung (MBML) Annual Retreat, Giessen, Germany 2006*
2. Role of Glycogen Synthase Kinase 3ß / ß catenin signaling system in Pulmonary Arterial Hypertension *Molecular Biology and Medicine of the Lung (MBML) Annual Retreat, Giessen, Germany 2007*

12. **Declaration**

I declare that I have completed this dissertation single-handedly without the unauthorized help of a second party and only with the assistance acknowledged therein. I have appropriately acknowledged and referenced all text passages that are derived literally from or are based on the content of published or unpublished work of others, and all information that relates to verbal communications. I have abided by the principles of good scientific conduct laid down in the charter of the Justus Liebig University of Giessen in carrying out the investigations described in the dissertation.

13. Acknowledgements

I would like to express my greatest appreciation and gratitude for my supervisor Prof. Dr. rer. nat. Ralph Schermuly for the precious assistance and guidance. Thank You for giving me opportunity to be a part of your scientific group and for providing me all possible support not only scientific that made my PhD disputation possible. Thank You for being a great boss.

I especially would like to thank my Co-supervisor Prof. Jeanine D'Armiento at Columbia University, New York for giving me opportunity to work on the research project in her laboratory. Thank You for your great assistance, all suggestions and encouragement I received which helped me to enjoy science. Thank You for unvaluable help me and my wife experienced from You.

I would like to thank also my postdoc Dr. Soni Pullamsetti for her great assistance and guidance which encouraged and motivated me through my research projects.

Special thanks to Dr. Med. Takayuki Shiomi who always was there for me when I needed his professional advice. Thank You for everything.

I would also like to thank Dr. Pat Geraghty for proofreading my thesis and for being a good friend.

For solving technical problems and for great scientific discussions I would like to thank Dr. Rajkumar Savai and Dr. Marcus Roth.

To all my great labmates: Ewa, Xia, Ying-Ju, Kathrin, Matze, Sevda, Sergey, Ola, Jo, Kati, Hamza, Pavan, Asahiro, Taka, Vincent, Polina, Jules, Bob, Anita and Pat for creating great atmosphere, Thank You.

All my work is dedicated to my lovely wife Marta and my wonderful parents for support I can always count on and unconditional love ... Thank You that you are with me ..